

UCSF

UC San Francisco Electronic Theses and Dissertations

Title

Regulation of axon outgrowth and guidance in *C. elegans*

Permalink

<https://escholarship.org/uc/item/0jm297t8>

Author

Zallen, Jennifer A.

Publication Date

1999

Peer reviewed|Thesis/dissertation

Regulation of Axon Outgrowth and Guidance
in *C. elegans*

by
Jennifer A. Zallen

DISSERTATION

Submitted in partial satisfaction of the requirements for the degree of

DOCTOR OF PHILOSOPHY

in

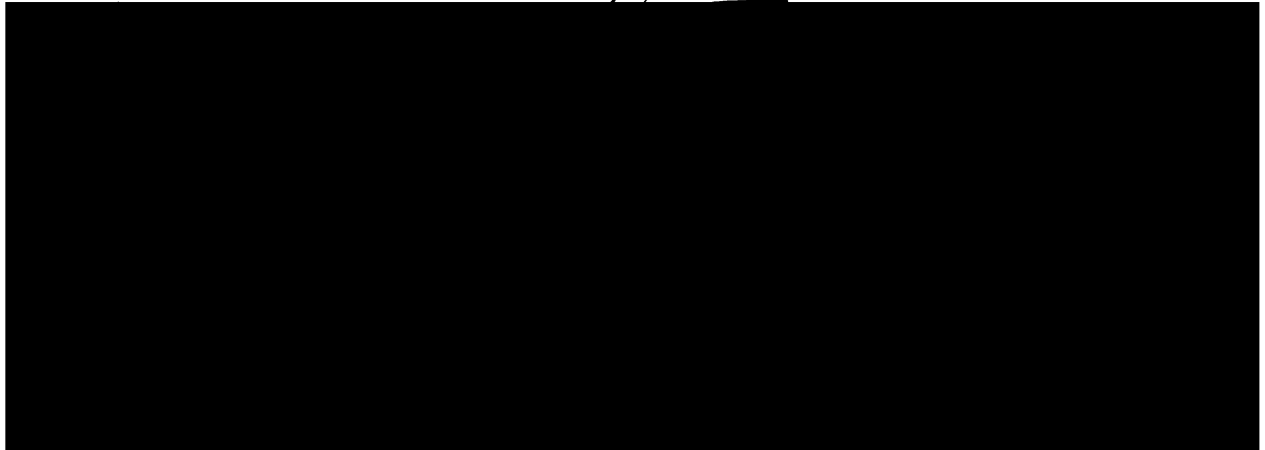
Biochemistry

in the

GRADUATE DIVISION

of the

UNIVERSITY OF CALIFORNIA SAN FRANCISCO



Date

University Librarian

Degree Conferred:

Copyright 1999
by
Jennifer A. Zallen

**this thesis is dedicated to my parents
and my brother Avi**

Jennifer Zallen
University of CA, San Francisco
513 Parnassus Avenue, Box 0452
San Francisco, CA 94143-0452
May 24, 1999

Cell
Cell Press
1050 Massachusetts Avenue
Cambridge, MA 02138

To whom it may concern:

I would like to request permission to include in my thesis dissertation a copy of the following paper:

Zallen, JA; Yi, BA; Bargmann, CI
The conserved immunoglobulin superfamily member SAX-3/Robo directs multiple aspects of axon guidance in *C. elegans*
Cell, 1998 Jan 23, 92(2): 217-227.

This dissertation will be microfilmed by University Microfilms Incorporated and they request permission to supply single copies upon demand. Since I must submit my thesis May 28, I would greatly appreciate it if you could respond within the next few days by fax to (415) 476-3493.

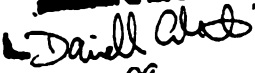
Thank you very much.

Sincerely,



Jennifer Zallen
Department of Anatomy
University of CA, San Francisco

Permission granted subject to citation of the original manuscript, and release that copyright is held by Cell Press. (See copyright by copyright on permission of the author.)



5-26-99

Date: Thu, 27 May 1999 09:32:48 -0700
From: "Corey S. Goodman" <goodman@uclink4.berkeley.edu>
To: "J. Zallen" <jzallen@itsa.ucsf.edu>
Subject: Re: copyright permission

Ms. Zallen -- we grant your request.
Corey Goodman
Associate Editor, Development

>Thursday, May 27, 1999

>

>Development

>

>To whom it may concern:

>>I would like to request permission to include in my thesis dissertation a
>copy of the following manuscript currently under review at Development
>(manuscript number 8610):

>

>Zallen JA; Kirch SA; Bargmann CI.

>Genes required for axon pathfinding and extension in the *C. elegans* nerve
>ring.

>

>The dissertation will be microfilmed by University Microfilms Incorporated
>and they request permission to supply single copies upon demand. Since I
>must submit my thesis June 1, I would greatly appreciate it if you could
>respond within in the next few days by fax to: (415) 476-3493. I have
>also sent a faxed copy of this request. Please contact me at
>(415) 476-3557 if you have questions.

>

>Thank you very much.

>

>Sincerely,

>

>Jennifer Zallen

>Department of Anatomy

>UC San Francisco

Prof. Corey S. Goodman
Howard Hughes Medical Institute
Department of Molecular and Cell Biology
519 LSA
University of California, Berkeley
Berkeley, CA 94720 USA

phone: 510 643-9949
office phone: 510 643-9948
lab phone: 510 642-9084

Acknowledgments

Many people deserve my gratitude for their immense contributions to my work and well-being during the course of this thesis. First and foremost, I would like to thank my parents and my brother Avi, as well as many members of my extended family, for their support and encouragement throughout graduate school and in the formative years leading up to this point.

My advisor Cori Bargmann has had a tremendous impact on my education. Cori has been incredibly supportive, and I have valued her input in all areas of science, from her ability to derive insightful conclusions from routine results and her perspective on fruitful long-term research directions to her rigor and precision in designing, interpreting, and presenting experiments. Cori's generosity with her ideas, energy and expertise has made graduate school both exciting and rewarding for me and I feel extremely lucky to have had her as my advisor. I would also like to thank the members of my thesis committee, Marc Tessier-Lavigne and Andrew Murray, for help with both focusing my research and communicating my work to the scientific community.

This thesis would not have been possible without the contributions of many people with whom I have collaborated scientifically. Alex Yi assisted in the cloning of *sax-3* described in Chapter 2. Sue Kirch conducted the analysis of the *sax* mutants at single-neuron resolution in Chapter 3. Erin Peckol and I worked together to explore the interactions between *sax-1*, *rhoA* and activity-dependent regulation of neuronal morphology in Chapter 4. David Tobin pioneered reverse genetics in the lab and enabled the isolation of a *sax-1* deletion mutant in Chapter 4. Joe Hao and Erik Lundquist identified *sax(ky112)* as an allele of *vab-3* and performed interesting and informative double mutant analyses. Tim Yu carried the *sax-3* project to the next level and provided many stimulating and thoughtful conversations. Joe Hao is studying the Slit ligand and his work has provided a deeper understanding of the SAX-3 receptor. Katja Brose, Tom

Kidd, Corey Goodman and Marc Tessier-Lavigne were generous with reagents, information and key experimental insights and provided real camaraderie as scientific collaborators studying the Robo receptor. I am also grateful to Shannon Grantner, May Zhang and LiQin Tong for speedy sequencing assistance on innumerable occasions.

I would like to thank the members of the Bargmann lab and past and present members of the 14th floor scientific community for making the lab an incredible place to work. Every single person has helped me out at some point with advice, reagents, or sitting through endless practice talks. In particular, Piali Sengupta provided guidance and support early on. Noelle Dwyer shared a bay with me for many years, and the people who know us will probably agree that we think as differently as two people possibly can. But Noelle has always helped me to see things in a new way, and I am grateful for her help with some major scientific decisions as well as many trivial ones.

Many good friends were truly essential parts of my life during graduate school. In particular, I would like to thank Katja, Mimi, Ann, Debbie, Lena, Sarah, Dave, Noelle, Natasha, Tali, Michele, Kerstin, Laura, Dylan, Zoë, Erin, Piali, David and Penny. I can't fully express my gratitude and affection for these people in this space, but I hope to be able to convey it in my words and actions in person. And finally I want to give my deepest thanks to Zemer, for bringing me a lot of happiness in the last two years.

Advisor statement

The work described in Chapters two, three and four of this thesis were conducted in collaboration with other members of the Bargmann lab, whose contributions are as described above. All other work was done by Jennifer Zallen.

A handwritten signature in black ink that reads "Cori Bergmann". The signature is written in a cursive, flowing style with a long horizontal tail at the end.

Regulation of Axon Outgrowth and Guidance in *C. elegans*

Jennifer A. Zallen

Abstract

Over half of the neurons in *C. elegans* project axons to the nerve ring, a major neuropil in the head of the animal. Screens for mutants with defects in the morphology of sensory neurons that contribute axons to the nerve ring identified eight new *sax* genes required for the establishment (*sax-3*, *sax-5* and *sax-9*) or maintenance (*sax-1*, *sax-2*, *sax-6*, *sax-7* and *sax-8*) of sensory neuron morphology. An examination of the functions of known guidance molecules in nerve ring development revealed that SAX-3/Robo acts in parallel to the VAB-1/Eph receptor and the UNC-6/netrin, UNC-40/DCC guidance systems for ventral guidance in the amphid commissure, a major route of axon entry into the nerve ring.

sax-3 encodes a transmembrane protein in the immunoglobulin superfamily that is required for the guidance of multiple nerve ring axons. SAX-3 is related to *Drosophila* Robo, and both proteins act to prevent aberrant axon crossing of the ventral midline. *sax-3* mutants exhibit axon defects throughout the *C. elegans* nervous system and *sax-3* function is required at the time of axon outgrowth, consistent with a direct role in axon guidance. SAX-3 acts cell autonomously to mediate ventral guidance of the AVM axon, suggesting that SAX-3 functions as a guidance receptor.

The *sax-1* gene is required for the maintenance of cell shape and polarity in *C. elegans* sensory neurons. *sax-1* encodes an Ndr serine/threonine kinase that belongs to a family of kinases whose members function in cell shape regulation in yeast and flies. Disruption of the *C. elegans* RHOA GTPase causes cell shape defects similar to those of *sax-1* mutants, and GTPase signaling influences neuronal cell shape in a pathway that acts

in parallel to SAX-1. SAX-1 also functions in parallel to sensory activity in the regulation of neurite outgrowth. Both SAX-1 and activity-dependent pathways can be modulated by the UNC-43 calcium/calmodulin-regulated kinase, suggesting that they converge on common targets in the regulation of neuronal morphology.

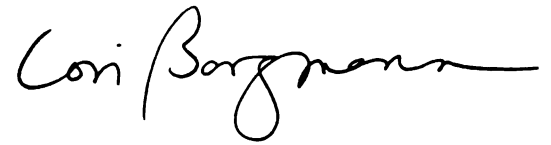
A handwritten signature in black ink that reads "Cori Bargmann". The signature is written in a cursive style with a long horizontal stroke at the end.

Table of Contents

Chapter One: Introduction	1
Chapter Two: Genes required for axon pathfinding and extension in the <i>C. elegans</i> nerve ring	27
Chapter Three: The conserved immunoglobulin superfamily member SAX-3/Robo directs multiple aspects of axon guidance in <i>C. elegans</i>	71
Chapter Four: Neuronal cell shape and neuritogenesis are regulated by the Ndr kinase SAX-1, a member of the Orb6/COT-1/Warts serine/threonine kinase family	83
Chapter Five: Future directions	121
Bibliography	132
Appendices	161

List of Tables

Chapter Two

Table 1-1. Genes required for normal amphid axon trajectories.	66
Table 2-1. Amphid axon defects in <i>sax</i> mutants.	67
Table 3-1. Axon defects in the ASI amphid neurons.	68
Table 4-1. Ventral guidance and midline crossover defects in <i>sax</i> mutants.	69
Table 5-1. CAN cell migration and axon outgrowth defects in <i>sax</i> mutants.	70

Chapter Three

Table 3-1. Axon defects in ventral cord interneurons in <i>sax-3</i> mutants.	74
Table 3-2. Axon defects in HSN motor neurons in <i>sax-3</i> mutants.	76

Chapter Four

Table 4-1. Some neuronal morphology defects in <i>sax-1</i> and <i>sax-2</i> mutants are temperature sensitive.	120
---	-----

Appendices

Appendix B. Amphid axon pathfinding and cell migration defects in <i>sax-3</i> mutants.	165
Appendix C. Axon outgrowth and cell migration defects in the ASI neuron produced by a high copy <i>sax-3(+)</i> transgene.	167
Appendix D. Map positions of <i>sax</i> mutants.	168
Appendix E. Mosaic analysis of <i>sax-3</i> .	169
Appendix F. Axon defects in amphid sensory neurons and HSN motor neurons in known mutants.	171
Appendix G. Candidate cosmids injected into <i>sax-2</i> and <i>vab-13</i> mutants.	172

List of Figures

Chapter Two

- Figure 2-1. Amphid axon trajectories in wild-type and *sax* mutant animals. 53
- Figure 2-2. ASI axon trajectories in wild-type and *sax* mutant animals. 56
- Figure 2-3. HSN and interneuron axon trajectories in wild-type and *sax* mutant animals. 58
- Figure 2-4. CAN neuron positions in wild-type and *sax* mutant animals. 60
- Figure 2-5. Amphid ventral guidance defects in *sax-3*, *vab-1*, *unc-6* and *unc-40* single and double mutants. 62
- Figure 2-6. The AVM ventral guidance defect of *sax-3* mutants is rescued cell-autonomously. 64

Chapter Three

- Figure 3-1. Disrupted guidance of interneuron axons to and within the ventral nerve cord of *sax-3* mutants. 73
- Figure 3-2. Disrupted guidance of HSN motor neuron axons to and within the ventral nerve cord of *sax-3* mutants. 75
- Figure 3-3. Molecular analysis of *sax-3*. 77
- Figure 3-4. Expression of *sax-3::GFP*. 78
- Figure 3-5. *sax-3* activity is required at different times for different axon guidance events. 79

Chapter 4

- Figure 4-1. Morphological defects in amphid sensory neurons of *sax-1* and *sax-2* mutants. 108

Figure 4-2. <i>sax-1</i> and <i>sax-2</i> morphological defects appear late in development and do not lead to severe behavioral defects.	110
Figure 4-3. <i>sax-1</i> encodes a serine/threonine kinase.	112
Figure 4-4. SAX-1::GFP expression and site of action.	114
Figure 4-5. ASJ ectopic neurite defects in <i>sax-1</i> , <i>tax-4</i> , <i>unc-43</i> and <i>sax-2</i> single and double mutants.	116
Figure 4-6. Regulation of ASER amphid neuron morphology by expression of <i>rhoA</i> alleles in wild-type and mutant backgrounds.	118

Appendices

Appendix A. Double mutant analysis between genes involved in axon guidance.	163
---	-----

Chapter One

Introduction

Overview

A fundamental advance in the evolution of living organisms is the emergence of the nervous system, a cellular network that allows an animal to perceive, interpret and respond to its surroundings. Precise and elaborate neural circuits communicate information from sensory neurons that receive input from the environment to interneurons that integrate this information and motor neurons that execute an appropriate behavioral response. During development, neuronal cells project axons that navigate along stereotyped trajectories to contact their targets. Evidence from many systems indicates that axons are actively guided along their trajectories (Tessier-Lavigne and Goodman, 1996; Mueller, 1999). Subsequent to initial axon guidance, distinct mechanisms govern the maintenance of neuronal morphology, often relying on properties of neuronal function (Goodman and Shatz, 1993).

Several of the extracellular signals that provide guidance information to growing axons are present in both invertebrates and vertebrates, demonstrating that analysis of simple model systems can provide insight into conserved developmental mechanisms. This thesis describes a genetic approach to understanding the establishment and maintenance of neuronal morphology in the nematode *C. elegans*. The simple *C. elegans* nervous system contains 302 neurons whose positions, axonal trajectories and synaptic connections are well characterized (White *et al.*, 1976; White *et al.*, 1986). A primary function of the *C. elegans* nervous system is to locate food sources and avoid unfavorable conditions created by overcrowding, food scarcity, noxious substances and nonoptimal temperatures. The largest nematode sensory organ is the amphid, composed of 12 bilaterally symmetric amphid neuron pairs that detect chemicals, touch and temperature (Ward *et al.*, 1975; Ware *et al.*, 1975). Amphid sensory neurons contain a ciliated dendrite that is exposed to the environment through an opening in the anterior cuticle (Perkins *et al.*, 1986). Each amphid neuron projects a single axon that travels

circumferentially in the nerve ring, the largest axon bundle in the animal. Within the nerve ring, amphid sensory axons contact sensory and interneuron targets (White *et al.*, 1986), establishing neural circuits essential to sensation and behavior.

The navigation of sensory axons in the nerve ring is largely completed by the end of embryogenesis. However, nerve ring axons continue to grow as the animal grows in size during postembryonic development. In the larval and adult stages, nerve ring axons increase 2.5-fold in length, while retaining the spatial organization established during embryogenesis. These axon growth and maintenance processes may have requirements that are distinct from initial axon development. For some amphid sensory neurons, maintenance of appropriate axon morphology is regulated by neuronal electrical activity (Coburn and Bargmann, 1996; Coburn *et al.*, 1998; Peckol *et al.*, 1999).

This thesis describes a genetic approach in *C. elegans* to identify and characterize molecules involved in the establishment of the nerve ring and in the subsequent maintenance of sensory morphology throughout larval and adult development. Chapter 1 presents an introduction describing the identified molecular mechanisms that regulate axon guidance (part I) and cell shape (part II). Part I describes several well-characterized guidance cues and their neuronal receptors, with a focus on the guidance pathways that are examined in the *C. elegans* nerve ring and ventral midline in Chapters 2 and 3. Part II describes pathways implicated in regulation of cell shape and polarity, with particular attention to GTPase and kinase signaling pathways examined in Chapter 4. Chapter 2 describes screens for mutants with sensory axon defects (*sax* mutants) and the characterization of eight new *sax* genes that are required for the establishment (*sax-3*, *sax-5* and *sax-9*) or maintenance (*sax-1*, *sax-2*, *sax-6*, *sax-7* and *sax-8*) of amphid neuron morphology. The functions of known axon guidance pathways are examined in the nerve ring, and genetic interactions between components of different pathways reveal how different guidance systems function together to create unique axon trajectories. Chapter 3 presents the cloning and characterization of SAX-3/Robo, a transmembrane protein in the

immunoglobulin superfamily that prevents aberrant axon crossing of the ventral midline in *C. elegans* and *Drosophila*. *sax-3* is required for multiple axon guidance events in *C. elegans* and functions at the time of axon outgrowth, consistent with a direct role in a guidance interaction. Chapter 4 presents the cloning and characterization of SAX-1, a serine/threonine kinase related to *Drosophila* and human Ndr kinases. *sax-1* is required for the maintenance of amphid cell shape and polarity in *C. elegans* and functions in parallel to sensory activity in the regulation of neuronal morphology. The RHOA GTPase is shown to influence neuronal morphology in a similar manner, and the intersection between signaling pathways mediated by the SAX-1 kinase and the RHOA GTPase is examined. Chapter 5 presents a perspective on short-term and long-term experimental directions suggested by this work. Results from preliminary experiments that others may wish to extend are described in the Appendices.

Part I. Regulation of axon guidance

Growing axons often navigate long distances and through diverse environments to contact their targets, responding to attractive or repellent guidance information from local or distant sources. Four classes of guidance cues have been identified and extensively characterized — netrins, ephrins, semaphorins and slits — all of which display both attractive and repulsive properties (Mueller, 1999; Zinn and Sun, 1999). Receptor proteins that mediate responses to these guidance cues have also been identified (Mueller, 1999). The characterization of these ligand-receptor interactions has provided insight into the initial steps of axon guidance, where a directional map of guidance information is established in the environment and detected by proteins that initiate a response in the growing axon. This section of the introduction provides a description of several well-characterized classes of guidance molecules, their corresponding receptors, and the regulation of these guidance systems in different contexts to achieve diverse axonal responses. The functions of several components of these guidance pathways are examined in the *C. elegans* nerve ring in Chapters 2 and 3.

Netrins

The netrin family of secreted axon guidance molecules was first identified in the nematode *C. elegans*, where the *unc-6* laminin-related gene is required for the guidance of axons along the dorsoventral axis (Hedgecock *et al.*, 1990; Ishii *et al.*, 1992). Vertebrate UNC-6 homologs, netrin-1 and netrin-2, were independently purified based on their ability to promote outgrowth of spinal cord commissural axons (Serafini *et al.*, 1994) and were shown to actively function as chemoattractants (Kennedy *et al.*, 1994; de la Torre *et al.*, 1997).

Netrins can act as long-range diffusible guidance cues. Netrin is expressed at the ventral midline in vertebrates and invertebrates (Kennedy *et al.*, 1994; Harris *et al.*, 1996; Mitchell *et al.*, 1996; Wadsworth *et al.*, 1996) and netrin function is required to guide axons ventrally to the ventral midline *in vivo* (Hedgecock *et al.*, 1990; Ishii *et al.*, 1992; Harris *et al.*, 1996; Mitchell *et al.*, 1996; Serafini *et al.*, 1996). In vertebrates, specialized floor plate cells at the ventral midline of the vertebrate spinal cord function as an intermediate target in the guidance of spinal cord axons (reviewed in Colamarino and Tessier-Lavigne, 1995b). Recombinant netrin has been shown to be sufficient for some floor plate guidance activities (Kennedy *et al.*, 1994; Serafini *et al.*, 1994; Colamarino and Tessier-Lavigne, 1995a; Shirasaki *et al.*, 1995; Shirasaki *et al.*, 1996; Varela-Echavarría *et al.*, 1997). However, floor plate cells from *netrin-1* mutant mice retain some guidance functions, indicating that these guidance events can be mediated by other floor plate components (Serafini *et al.*, 1996).

Netrins can also act as local guidance cues. In worms, flies and mice, mutants defective in netrin function exhibit defects in axon crossing of the ventral midline, suggesting that netrins are required locally to promote midline crossing (Harris *et al.*, 1996; Mitchell *et al.*, 1996; Serafini *et al.*, 1996; Wadsworth *et al.*, 1996). Similarly, netrin may also function locally to guide retinal axons into the optic nerve; netrin expression is observed at the optic nerve head, and axons accumulate at the retinal exit point in netrin mutant mice (de la Torre *et al.*, 1997; Deiner *et al.*, 1997).

Netrins attract some axons and repel others. In some cases, different netrin receptors are used for attraction and repulsion. Attraction to netrins is mediated by UNC-40/DCC, a member of the immunoglobulin superfamily that is thought to act directly as a netrin receptor on growing axons (Hedgecock *et al.*, 1990; Chan *et al.*, 1996; Keino-Masu *et al.*, 1996; Kolodziej *et al.*, 1996; de la Torre *et al.*, 1997; Deiner *et al.*, 1997; Fazeli *et al.*, 1997; Ming *et al.*, 1997). Repulsion from netrins is mediated by UNC-5, a transmembrane receptor that acts in combination with UNC-40/DCC (Hedgecock *et al.*,

1990; Leung-Hagesteijn *et al.*, 1992; Hamelin *et al.*, 1993; Ackerman *et al.*, 1997; Leonardo *et al.*, 1997; Colavita and Culotti, 1998). Expression of UNC-5 on an axon can be sufficient to convert its response from attraction to repulsion, and both responses require UNC-40 function (Hamelin *et al.*, 1993; Colavita and Culotti, 1998).

In addition to different netrin receptors, some aspects of neuronal signaling can also influence netrin response. For example, vertebrate axons attracted to the source of netrin expression at the ventral midline lose netrin responsiveness after crossing the midline, despite the fact that these axons still express DCC (Shirasaki *et al.*, 1998). Cultured *Xenopus* spinal cord neurons exposed to a netrin point source can rapidly switch from attraction to repulsion in the presence of inhibitors of the cAMP-dependent protein kinase A (Ming *et al.*, 1997). These results suggest that second messenger signaling within a neuron can influence the axonal response.

Semaphorins

Semaphorin guidance cues have been implicated primarily in repulsion of migrating axons, though they may have attractive properties as well (Kolodkin, 1996; Kolodkin and Ginty, 1997). At least 30 semaphorins have been identified in a ligand family that is conserved from worms to humans (Kolodkin *et al.*, 1993). Semaphorins can be transmembrane, GPI-linked or secreted. All share a 500 amino acid sema domain and are divided into seven classes based on sequence similarity. Semaphorins can induce growth cone collapse in sensory neurons (Luo *et al.*, 1993) and are capable of repelling axon growth *in vitro* (Fan and Raper, 1995; Messersmith *et al.*, 1995; Puschel *et al.*, 1995; Puschel, 1996; Adams *et al.*, 1997; Varela-Echavarria *et al.*, 1997). Semaphorins are also required for axon guidance *in vivo*; mice defective in the secreted Sema 3A ligand (Sema III/Sema D/Collapsin I) exhibit axon defasciculation and excessive axon growth in peripheral nerves (Behar *et al.*, 1996; Taniguchi *et al.*, 1997). Similarly, disruption of the

transmembrane Sema 1a ligand leads to defects in motor axon guidance in *Drosophila* (Yu *et al.*, 1998).

Semaphorins are recognized by plexin or neuropilin receptors *in vitro* (Chen *et al.*, 1997; He and Tessier-Lavigne, 1997; Kolodkin *et al.*, 1997; Winberg *et al.*, 1998). Neuropilin receptors are neuronally expressed (Takagi *et al.*, 1991; Fujisawa *et al.*, 1995; Takagi *et al.*, 1995; Kawakami *et al.*, 1996) and bind to type 3 semaphorins (He and Tessier-Lavigne, 1997; Kolodkin *et al.*, 1997). Antibodies to neuropilin 1 prevent axon collapse and repulsion by semaphorin 3A (He and Tessier-Lavigne, 1997; Kolodkin *et al.*, 1997). Semaphorin 3A and neuropilin 1 are likely to interact *in vivo*, since the mouse neuropilin mutant exhibits axon defects similar to those in Sema 3A mutant mice, and sensory neurons lacking neuropilin are resistant to the collapse-inducing effect of Sema 3A (Kitsukawa *et al.*, 1997). The transmembrane protein plexin also functions as a semaphorin receptor. Plexins are neuronally-expressed proteins that have a sema domain (Takagi *et al.*, 1995; Maestrini *et al.*, 1996) that can function as cell adhesion molecules (Ohta *et al.*, 1995). A member of the plexin family was purified biochemically as a semaphorin binding protein (Comeau *et al.*, 1998) and *Drosophila* Plexin A binds to the transmembrane ligands Sema 1a and Sema 1b (Winberg *et al.*, 1998). Furthermore, *plexin A* mutant flies exhibit axon defects similar to those seen in *sema 1a* mutants, and genetic interactions between these genes suggest that they may function in a common pathway (Winberg *et al.*, 1998).

As with the netrins, semaphorin ligands can repel some axons and attract others. Sema 3C has been shown to attract cortical axons (Bagnard *et al.*, 1998) and repel sensory and sympathetic axons (Adams *et al.*, 1997). Sema 3A can inhibit cortical axon branching (Bagnard *et al.*, 1998). Moreover, Sema 3B and 3C can act as competitive antagonists of Sema 3A-mediated repulsion in neurons that express the neuropilin 1 receptor, but they act as repulsive factors to neurons that express neuropilin 2 (Takahashi *et al.*, 1998). The mechanisms by which semaphorins exert these diverse effects may reflect differences in

receptor expression or ligand presentation (Chalfie and Thomson, 1979; Chen *et al.*, 1997; Chedotal *et al.*, 1998; Chen *et al.*, 1998).

Ephrins

Ephrin ligands, in either GPI-linked (ephrin A) or transmembrane (ephrin B) forms, associate with Eph receptor tyrosine kinases in guidance pathways that function primarily in axon repulsion (Flanagan and Vanderhaeghen, 1998), although there is also evidence that ephrins can function in attraction (Castellani *et al.*, 1998). Mouse knockouts of the EphB2, EphB3 and EphA8 receptors all cause defects in axonal trajectories (Henkemeyer *et al.*, 1996; Orioli *et al.*, 1996; Park *et al.*, 1997). The anterior-posterior axis of the topographic map formed by retinal axons at their tectal target is mediated in part by gradients of Eph receptors expressed on vertebrate retinal axons that detect complementary gradients of ephrin-A2 and ephrin-A5 ligands in the optic tectum (Cheng *et al.*, 1995; Drescher *et al.*, 1995). Retinal axons avoid substrates containing ephrin-A2 and ephrin-A5 *in vitro* and they avoid ephrin-A2-expressing tectal cells *in vivo*, consistent with a role as a repellent (Drescher *et al.*, 1995; Nakamoto *et al.*, 1996; Monschau *et al.*, 1997). Ephrin expression in the optic tectum is highest in the posterior regions and may define the posterior limit of axon innervation by selectively repelling axons with higher Eph receptor expression levels. Consistent with this possibility, ephrin-A2 and ephrin-A5 are more repulsive to the temporal axons (high Eph receptor) that project to the anterior tectum than to the nasal axons (low Eph receptor) that project to more posterior regions (Nakamoto *et al.*, 1996; Monschau *et al.*, 1997). Ephrin-A5-containing substrates also inhibit axon branching (Roskies and O'Leary, 1994) and promote axon fasciculation (Winslow *et al.*, 1995), which may reflect different geometries of presentation of a repulsive ligand. Ephrins can function as bifunctional guidance cues; ephrin-A5 promotes axon outgrowth and sprouting of specific subsets of cortical neurons, but inhibits axon outgrowth in other

cortical neuron types (Castellani *et al.*, 1998). These results suggest that ephrins, like netrins and semaphorins, can elicit diverse neuronal responses.

Ephrins act as ligands in the retinotectal system, but in other regions of the brain Eph receptors signal to ephrin-expressing cells. Axons of the anterior commissure express ephrin-B and grow on substrate cells that express the EphB2 receptor. Guidance of anterior commissure axons requires EphB2 but not the Eph receptor cytoplasmic domain, suggesting that EphB2 acts as a ligand (Henkemeyer *et al.*, 1996). The cytoplasmic domain of ephrin-B ligands is tyrosine phosphorylated upon association with the EphB2 receptor, suggesting that ephrins may signal to the cells that express them (Bruckner *et al.*, 1997; Holland *et al.*, 1997). These results indicate that guidance molecules may achieve an additional level of versatility by functioning as either ligands or receptors.

The *C. elegans vab-1* Eph receptor homolog is required in neurons for interactions among neuroblasts during gastrulation as well as for the cell migrations of overlying epidermal cells (George *et al.*, 1998). From these results, VAB-1 could function as a ligand or a receptor in neuron-neuron interactions, or as a ligand in neuron-epidermis interactions. Complete loss of *vab-1* function causes more severe defects than mutations in the kinase domain alone. These results raise the possibility that VAB-1 could function both as a receptor, in a pathway requiring the activity of its cytoplasmic kinase domain, and as a ligand, in a pathway that may require the extracellular domain.

Slits

The conserved Roundabout (Robo) family of immunoglobulin superfamily members regulates axon guidance at the ventral midline in *Drosophila* and *C. elegans* (Kidd *et al.*, 1998a; Zallen *et al.*, 1998/Chapter 3). Axons approaching the midline make divergent guidance decisions: some axons cross the midline while other axons do not cross the midline and remain on the ipsilateral side. Midline crossing is tightly regulated;

axons that cross the midline once often remain closely associated with it without crossing again, while other axons near the midline never cross at all. Genetic screens in *Drosophila* (Seeger *et al.*, 1993) and *C. elegans* (Chapter 2) have identified genes required for the proper regulation of midline crossing. In mutants defective in the *Drosophila* Robo receptor or the related *C. elegans* SAX-3 protein, axons cross the midline inappropriately (Kidd *et al.*, 1998a; Zallen *et al.*, 1998/Chapter 3). *sax-3* mutants also exhibit defects in the ventral guidance of axons to the midline, suggesting that Robo family members may be involved in additional guidance decisions. Cell-specific expression studies indicate that SAX-3/Robo can function cell autonomously in midline guidance (Kidd *et al.*, 1998a) and in ventral guidance (Zallen *et al.*, submitted/Chapter 2), consistent with a role as a receptor. The Robo receptor could function to prevent aberrant midline crossing by sensing a repellent guidance cue expressed at the midline; alternatively, Robo could detect an attractive guidance cue expressed by longitudinal axons.

The Slit family of secreted proteins are candidate Robo ligands in *Drosophila* and vertebrates (Brose *et al.*, 1999; Kidd *et al.*, 1999; Li *et al.*, 1999; Wang *et al.*, 1999). Slit proteins are large extracellular matrix molecules with leucine rich and EGF repeats that are conserved from *C. elegans* to humans (Itoh *et al.*, 1998; Nakayama *et al.*, 1998; Brose *et al.*, 1999; Li *et al.*, 1999 J. Hao, J. A. Z. and C. Bargmann, unpublished results). Slit proteins have been shown to interact biochemically and genetically with the Robo receptor. The human Slit2 protein associates with cells expressing vertebrate Robo1 or Robo2 receptors; conversely, the soluble Robo1 extracellular domain binds to cells expressing Slit1 or Slit2 protein (Brose *et al.*, 1999). Similar association occurs between the *Drosophila* Slit protein and *Drosophila* Robo, indicating that this binding interaction is conserved (Brose *et al.*, 1999).

Different isoforms of the Slit ligand may perform distinct physiological functions. Slit1 and Slit2 are proteolytically processed into a larger N-terminal fragment (Slit2-N, 140 kD) and a smaller C-terminal fragment (Slit2-C, 55-60 kD), both in cultured cells and

in vivo (Brose *et al.*, 1999; Wang *et al.*, 1999). Full length Slit2 and Slit2-N are tightly associated with membranes, while Slit2-C is more diffusible, raising the possibility that these fragments behave differently *in vivo* (Brose *et al.*, 1999). Interestingly, the Slit2-N fragment associates with the Robo receptor, while Slit2-C does not (K. Brose and M. Tessier-Lavigne, personal communication).

Slit proteins repel growing motor and sensory axons in culture, consistent with a role in a repulsive guidance mechanism (Brose *et al.*, 1999; Li *et al.*, 1999; Nguyen Ba-Charvet *et al.*, 1999). In particular, the Robo-binding N-terminal fragment of Slit2 is sufficient to repel spinal cord motor neurons (K. Brose and M. Tessier-Lavigne, personal communication). However, Slit2-N also promotes axon outgrowth and branching of DRG sensory neurons (Wang *et al.*, 1999), demonstrating that Slit can operate as a positive factor for some axons. The mechanisms by which Slit exerts positive or negative effects on axon growth are not clear, but one possibility is that these differences may reflect differential protein expression: DRG sensory neurons express Robo2 (Wang *et al.*, 1999), while motor neurons express both Robo1 and Robo2 (Brose *et al.*, 1999). It is not clear which Robo receptor is expressed by olfactory neurons, which are repelled by Slit (Brose *et al.*, 1999; Li *et al.*, 1999; Nguyen Ba-Charvet *et al.*, 1999). Alternatively, some Slit-induced axon guidance events may be mediated by non-Robo receptors.

Drosophila Slit protein is expressed by midline glial cells but is not required for their differentiation (Rothberg *et al.*, 1988; Rothberg *et al.*, 1990; Sonnenfeld and Jacobs, 1994). Since Slit is expressed in a region that Robo-expressing axons avoid, Slit may function as a repellent ligand detected by the Robo receptor. Consistent with this possibility, weak *slit* mutants exhibit midline crossover defects reminiscent of those observed in *robo* mutants (Kidd *et al.*, 1999). *robo* and *slit* exhibit dosage-sensitive genetic interactions that are suggestive of a common function (Kidd *et al.*, 1999). However, strong *slit* alleles cause complete collapse of longitudinal axon tracts at the ventral midline (Rothberg *et al.*, 1990), a phenotype distinct from that of *robo* mutants.

Furthermore, Slit misexpression on muscle cells causes axon guidance defects that do not require the Robo receptor, indicating that some aspects of Slit function are Robo-independent (Kidd *et al.*, 1999). Therefore, further analysis of Slit and its receptors, perhaps including *Drosophila* Robo2 (Kidd *et al.*, 1999), will be required to understand the relation between the *in vivo* guidance pathways mediated by Slit and Robo. In support of a Slit-Robo interaction *in vivo*, Slit misexpression in *C. elegans* causes repulsion of ventrally-directed axons in a SAX-3-dependent manner (J. Hao, M. Tessier-Lavigne and C. Bargmann, personal communication). However, the role of the Slit ligand in regulating axon crossover at the *C. elegans* midline remains to be determined.

Drosophila Robo is regulated by Commissureless (Comm), a novel transmembrane protein expressed by midline glia (Tear *et al.*, 1996). Comm functions to downregulate Robo expression in axon segments spanning the midline (Kidd *et al.*, 1998b), suggesting a mechanism by which Robo-mediated midline avoidance is transiently suppressed in axons that cross the midline. In *comm* mutants, no axons cross the midline, but axon crossing is restored by additional removal of the *robo* gene (Seeger *et al.*, 1993). These results suggest that the defects caused by Comm loss of function are due to Robo overexpression. Therefore, axon guidance mechanisms can be refined through regulation of the subcellular localization of guidance receptors. No Comm homologs have been identified in the *C. elegans* genome, although a divergent protein may perform similar regulatory functions.

Conclusion

The identification of guidance cues and their receptors provides a strong foundation for the study of many outstanding questions in the field of axon guidance. The mechanisms by which a single guidance cue can influence axon behavior in several ways are not fully understood, but may reflect differences in ligand presentation, growth cone receptor expression and localization, and distinct mechanisms of signaling to second

messengers and the cytoskeleton. The identification of catalytic and protein-binding motifs in the cytoplasmic domain of guidance receptors provides a starting point for the analysis of downstream signaling pathways. The elucidation of these pathways should reveal how ligand-receptor interactions ultimately communicate to the cytoskeleton to regulate the dynamic morphogenetic processes that contribute to axon growth and guidance.

Part II. Regulation of cell shape and polarity

Cells perform diverse functions through specialized features of cell shape and polarity. Cell shape and polarity are created through the precise spatial and temporal regulation of actin, tubulin and intermediate filaments that make up the cellular cytoskeleton. Different cytoskeletal structures direct morphological transitions during development. For example, neuronal precursor cells form a mitotic spindle to govern the cell divisions that produce neurons, neurons carry out actin-based motility to migrate from their site of birth to their final locations, and postmigratory cells differentiate structurally distinct axonal and dendritic projections to create the precise circuitry essential to nervous system function. Subsequent to these initial developmental processes, mechanisms operate to maintain or refine cell shape during the final stages of neuronal maturation. In particular, regulation of the actin cytoskeleton has been implicated in several morphogenetic processes, including cell shape, division, motility and intracellular trafficking (Devreotes and Zigmond, 1988; Bretscher, 1991; Hall, 1994; Symons, 1996).

Rho GTPases influence cell morphology

Fibroblasts contain actin subpopulations that form three types of structures: the cortical actin network, actin stress fibers and cell surface projections. Fibroblasts in culture can redistribute these actin populations in response to extracellular signals. For example, quiescent Swiss 3T3 fibroblasts rapidly form actin stress fibers and focal adhesion complexes in response to serum or lysophosphatidic acid (LPA) (Ridley and Hall, 1992), membrane ruffles or lamellipodia when exposed to the growth factors PDGF or EGF (Ridley and Hall, 1992), and filopodia when exposed to bradykinin (Kozma *et al.*, 1995; Nobes and Hall, 1995). These distinct morphological changes can be reproduced by activation of specific GTPases in the Rho family, while treatments that inactivate Rho GTPases selectively block the formation of certain structures, suggesting

that GTPases are downstream of the signals that lead to cytoskeletal reorganization (Hall, 1994).

Rho GTPases belong to the Ras superfamily of small GTP-binding proteins, which function in a number of cell biological processes, including cell proliferation and differentiation, intracellular vesicle transport), nuclear protein import and cytoskeletal regulation (Hall, 1994). The Rho subfamily includes the Rho, Rac and Cdc42 GTPase subtypes that are involved in cytoskeletal regulation, as well as transcriptional activation, endocytosis and cell cycle progression. This section will focus on the Rho GTPase and its role in regulating stable cytoskeletal structures that contribute to cell shape.

The cycling of Rho proteins between the active (GTP-bound) and inactive (GDP-bound) states is regulated by several cofactors. Rho GTPases are activated by guanine nucleotide exchange proteins (GEFs), which stabilize the nucleotide-free state of Rho, increasing the rate of nucleotide exchange and thereby enhancing levels of GTP-bound Rho (Quilliam *et al.*, 1995). In an opposing pathway, specific GTPase activating proteins (GAPs) increase the rate of GTP hydrolysis and reduce the levels of active, GTP-bound Rho (Boguski and McCormick, 1993; Lamarche and Hall, 1994). Rho- and Rac-type GTPases are also sequestered in an inactive form by Rho guanine nucleotide dissociation inhibitors (Rho-GDIs), which inhibit GDP dissociation and maintain the GTPase in a GDP-bound form (Hall, 1994).

An understanding of the Rho GTPase cycle has provided useful tools for the experimental manipulation of Rho function. Gain of function Rho proteins can be created through mutations that reduce GTPase activity and sensitivity to GAPs (glycine to valine at residue 14 in Rho and Rac or residue 12 in Ras and Cdc42; glutamine to leucine at residue 63 in Rho or residue 61 in Ras, Rac and Cdc42), producing proteins that are constitutively bound to GTP (Der *et al.*, 1986a; Feig and Cooper, 1988; Garrett *et al.*, 1989; Bourne *et al.*, 1991) Mutations that decrease GTP affinity (threonine to asparagine at residue 17 in Ras or residue 19 in Rho, Rac and Cdc42) can act as dominant negative alleles by

associating with GEF proteins in nonproductive complexes with nucleotide-free Rho, reducing their ability to activate wild-type Rho (Der *et al.*, 1986b; Quilliam *et al.*, 1995).

The Rho subtype of the Rho GTPase family has been implicated in the formation of actin stress fibers and focal adhesion complexes. In quiescent Swiss 3T3 fibroblasts, exposure to the growth factor LPA or microinjection of activated RhoA^{V14} leads to stress fiber and focal adhesion formation within minutes, while Rho inhibition prevents induction of stress fibers and focal adhesions by LPA, demonstrating that Rho is a downstream component of LPA in cytoskeletal regulation (Paterson *et al.*, 1990; Ridley and Hall, 1992). In REF52 fibroblasts, which normally contain stress fibers and focal adhesions, Rho inhibition leads to a disruption of both of these structures (Chihara *et al.*, 1997). These results are consistent with an active requirement for Rho in both the establishment and maintenance of stress fibers and focal adhesions.

Stress fibers consist of long bundles of antiparallel actin and myosin filaments anchored to the extracellular matrix through focal adhesion complexes at the plasma membrane (Yamada and Geiger, 1997). Focal adhesions represent a large complex of proteins, including structural (talin, vinculin, α -actinin and actin) and regulatory (protein kinase C, p60^{v-src} and p125^{FAK}) components; additional focal adhesion proteins, such as paxillin, tensin and zyxin, may also have some regulatory functions (Turner and Burridge, 1991). The formation of stress fiber and focal adhesion structures in response to Rho GTPase signaling suggest a role for Rho in regulating stable properties of cell shape.

By contrast, the Rac and Cdc42 GTPases are involved in the generation of dynamic actin structures that underlie cell motility. An activated Rac1^{V12} mutant leads to membrane ruffling, while the dominant negative Rac1^{V12N17} mutant blocks ruffling induced by PDGF, indicating that Rac1 is necessary and sufficient for ruffling (Ridley *et al.*, 1992). Disruption of Rho function does not interfere with membrane ruffling; however, stress fibers that emerge after a delay following PDGF or Rac1 activation are dependent on Rho function (Ridley *et al.*, 1992). Activated Cdc42^{V12} causes the rapid

induction of filopodia, while the dominant negative Cdc42^{N17} mutant blocks filopodia induced by bradykinin, indicating that Cdc42 is necessary and sufficient for filopodia formation (Kozma *et al.*, 1995; Nobes and Hall, 1995). Membrane ruffles and stress fibers also appear as a delayed response to activated Cdc42^{V12} and this response requires Rac1 function. These results suggest a model where the Cdc42 GTPase leads to sequential activation of Rac and then Rho in a signaling cascade.

Rho GTPase function *in vivo*

Insight into the regulation of cell shape and polarity by GTPases has come from studies of bud site selection in *S. cerevisiae*, where cellular materials for the emerging daughter cell are selectively transported to one part of the mother cell in a pattern regulated by genotype (Chant and Herskowitz, 1991). Three GTPase cycles are required for different morphogenetic changes that occur during budding. Mutations in the Ras-type Bud1 GTPase, its inhibitory GAP (Bud2) or its activating GEF (Bud5) disrupt bud pattern and cause yeast cells to bud in random locations (Bender and Pringle, 1989; Chant *et al.*, 1991; Chant and Herskowitz, 1991; Park *et al.*, 1993). By contrast, disruption of the Rho-type Cdc42 GTPase, its activating GEF (Cdc24) or its inhibitory GAP (Bem3) prevents bud assembly, causing yeast cells to grow uniformly without budding (Hartwell, 1973; Adams *et al.*, 1990; Johnson and Pringle, 1990). In a third process, disruption of the Rho1 GTPase, its two activating GEFs Rom1 and Rom2, or the two Rho-related GTPases Rho3 and Rho4 causes cells to arrest with small buds, indicating that bud site selection and bud initiation occur normally, but bud growth is defective (Matsui and Toh-E, 1992; Yamochi *et al.*, 1994; Ozaki *et al.*, 1996). Furthermore, growth-arrested diploid cells lacking Rho3 and Rho4 exhibit delocalized chitin and actin patches, suggesting an additional defect in cell polarity (Matsui and Toh-E, 1992). Interestingly, genetic interactions between components of these GTPase cycles indicate a mechanism for the regulation of genes required for bud formation by genes required for bud pattern.

Cells of the fission yeast *S. pombe* have a rod-shaped morphology that continues to elongate during cell growth, with localized actin structures at its growing ends. At least two GTPase cycles are required to establish and maintain this morphology, and in their absence cells become spherical. These include *ras1* (Fukui *et al.*, 1986) and *cdc42sp* (Fawell *et al.*, 1992; Miller and Johnson, 1994). As in *S. cerevisiae*, oriented cell growth prior to cell division in *S. pombe* is regulated by hierarchical regulation of GTPase cycles (Chang *et al.*, 1994).

In *Drosophila*, disruption of RhoA function causes a number of phenotypes that may reflect defects in cell proliferation or viability, as well as disruption of tissue polarity in the eye and epithelial cell shape changes during gastrulation (Barrett *et al.*, 1997; Strutt *et al.*, 1997). Rac is also required for epithelial morphogenesis, as well as for the proper formation of cell-cell junctions (Eaton *et al.*, 1995; Harden *et al.*, 1995). By contrast, Cdc42 is required for epithelial cell elongation (Eaton *et al.*, 1995). The different phenotypes caused by perturbation of different GTPases are reminiscent of the requirements for multiple GTPase cycles in regulation of distinct properties of cell shape in *S. cerevisiae*. These early developmental defects caused by loss of RhoA function may obscure later roles for RhoA in other processes, such as neuronal development. Neuron-specific expression of dominant negative GTPase mutants has revealed a role for Rac and Cdc42 in axon extension, while Cdc42 is also required for dendrite extension (Luo *et al.*, 1994).

The *C. elegans* MIG-2 GTPase, which is equally related to Cdc42 and Rac, is required for specific cell migrations, while gain of function *mig-2* mutations disrupt axon pathfinding (Zipkin *et al.*, 1997). These results suggest that altered MIG-2 activity may interfere with other GTPase pathways that function in axon guidance. Mutations in the Rac-specific UNC-73 GEF also disrupt axon pathfinding, implicating Rac GTPase in this process (Steven *et al.*, 1998). A single *C. elegans* Rho GTPase has been identified (Chen

and Lim, 1994), but its function is not known. Further analysis of the role of *C. elegans* RHOA in the regulation of neuronal morphology is presented in Chapter 4.

Signaling downstream of Rho GTPase: Rho kinase and Protein kinase C

Since the GTP-bound form of Rho GTPase is active, proteins that specifically bind to Rho-GTP have been implicated as candidate effectors. Serine/threonine kinases in the Rho kinase family were isolated based on their association with GTP-bound RhoA (Leung *et al.*, 1995; Ishizaki *et al.*, 1996; Matsui *et al.*, 1996). The Rho kinase family includes additional Rho kinase relatives (Leung *et al.*, 1996; Nakagawa *et al.*, 1996), LET-502 (Wissmann *et al.*, 1997), Genghis Khan (GEK) (Luo *et al.*, 1997), Citron (Di Cunto *et al.*, 1998; Madaule *et al.*, 1998) and MRCK (Leung *et al.*, 1998). Rho kinase contains an N-terminal serine/threonine kinase catalytic domain and a C terminal region that mediates GTPase association. Rho-GTP enhances the ability of Rho kinase to autophosphorylate and to phosphorylate exogenous substrates (Ishizaki *et al.*, 1996; Matsui *et al.*, 1996). Rho kinases do not associate with Rac or Cdc42 *in vitro* (Leung *et al.*, 1995; Ishizaki *et al.*, 1996; Matsui *et al.*, 1996). Furthermore, Rho kinase activity is not activated by Rac1 or Ras (Matsui *et al.*, 1996) and a dominant negative Rho kinase mutant does not block Rac-induced membrane ruffling (Ishizaki *et al.*, 1997). However, related kinases such as Genghis Khan and MRCK associate with Cdc42 (Luo *et al.*, 1997; Leung *et al.*, 1998) and the Citron kinase associates with Rho and Rac (Madaule *et al.*, 1995; Di Cunto *et al.*, 1998; Madaule *et al.*, 1998). These results suggest that many Rho kinases function specifically in a Rho signaling pathway, although related kinases may function in other GTPase pathways.

Rho kinase is a compelling candidate Rho effector in cytoskeletal regulation. The *C. elegans* Rho kinase LET-502 is required *in vivo* for epidermal cell shape changes during gastrulation (Wissmann *et al.*, 1997) and mutations Genghis Khan produce abnormal actin accumulation in the *Drosophila* egg chamber (Luo *et al.*, 1997). In

cultured cells, constitutively active RhoA^{V14} or Rho kinase induces stress fibers and focal adhesions (Leung *et al.*, 1996; Amano *et al.*, 1997; Ishizaki *et al.*, 1997). In epistasis experiments, a dominant negative Rho kinase mutant blocks the ability of RhoA^{V14} to induce stress fibers and focal adhesions (Ishizaki *et al.*, 1997). Conversely, the effects of Rho kinase are insensitive to disruption of Rho function (Leung *et al.*, 1996; Amano *et al.*, 1997). These results indicate that Rho kinase acts downstream of Rho in a pathway that leads to the formation of stress fibers and focal adhesions.

What information do these experiments provide about the function and regulation of Rho kinase? The activity of truncated Rho kinase mutants demonstrate that the Rho-binding domain is not required for its biological effects in cultured cells (Amano *et al.*, 1997; Ishizaki *et al.*, 1997). However, the stress fibers formed by truncated Rho kinase are qualitatively different from those produced by activated Rho or full-length Rho kinase: instead of adjoining the plasma membrane, they aggregate aberrantly in the cell interior (Leung *et al.*, 1996; Amano *et al.*, 1997; Ishizaki *et al.*, 1997). This difference suggests that the C terminus is required for proper localization or regulation of Rho kinase function. Several domains from the Rho kinase C terminus inhibit the ability of full-length Rho kinase to stimulate focal adhesion and stress fiber formation; however, the truncated Rho kinase catalytic domain is resistant to this inhibition (Amano *et al.*, 1997). Therefore, these domains do not appear to function by titrating out effectors, but may bind to factors required for Rho kinase localization or activation. Consistent with this possibility, the C-terminal region of the related Citron kinase is required for its colocalization with actin (Di Cunto *et al.*, 1998) and activated RhoA^{V14} promotes the translocation of Rho kinase to membranes (Leung *et al.*, 1995).

Another candidate Rho effector is the serine/threonine kinase protein kinase C. Disruption of the *S. cerevisiae* PKC1 gene causes cells to arrest with small buds (Levin *et al.*, 1990), a phenotype similar to that of *rho1* mutants (Yamochi *et al.*, 1994). Pkc1 interacts with activated Rho1 in the yeast two-hybrid assay in an interaction mediated by

the Pkc1 C1 motif (Nonaka *et al.*, 1995). Interestingly, a dominant mutation in the *pkc1* gene suppresses the growth defect of yeast defective in *rho1* function (Nonaka *et al.*, 1995). The dominant *pkc1* mutation disrupts a conserved pseudosubstrate site which is predicted to maintain the kinase in an inactive state (Hug and Sarre, 1993). These results indicate that Pkc1 may function downstream of Rho signaling. However, the dominant *pkc1* allele cannot suppress the growth defect of a *rho1* null mutant, indicating that Pkc1 is not the only Rho1 target.

How does Rho kinase communicate to the cytoskeleton?

The identification of several kinases in the Rho signaling pathway suggests that regulated phosphorylation of specific downstream targets is essential to the biological functions of Rho. Myosin and actin are the two primary components of stress fibers, and myosin motor proteins hydrolyze ATP to power their translocation along actin filaments (Tan *et al.*, 1992). Levels of active, phosphorylated myosin are controlled by the opposing activities of myosin light chain kinase and myosin light chain phosphatase. Rho kinase can phosphorylate myosin light chain *in vitro* (Amano *et al.*, 1996), activating myosin ATPase activity and increasing its ability to assemble into filaments and bundle actin filaments (Tan *et al.*, 1992; Chrzanowska-Wodnicka and Burridge, 1996). In addition, Rho kinases can phosphorylate the myosin-binding subunit (MBS) of myosin light chain phosphatase (Matsui *et al.*, 1996) in a reaction that is enhanced by activated Rho (Kimura *et al.*, 1996; Matsui *et al.*, 1996). MBS phosphorylation leads to decreased phosphatase activity (Kimura *et al.*, 1996), which is predicted to further increase the levels of active myosin.

In *C. elegans*, mutations in the LET-502 Rho kinase are suppressed by mutations in the MEL-11 myosin phosphatase regulatory subunit, consistent with a model where Rho kinase functions *in vivo* to enhance myosin phosphorylation in a pathway opposed by myosin phosphatase (Wissmann *et al.*, 1997). In cultured cells, LPA or RhoA stimulation

leads to an increase in myosin light chain phosphorylation and the redistribution of diffuse subcellular myosin to actin stress fibers (Kolodney and Elson, 1993; Chrzanowska-Wodnicka and Burridge, 1996). LPA or RhoA-induced stress fibers and focal adhesions are blocked by inhibitors of myosin or myosin light chain kinase (Lamb *et al.*, 1988; Chrzanowska-Wodnicka and Burridge, 1996). These results support a model where Rho GTPase signals to Rho kinase in a pathway that leads to stress fiber and focal adhesion formation through the regulation of actin-myosin contractility.

Kinases in the Orb6/COT-1/Warts family influence cell shape *in vivo*

A distinct family of serine/threonine kinases related to Rho kinase is required for normal cell morphology in organisms from yeast to flies. Members of the Orb6/COT-1/Warts kinase family define pathways for the regulation of specific properties of cell shape, similar to the functions of Rho GTPase and Rho kinase. However, these kinases have divergent N-termini, lack the C-terminal domain of Rho kinase, including the Rho binding domain, and contain an additional spacer region between conserved motifs VII and VIII of the kinase domain. Orb6 is required for the elongate morphology of fission yeast cells; *orb6* mutants appear spherical (Verde *et al.*, 1995; Verde *et al.*, 1998). Orb6 protein colocalizes with actin at sites of cell growth, where it may function to anchor actin structures to the plasma membrane. Consistent with this model, actin is uniformly distributed on the surface of *orb6* mutant cells. Interestingly, arrested cells rapidly lose their normal shape when Orb6 function is removed, indicating that Orb6 is actively required for cell shape maintenance. *orb6* mutants also progress more rapidly through the cell cycle than wild-type fission yeast, leading to the production of abnormally small daughter cells. Conversely, cells overexpressing Orb6 are delayed in the cell cycle, suggesting that Orb6 may play a dose-dependent role in cell cycle regulation in addition to its role in maintaining cell morphology.

In *Drosophila*, the Orb6-related serine/threonine kinase Warts/Lats also functions in the regulation of both cell morphology and cell division (Justice *et al.*, 1995; Xu *et al.*, 1995). Mutations in the *warts* gene cause apical expansion of imaginal disc cells, producing a surface cuticle that appears irregular rather than smooth. The cell shape defects of *Drosophila warts/lats* mutants are selective; epidermal cells undergo aberrant expansion in their apical regions but retain the septate and adherens junctions characteristic of polarized cells (Justice *et al.*, 1995). In addition, *warts/lats* mutants exhibit increased cell proliferation leading to tumors in flies and mice (Justice *et al.*, 1995; Xu *et al.*, 1995; St. John *et al.*, 1999), suggesting that Warts/Lats may play a role similar to that of fission yeast Orb6 in negatively regulating cell cycle progression.

The COT-1 member of this serine/threonine kinase family is required for normal cell morphology in the fungus *Neurospora* (Yarden *et al.*, 1992). Growing *Neurospora* cells normally extend exclusively at their hyphal tip, with minimal side branching along the stem, but in *cot-1* mutants, excessive side branching initiates at the expense of tip elongation. This side branching is unlikely to be an indirect effect of tip growth cessation, since other tip growth mutants do not lead to the production of ectopic side branches by default. COT-1 may therefore function to restrict cell growth and spreading in inappropriate locations, perhaps through stabilizing regions of the actin cytoskeleton.

A relative of these serine threonine kinases was identified in the *C. elegans* expressed sequence tag (EST) database, and *Drosophila* and human homologs of this gene were named Ndr proteins, for nuclear Dbf2-related kinases (Millward *et al.*, 1995). The Ndr proteins form a subset of the Orb6/Warts/COT-1 kinase family, and are more closely related to Rho kinase than to Dbf2. The function of Ndr kinase is unknown, but the protein is widely expressed in human tissues and is localized to the nucleus and the cell periphery in culture. The physiological functions of these two subcellular populations of hNdr protein are unknown. In particular, Ndr nuclear localization requires the conserved spacer region within the kinase domain, and it will be interesting to determine if this spacer

region is required for the *in vivo* function of the Ndr homologs. Interestingly, human Ndr interacts with the calcium-binding protein S100b, and its kinase activity in cultured cells is stimulated by calcium influx (Millward *et al.*, 1998). The regulation of hNdr by calcium is dependent on a region in its N-terminal domain that is conserved in Orb6, COT-1 and Warts, raising the possibility that members of this serine/threonine kinase family could be regulated by calcium levels *in vivo*.

Although kinases in the Orb6/COT-1/Warts family are related to Rho kinases, they form a distinct class that lacks the Rho-binding domain, along with several other domains in the Rho kinase C-terminus that are proposed to have signaling or regulatory functions. It is not known whether Orb6/COT-1/Warts family kinases are regulated by GTPase pathways. In support of this possibility, the *orb6* mutant phenotype is similar to the cell shape defect caused by disruption of the Cdc42sp GTPase (Miller and Johnson, 1994). Furthermore, increased *orb-6* copy number can partially rescue the cell shape defects caused by a mutation in the Pak1/Shk1 kinase (Verde *et al.*, 1998), which has been shown to function with Cdc42sp at the same step in a pathway regulating cell shape (Marcus *et al.*, 1995; Otilie *et al.*, 1995). Moreover, Orb6 localization is disrupted in a *pak1/shk1* mutant, consistent with a role for the Orb6 kinase downstream of Pak kinase (Verde *et al.*, 1998). Therefore, it is possible that kinases in the Orb6/COT-1/Warts family, like the related Rho kinases, may also function in a GTPase signaling pathway.

Spatial regulation of GTPase signaling pathways

The requirement for Rho GTPase in defining cell morphology may provide information about how these pathways are spatially regulated. Rho GTPases associate with the plasma membrane as a result of protein prenylation (Seabra, 1998) and activated Rho has been shown to localize to the cell cortex (Drechsel *et al.*, 1997). Furthermore, RhoGDI proteins retain Rho GTPase in the cytoplasm, and this interaction is facilitated by phosphorylation of RhoA by protein kinase A (Lang *et al.*, 1996). Therefore, interactions

between GTPases and regulatory kinases or binding proteins may serve to regulate Rho localization.

Locally active GTPase subpopulations may lead to the local activation of GTPase effectors. For example, Rho kinase translocates to the cell cortex upon cotransfection with activated RhoA^{V14} (Leung *et al.*, 1995). Both Rho1 and Pkc1 colocalize with actin at the incipient bud site and the growing bud of *S. cerevisiae* (Yamochi *et al.*, 1994; Nonaka *et al.*, 1995), suggesting that localized components of this signaling pathway may be required for the polarization of cytoskeletal structures and growth material toward the emerging bud. The mechanisms by which Rho1 and Pkc1 are localized to the bud site are not known, but the upstream Cdc42 GTPase is also localized to the bud site (Ziman *et al.*, 1993), and may play a role in recruiting Rho1 in a GTPase cascade similar to that observed in fibroblasts. In addition, the Rho kinase relative Orb6 localizes to points of actin-membrane contact in *S. pombe* (Verde *et al.*, 1998), suggesting that these related pathways may also display precise spatial regulation.

Conclusion

The mechanism by which cell shape and polarity are established and communicated throughout the cytoplasm are not well understood, although rigid, extensive and polar cytoskeletal structures provide an ideal framework for polarized membrane and organelle traffic. The identification of GTPase and kinase proteins required for specific aspects of cell morphology provides a useful starting point for the identification of signaling pathways that link intrinsic and extrinsic cellular asymmetries to the structural cytoskeleton.

Chapter Two
Genes required for axon pathfinding and extension
in the *C. elegans* nerve ring

SUMMARY

Over half of the neurons in *C. elegans* send axons to the nerve ring, a large neuropil in the head of the animal. A genetic screen in animals that express the green fluorescent protein in a subset of sensory neurons identified eight new *sax* genes that affect the morphology of nerve ring axons. *sax-3/robo* mutations disrupt axon guidance in the nerve ring, while *sax-5*, *sax-9* and *unc-44* disrupt both sensory axon extension and guidance. By contrast, while axon extension and guidance proceeded normally in *sax-1*, *sax-2*, *sax-6*, *sax-7* and *sax-8* mutants, these animals exhibited later defects in the maintenance of nerve ring structure. The functions of existing guidance genes in nerve ring development were also examined, revealing that SAX-3/Robo acts in parallel to the VAB-1/Eph receptor and the UNC-6/netrin, UNC-40/DCC guidance systems for ventral guidance in the amphid commissure, a major route of axon entry into the nerve ring. In addition, SAX-3/Robo and the VAB-1/Eph receptor both function to prevent aberrant axon crossing at the ventral midline. Together, these genes define pathways required for axon growth, guidance, and maintenance during nervous system development.

INTRODUCTION

During development, neurons project axons that often travel long distances through diverse environments to contact their targets (Tessier-Lavigne and Goodman, 1996; Mueller, 1999). The nematode *C. elegans* provides a simple and well characterized organism in which to study axon development. There are only 302 neurons in the adult hermaphrodite, and the stereotyped position of each neuron, its processes, and its putative synaptic connections are known from serial section electron micrographs (White *et al.*, 1986). 180 of these neurons send axons into the nerve ring, which is the largest axon

bundle in the animal. These axons must navigate to the nerve ring, recognize and enter the nerve ring, make specific contacts with each other and maintain these contacts during growth. Little is known about the genes that control nerve ring development.

Several conserved classes of guidance molecules direct axon guidance in *C. elegans* and other organisms. The UNC-6/netrin diffusible guidance cue is required for axon guidance along the dorsal-ventral axis in *C. elegans*, *Drosophila* and vertebrates (reviewed in Tessier-Lavigne and Goodman, 1996 and Culotti and Merz, 1998). Netrins can function to attract or repel different subsets of axons in vivo and in vitro. Attraction to netrins is mediated by UNC-40/DCC, an immunoglobulin superfamily member that is thought to act as a netrin receptor on growing axons, while repulsion from netrins can be mediated by UNC-5, a transmembrane receptor that acts in combination with UNC-40/DCC. UNC-6 is present in the region of the nerve ring (Wadsworth *et al.*, 1996), and both the UNC-40/DCC and UNC-5 receptors are expressed in nerve ring neurons (Leung-Hagesteijn *et al.*, 1992; Chan *et al.*, 1996), but it is not known whether these molecules influence nerve ring axon guidance.

Nerve ring neurons also express SAX-3/Robo, a transmembrane protein in the immunoglobulin superfamily that is related to *Drosophila* and vertebrate Roundabout (Robo) proteins. Disruption of Robo function in *Drosophila* and *C. elegans* leads to inappropriate axon crossing of the ventral midline (Kidd *et al.*, 1998; Zallen *et al.*, 1998/Chapter 3). *sax-3* mutants are also defective in the ventral guidance of motor and interneuron axons toward the midline, suggesting a role for SAX-3/Robo in multiple axon guidance events (Zallen *et al.*, 1998/Chapter 3).

A third guidance molecule expressed in the *C. elegans* nerve ring is the *vab-1* Eph receptor tyrosine kinase (George *et al.*, 1998). Eph receptors recognize transmembrane or GPI-linked ephrin ligands, which have been implicated primarily in repulsion of growing axons, though they may have attractive properties as well (see Kolodkin, 1996; Flanagan and Vanderhaeghen, 1998 for review). The *vab-1* Eph receptor is required for normal

epithelial cell migrations in *C. elegans* (George *et al.*, 1998), but its role in axon guidance has not been described.

We initiated a genetic analysis of axon guidance in the *C. elegans* nerve ring by focusing on a subset of nerve ring sensory neurons. The primary nematode sensory organ, the amphid, consists of twelve bilaterally symmetric amphid neuron pairs that function to detect chemicals, touch and temperature. Each amphid neuron has a single axon that extends in the nerve ring and a ciliated sensory dendrite that connects to an opening in the anterior cuticle (White *et al.*, 1986). Most amphid axons reach the nerve ring after first growing ventrally in the amphid commissure, while one pair projects directly to the ring in a lateral position. The navigation of sensory axons in the nerve ring is largely completed by the end of embryogenesis. However, nerve ring axons continue to grow as the animal grows during the larval stages. During larval development, nerve ring axons increase 2.5-fold in length, while retaining the spatial organization established during embryogenesis. The organization of processes in the nerve ring places amphid sensory axons in contact with sensory and interneuron targets, establishing neural circuits essential to sensation and behavior (White *et al.*, 1986).

While little is known about the mechanisms that direct amphid axon guidance, three cytoplasmic proteins have been shown to be required for amphid axon extension: UNC-33/CRMP, the UNC-44 ankyrin-related protein, and UNC-76 (Hedgecock *et al.*, 1985; Siddiqui and Culotti, 1991; McIntire *et al.*, 1992; Otsuka *et al.*, 1995; Bloom and Horvitz, 1997). In addition, the *ina-1* α -integrin is required for amphid axon fasciculation (Baum and Garriga, 1997). Later axon growth and maintenance in the larval stages may have requirements that are distinct from initial axon development. For some amphid sensory neurons, maintenance of appropriate axon morphology is regulated by neuronal electrical activity (Coburn and Bargmann, 1996; Coburn *et al.*, 1998; Peckol *et al.*, 1999).

To obtain information about the mechanisms of axon extension, guidance, and maintenance in the *C. elegans* nerve ring, we conducted screens for mutants with altered

morphology of nerve ring sensory axons. We used a behavioral enrichment based on the functions of specific sensory neurons, followed by a visual screen of GFP-labeled axons to isolate mutants with sensory axon defects. Using this approach, we isolated mutations in 12 genes, including 8 new genes. Some mutations disrupted the initial outgrowth and guidance of nerve ring axons, as well as axon guidance in other locations, while other mutations disrupted later aspects of nerve ring maintenance. In addition, we have identified roles for the SAX-3/Robo, VAB-1/Eph receptor and UNC-6/netrin, UNC-40/DCC guidance systems in ventral guidance of sensory axons in the amphid commissure.

MATERIALS AND METHODS

Strain Maintenance

Worms were maintained using standard methods (Brenner, 1974). Strains were grown at 20°C, with the exception of *sax-1*, *sax-2*, *sax-3(ky200ts)*, *sax-6*, *sax-9*, and *sax(ky213)* mutants which were grown at 25°C, where their amphid axon defects were more penetrant than at 20°C or 15°C. No temperature sensitive amphid axon defects was observed in the other mutants, although all *sax-3* alleles showed substantially decreased viability at 25°C. Mutants characterized at multiple temperatures are indicated in each table.

Strain Construction

The *ceh-23::gfp* transgene was constructed by inserting a Ecl136 (Fermentas) /KpnI partial digest fragment of the *ceh-23::lacZ* construct (Wang *et al.*, 1993) into a Sma/KpnI partial digest of the *unc-76::lacZ* vector p76-L18 (Bloom, 1993). In parallel, the GFP coding region from the vector Tu65 (Chalfie *et al.*, 1994) was subcloned into the

p76L18 vector using AgeI/EcoRI sites. From this intermediate, GFP was cloned into the *ceh-23::unc-76* fusion as an AgeI/ApaI fragment. The *ceh-23::gfp* construct was introduced into a *lin-15(n765ts)* mutant strain with the *lin-15* plasmid pJM23 (Huang *et al.*, 1994) by germ-line transformation, and stable transgenic strains were generated by gamma irradiation as described (Mello and Fire, 1995; Sengupta *et al.*, 1996) to generate *kyIs4*. *kyIs4* was outcrossed six times and mapped to LGXR. The *lin-15(n765ts)* mutation may still be present in this strain. In *kyIs4*, GFP expression was consistently observed in the following neuron pairs: ADF, ADL, AFD, ASE, ASG, ASH, and AWC in the amphid, BAG and AIY in head, CAN in the midbody, and PHA and PHB in the tail. In addition, variable expression was detected in the ASI amphid neuron pair. These neurons had wild-type cell positions and process morphology in *kyIs4* animals (White *et al.*, 1986). *kyIs4* animals displayed normal chemotaxis responses to the odorants benzaldehyde, 2-butanone, and isoamyl alcohol, indicating that the AWC neurons were functional (Bargmann *et al.*, 1993).

The *mec-7::sax-3* transgene was constructed by engineering a KpnI site at the 5' end of the *sax-3* cDNA by PCR and cloning a KpnI-NheI fragment of the *sax-3* cDNA into a *sax-3* genomic subclone. A KpnI-AflIII(blunted) fragment containing the *sax-3* coding region (nucleotides 1-1343 of the *sax-3* cDNA linked to the *sax-3* genomic region beginning at the NheI site and ending at the AflIII site in the *sax-3* 3' UTR) was cloned into the KpnI-EcoRI(blunted) sites of the ppD96.41 *mec-7* promoter vector (A. Fire, personal communication), resulting in the addition of the *unc-54* 3'UTR which is predicted to increase expression. This *mec-7::sax-3* construct was injected at 10 ng/μl into *sax-3(ky123)* mutant animals using 50 ng/μl of *str-1::gfp* (Troemel *et al.*, 1997) as a coinjection marker.

Visualization of Neuronal Morphology

DiI staining of amphid neurons was conducted by exposing adult animals to a 15 $\mu\text{g/ml}$ solution of DiI in M9 buffer for 1.5 hours. DiO staining was conducted as previously described (Herman and Hedgecock, 1990; Coburn and Bargmann, 1996). These techniques label the following amphid neuron pairs: ADL, ASH, ASI, ASJ, ASK, and AWB.

The *str-3::gfp* transgene CX3596 *kyIs128* X (E. Troemel and C.I.B., unpublished results) and the *glr-1::gfp* transgene CX2835 *kyIs29* X (Maricq *et al.*, 1995) were introduced into the *sax* mutants. In *kyIs29*, GFP expression was detected in the interneurons AVA, AVB, AVD, AVE, AVG, PVC, RIF, AIB and motor neurons RMD, RIM and SMD. PVQ and URY stained faintly. The *mec-4::gfp* strain ZB163 *bzIs7* IV (generously provided by Ed Wu and Monica Driscoll) was used to visualize the AVM and PVM neurons and the ALM and PLM neuron pairs (Mitani *et al.*, 1993).

The HSN neurons were visualized with antibodies to serotonin (Desai *et al.*, 1988). Quantitation of HSN phenotypes in Table 4 was conducted on mutant strains that did not contain any GFP transgenes.

Fluorescent animals were visualized using a Zeiss Axioplan equipped with the Zeiss 487909 filter set. Worms were mounted on 2.5% agarose pads containing 5 mM sodium azide. Phenotypes were scored in adults at 40X magnification. Photographs in Figures 1, 3, 4 and 6 were taken using Kodak Ektachrome T160 film, scanned into a computer graphics file using a Nikon Scanner, and assembled using the Adobe Photoshop program. Confocal images in Figure 2 were generated from optical sections collected on a Zeiss LSM410 Invert confocal microscope and three-dimensional reconstructions were created using NIH Image 1.61/ppc.

Chemotaxis Enrichment Screen

kyIs4 animals were mutagenized with EMS (Brenner, 1974). Mutagenized animals were grown at 25°C for two generations and their F2 progeny assayed for

chemotaxis to a point source of 5 nl benzaldehyde, an odorant detected by the AWC sensory neurons (Bargmann *et al.*, 1993). After one hour, animals at the benzaldehyde source were removed from the plate, and the remaining animals were washed off and their amphid axons scored by fluorescence. Mutants with an altered number of GFP-labeled cells were discarded, since they could alter cell fate or GFP expression. *sax-3(ky123, ky198, ky200, ky203)*, *sax-5(ky118)*, *sax-7(ky146)*, *sax-8(ky188, ky199, ky201)*, and *unc-44(ky110, ky115, ky116, ky186, ky256)* were obtained in the chemotaxis enrichment screen.

Mutant strains were backcrossed three times by *kyIs4* before characterization and outcrossed a fourth time by N2 to separate the *sax* mutation from the *ceh-23::gfp* transgene. All mutants exhibited similar amphid phenotypes assessed with DiO staining in the presence or absence of *ceh-23::gfp*. *sax-5* and *unc-44* mutants were severely uncoordinated, *sax-3* mutants were chemotaxis defective and mildly uncoordinated, and *sax-7* and *sax-8* mutants were wild type for these behaviors.

***daf-11* Suppression Screen**

daf-11(m47) V; kyIs4 X and *daf-11(m84) V; kyIs4 X* strains were mutagenized with EMS and grown for one generation at 15°C. F1 progeny were shifted to 25°C as L4 larvae to promote dauer formation in the F2 progeny. F2 nondauers were cloned and scored by fluorescence in the F3 generation for axon defects. *sax-1(ky211)*, *sax-2(ky216)*, *sax-9(ky212, 218)*, *unc-33(ky255)*, *unc-44(ky257)* and *unc-76(ky258)* were isolated as suppressors of *daf-11(m47)*. *sax-6(ky214)* and *sax(ky213)* were isolated as suppressors of *daf-11(m84)*. Mutations were not retested for suppression of *daf-11*. *unc-33*, *unc-44* and *unc-76* mutants were severely uncoordinated and *sax-1*, *sax-2* and *sax-9* mutants moved normally.

Mutant strains were outcrossed by a *him-5(e1490) V; kyIs4 X* strain to replace *daf-11* with the closely linked *him-5* mutation. Mutant *him-5* strains were outcrossed

again by *kyIs4* to separate the *sax* mutation from *him-5*. *sax-1*, *sax-2* and *sax-9* mutants were further outcrossed by *kyIs4* and N2 strains. *unc-76(ky258)* was not separated from the *daf-11* mutation.

Mapping

All of the *sax* mutations isolated were recessive. Mutations were mapped with respect to genetic markers. Linkage to chromosomes was established by two-factor mapping with recessive and dominant markers on each chromosome. Mutations were followed using the amphid axon phenotype detected by *kyIs4* or by DiO staining. Quadruply-marked strains were made with *kyIs4* and the triply-marked mutant strains MT464 *unc-5(e53) IV; dpy-11(e224) V; lon-2(e678) X* and MT465 *dpy-5(e61) I; bli-2(e768) II; unc-32(e189) III*. Additional strains used were MT4814 *unc-108(n501dm) dpy-5(e61) I*, MT6183 *bli-3(e767) unc-54(e1092) I*, MT4815 *sqt-1(sc1) II*, MT4817 *unc-103(e1597sd) III*, MT1747 *dpy-13(e184sd) unc-8(n491sd) IV*, MT4818 *unc-70(n493sd) V*.

Three-factor mapping was conducted using the following strains: MT530 *dpy-17(e164) unc-32(e189) III*, DR107 *dpy-4(e1166sd) unc-26(e205) IV*, CB3824 *eDf19/unc-24(e138) dpy-20(e1282ts) IV*, MT2211 *dpy-3(e27) unc-2(e55) X*, MT458 *unc-20(e112ts) lon-2(e678) X*, CX3546 *stDp2(X;II)/+ II; unc-18(e81) dpy-6(e14) X*, SP913 *mnDp57(X;I); unc-20(e112ts) X*, MT5339 *lon-2(e678) unc-3(e151) X*.

sax-1 mapped to X under the *mnDp57* duplication. *sax-2* mapped to III to the left or close to *dpy-17* (0/4 *dpy-17* non *unc-32* recombinants and 15/15 *unc-32* non *dpy-17* recombinants were mutant). *sax-3(ky123)* mapping and cloning is described in Zallen *et al.*, 1998/Chapter 3. *sax-5* mapped to IV between *unc-26* and *dpy-4* (13/19 *dpy-4* non *unc-26* recombinants were mutant). *sax-6* mapped to I (5/7 non *bli-3 unc-54* isolates were mutant and 2/7 were heterozygous). *sax-7* mapped to IV to the left or close to *unc-24* (0/7 *unc-24* non *dpy-20* recombinants and 1/1 *dpy-20* non *unc-24* recombinants were mutant).

sax-8(ky201) mapped to III between *dpy-17* and *unc-32* (1/4 *dpy-17* non *unc-32* recombinants and 4/6 *unc-32* non *dpy-17* recombinants were mutant). *sax-9(ky218)* mapped to IV to the left or close to *unc-26* (0/11 *unc-26* non *dpy-4* recombinants were mutant). *kyIs4* mapped to XR to the left of *unc-3* (1/12 *unc-3* non *lon-2* recombinants had *kyIs4*).

RESULTS

Identification of mutants with sensory axon defects

To visualize nerve ring axons in living animals, we generated transgenic strains expressing the green fluorescent protein (GFP) from the *ceh-23* cell-specific promoter. *ceh-23*, a homeobox gene linked to the *C. elegans* Hox cluster, is expressed in a subset of amphid sensory neurons (Wang *et al.*, 1993). The *ceh-23* promoter was joined in a translational fusion to the *gfp* coding region and a fragment of the *unc-76* gene to enhance labeling of neuronal processes (Bloom, 1993; Bloom and Horvitz, 1997). This gene fusion was expressed in nine pairs of neurons in the head, including seven amphid neuron pairs (Figure 1A, B), the BAG sensory neurons and the AIY interneurons. The *ceh-23::gfp* fusion was also expressed in the CAN neuron pair in the midbody (Figure 4A) and the PHA and PHB sensory neuron pairs in the tail. The *ceh-23::gfp* transgene did not appear to disrupt the position, morphology or function of these neurons (Materials and Methods).

Behavioral and developmental assays that require amphid sensory function were used to enrich for mutants that affect amphid neuron development (Materials and Methods). In one screen, mutagenized animals were tested for chemotaxis to an odorant sensed by the AWC amphid neuron to identify chemotaxis-defective and movement-defective mutants. These animals were then screened visually for altered axonal

morphology in *ceh-23::gfp*-labeled neurons. A second screen made use of *daf-11* mutants, which are growth arrested in the dauer larval stage (Riddle *et al.*, 1981). Dauer formation occurs in response to sensory stimuli, and disruption of amphid neuron function suppresses the constitutive dauer arrest of *daf-11* mutants (Vowels and Thomas, 1992; Schackwitz *et al.*, 1996; Coburn *et al.*, 1998). Mutagenized *daf-11* animals were screened for suppressed mutants that relieved the *daf-11* arrest and reached adulthood. These mutants were then examined visually for defects in axon morphology.

We screened 27,000 genomes using the chemotaxis enrichment strategy and isolated 15 mutations in 6 genes, determined by map position and complementation testing. We screened 6,000 genomes in the *daf-11* suppression screen and isolated 9 mutations in at least 7 genes. These screens identified different sets of genes, with the exception of one gene that was found in both screens (Table 1). The new genes were designated *sax* genes (for sensory axon defects). These genes defined three main categories: (1) one gene required for nerve ring axon guidance (*sax-3*), (2) three genes (*sax-5*, *sax-9* and *unc-44*) required for both nerve ring axon extension and guidance, and (3) five genes where initial development proceeded normally in mutant animals, but defects occurred in the subsequent maintenance of nerve ring morphology (*sax-1*, *sax-2*, *sax-6*, *sax-7* and *sax-8*).

Characterization of other neuron types in mutants with sensory axon defects

To further characterize the *sax* mutants identified in these screens, a variety of markers were used to analyze the morphology of sensory neurons, interneurons and motor neurons. The results of these experiments are presented in Tables 2-5; the conclusions for each mutant are discussed below.

Amphid sensory neurons were examined using the *ceh-23::gfp* transgene (Figure 1, Table 2) and the fluorescent dyes DiI or DiO (Figure 5) that label an overlapping set of

amphid neurons, including four pairs that do not express *ceh-23::gfp* (Materials and Methods). To characterize the trajectories of individual axons, we used the *str-3::gfp* transgene to specifically label the ASI neuron pair (Figure 2, Table 3, E. Troemel and C.I.B., unpublished results). Together, these techniques allowed the visualization of 11 of the 12 amphid neuron pairs. In all 24 mutants, these markers detected the correct number of neurons, confirming that the amphid neurons were present and retained structurally intact dendrites and sensory cilia. The *sax* genes are therefore likely to affect neuronal morphology and not cell fate.

Outside of the nerve ring, the second largest axon bundle in *C. elegans* is the ventral nerve cord along the ventral midline. The ventral nerve cord is asymmetric; over thirty axons travel on the right side of the ventral cord, while only four to six axons travel on the left side (White *et al.*, 1976). The decision to join one side of the ventral cord is made upon arrival at the ventral midline, and axons in the body region do not cross the midline subsequent to this choice. To characterize axons that travel in the ventral cord, we examined the HSN motor neuron pair in the lateral midbody using antibodies to the neurotransmitter serotonin (Figure 3A-E, Table 4; Desai *et al.*, 1988). The HSN axon grows ventrally to the ventral nerve cord without crossing the midline, joins the ipsilateral cord and travels anteriorly to the head. To visualize axons that travel in the right ventral cord, we used the *glr-1::gfp* reporter (Maricq *et al.*, 1995) to label eleven interneuron axons that run the length of the ventral cord (Figure 3F,G, Table 4). *glr-1*-expressing interneurons and motor neurons also contribute axons to the nerve ring, providing another marker for nerve ring morphology.

To determine if cell migrations were affected in the *sax* mutants, neuronal cell positions were examined. Amphid neurons are born at the anterior tip of the animal and undergo short-range posterior migrations (Sulston *et al.*, 1983). In addition to amphid neurons, two neurons in the midbody were examined to determine if the *sax* mutants had a general defect in cell migration. The two HSN neurons are born in the tail and migrate

anteriorly along half the length of the animal to reach the midbody; the two CAN neurons, labeled with the *ceh-23::gfp* transgene, migrate posteriorly from the head to the midbody (Sulston *et al.*, 1983; Figure 4, Table 5). Characterization of these neurons provided information about cell migrations in both directions along the longitudinal axis.

***sax-3/robo* mutations disrupt multiple aspects of amphid axon guidance**

Mutations in the *sax-3/robo* gene, a transmembrane protein that may function as a guidance receptor, caused amphid axons to extend inappropriately into the region anterior of the nerve ring (Figure 1E,H; Table 2). As few as one or as many as all *ceh-23::gfp*-labeled axons extended anteriorly in an individual mutant animal. When all seven labeled axon pairs were anteriorly misrouted, they were often able to complete the dorsal component of their trajectories, forming an anteriorly displaced structure that resembled the nerve ring. All neurons labeled by the *ceh-23::gfp* transgene, DiO and DiI exhibited defects in *sax-3* mutants, indicating that mutations in *sax-3* disrupted the pathfinding of at least 11 of the 12 amphid neuron pairs. In addition, the eight classes of interneurons and three classes of motor neurons that express *glr-1::gfp* in the nerve ring also exhibited anterior axons (97% defective in *sax-3(k123)*, n=31), indicating that *sax-3* is likely to affect the position of many or all nerve ring axons.

The severity of the amphid axon defects prompted us to examine the trajectories of individual axons in *sax-3* mutants. The ASI amphid neuron projects a single axon ventrally to the ventral midline in the amphid commissure and then dorsally within the nerve ring (Figure 2A). The *str-3::gfp* marker revealed that ASI axons in *sax-3* mutants often deviated anteriorly from their normal trajectory in the nerve ring (Figure 2B, Table 3). In addition to anterior misrouting, the ASI axons often failed to travel ventrally in the amphid commissure and instead projected directly to the nerve ring in a lateral position. In some animals laterally misrouted axons continued dorsally in the nerve ring, while in other animals they terminated in a lateral position, perhaps because of a failure to encounter their

normal substrates for entry into the nerve ring. A similar defect in the ventral guidance of six amphid neuron pairs was detected by DiI labeling (Figure 5). These results indicate that *sax-3* is required for two distinct guidance decisions of amphid sensory axons: initially to guide amphid commissure axons ventrally to the nerve ring entry point, and subsequently to prevent nerve ring axons from wandering anteriorly.

sax-3 mutations also disrupted the cell migrations of some neuron types. Amphid cell bodies were occasionally displaced anteriorly in *sax-3* mutants, as would occur if they did not complete their posterior cell migrations from the tip of the nose during development (Figure 1I, 22% of amphid neurons defective in *sax-3(ky123)* n=55). In addition, *sax-3* mutants exhibited defects in both the posteriorly-directed CAN migration (Figure 4B, Table 5) and the anteriorly-directed HSN migration (7% defective in *sax-3(ky123)*, n=27). These phenotypes indicate that *sax-3* is required for cell migrations in both directions along the longitudinal axis.

sax-3 mutants also exhibited a number of other phenotypes. Defects in head morphology produced a notched head phenotype (Figure 1I, 38% defective in *sax-3(ky123)* n=71). *sax-3* mutants exhibited a high incidence of embryonic lethality, with 82% of laid eggs (n=150) failing to hatch in the strong *sax-3(ky123)* allele, an 0.5 kb deletion mutation that removes the first exon (Zallen *et al.*, 1998/Chapter 3). The notched head phenotype and lethality are characteristic of mutants that affect epithelial cell migration and adhesion (George *et al.*, 1998). Consistent with the observation that *sax-3* mutations cause multiple neuronal defects, mutant animals were defective in a number of behaviors, including chemotaxis, locomotion and egg-laying.

***sax-5*, *sax-9* and *unc-44* mutations disrupt both extension and guidance of amphid axons**

Eleven mutations representing six genes caused amphid sensory axons to terminate prematurely before completing their trajectories in the nerve ring (Figures 1F, 2C; Tables

2, 3). In these mutants, most axons extended ventrally to join the nerve ring as in wild type, but terminated before reaching the dorsal midline. Three mutants in this category were immobile uncoordinated (Unc) and represent three previously identified genes: *unc-33* (1 allele), *unc-44* (6 alleles) and *unc-76* (1 allele). These genes were previously shown to cause axon defects in several neuron classes, including amphid neurons (Hedgecock *et al.*, 1985; Desai *et al.*, 1988; Siddiqui, 1990; Siddiqui and Culotti, 1991; McIntire *et al.*, 1992). In addition, a gene originally designated *sax-4(kyl12)* was found to be allelic to the previously identified *vab-3* gene (J. Hao, E. Lundquist, J.A.Z. and C.I.B., unpublished data). *vab-3* encodes a Pax family transcription factor (Chisholm and Horvitz, 1995), and characterization of the *vab-3* allele identified in our screen and previously identified *vab-3* alleles revealed severe defects in amphid axon extension (Figure 1F, 63% defective in *vab-3(e648)*, n=99 by DiI labeling).

Mutations in *sax-5*, *sax-9* and *unc-44* caused defects in amphid axon guidance as well as extension (Table 2). In *sax-5* and *unc-44* mutants, nearly all axons labeled by *ceh-23::gfp*, DiO and *str-3::gfp* were defective, suggesting that these mutations disrupt axon extension in at least 11 of the 12 amphid neuron pairs. Mutations in *sax-9* caused lower penetrance defects in amphid axon extension and guidance (Table 2). Because there are many *glr-1*-expressing axons in the nerve ring and they enter the ring at different points, their termination could not be scored reliably. However, both *sax-5* and *unc-44* mutants retained a ring of axons around the circumference of the nerve ring, excluding the possibility that these mutations cause a complete loss of the nerve ring.

Mutations in *sax-5*, *sax-9* and *unc-44* also caused misrouting of the HSN axon (Table 4), consistent with a role for these genes in axon pathfinding. Instead of growing directly to the ventral midline, the HSN axon often extended longitudinally in a lateral position or wandered and branched extensively in the vicinity of the cell body (Figure 3B). In some animals, the HSN axon grew posteriorly instead of anteriorly in the ventral cord, and when the axon did grow anteriorly as in wild type, it often terminated prematurely.

Consistent with previous reports, *unc-44* mutants exhibited defects in both HSN axon guidance and growth, with HSN axons often terminating prematurely (Table 4; McIntire *et al.*, 1992). The anterior and posterior CAN axons also terminated prematurely in *unc-44* mutants (Table 5). In addition, *unc-44* mutants exhibited ectopic HSN axons, with up to four axons from an individual neuron, suggesting a role for *unc-44* in axon initiation (Figure 3C, Table 4). Ectopic axons were also observed in *unc-33(e204)* mutants (data not shown).

sax-5 and *sax-9* mutations also disrupt axon guidance at the ventral midline. While wild-type HSN axons travel on opposite sides of the ventral cord (Figure 3D), axons often traveled together on the same side in *sax-5* and *sax-9* mutants (Figure 3E, Table 4). Similarly, *glr-1*-expressing interneuron axons that normally extend in the right ventral cord occasionally extend on the left side in *sax-5* mutants (Table 4). Mutations in *sax-5* and *sax-9* also disrupted the posteriorly-directed CAN cell migrations (Figure 4C, Table 5), while mutations in *sax-9* disrupted the anteriorly-directed HSN migration (7% defective, n=110). Cell migration defects were not observed in *unc-33*, *unc-44* or *unc-76* mutants.

***sax-1*, *sax-2* and *sax-6* mutations cause defects in maintenance of neuronal morphology**

Mutations in the *sax-1*, *sax-2* and *sax-6* genes caused amphid neurons to send aberrant processes into the region posterior to the nerve ring (Figure 1D). The *ceh-23::gfp* marker detected one to several aberrant posteriorly-directed processes per animal, in addition to a set of apparently normal axons in the nerve ring. Aberrant posteriorly-directed processes were observed both with the *ceh-23::gfp* transgene and with DiO and DiI filling, where some aberrant processes were traceable to the ASJ neuron. *sax-1*, *sax-2* and *sax-6* were identified as suppressors of *daf-11* dauer constitutivity, an assay that can detect subtle sensory defects. Laser ablation of the ASJ neuron pair suppresses the dauer

arrest of *daf-11* mutant animals (Schackwitz *et al.*, 1996). Therefore, it is possible that the ASJ axon defects in these mutants altered ASJ function.

To characterize the behavior of individual axons in *sax-1* and *sax-2* mutants, we examined the ASI neuron pair. In all cases, the posteriorly-directed processes were found to be ectopic neurites, since each ASI neuron also extended an apparently normal axon in the nerve ring (Figure 2D, Table 3).

To determine whether the phenotypes in *sax-1* and *sax-2* mutants reflect defects in initial development or in subsequent maintenance of neuronal morphology, we characterized the morphology of amphid neurons during development with the *ceh-23::gfp* marker. While the outgrowth of amphid axons is completed by the end of embryogenesis, few ectopic neurites were observed in first-stage (L1) larval *sax-1* and *sax-2* mutant animals (data not shown). Aberrant neurites began to appear in the L2 stage, accumulating to the high penetrance defects in adult animals. These results are consistent with a role for *sax-1* and *sax-2* in the maintenance, but not the establishment, of neuronal morphology during larval growth.

The *sax-1* and *sax-2* mutant phenotypes were not specific to amphid sensory neurons, since aberrant ectopic neurites were also observed in the CAN neurons (29% in *sax-1*, n=121; 53% in *sax-2*, n=36) and *glr-1::gfp*-labeled inter- and motor neurons (46% in *sax-1*, n= 54; 39% in *sax-2*, n=31). However, in *sax-1* and *sax-2* mutants the cell migrations and guidance of the primary axons in CAN neurons, HSN motor neurons and *glr-1::gfp*-labeled interneurons were normal. Consistent with the observation that these aspects of neuronal morphology are preserved in these mutants, mutant animals performed normally in a range of behavioral assays, including locomotion, egg-laying, and osmotic avoidance (data not shown).

***sax-7* and *sax-8* mutations disrupt the maintenance of nerve ring position**

In *sax-7* and *sax-8* mutants, the nerve ring contained an apparently normal complement of axons, and initial nerve ring morphology was wild type in postembryonic first-stage (L1) larvae. However, as mutant animals progressed through the four larval stages to adulthood, nerve ring axons became displaced posteriorly relative to the position of the cell bodies (Figure 1G). While the amphid cell bodies maintained their correct position, their axons became posteriorly displaced. These defects were first apparent in the L2 stage, and increased in penetrance in the L3 stage, when animals were as defective as adult populations (Table 2). Further characterization of the nerve ring in *sax-7* mutants revealed that *glr-1::gfp*-expressing axons were also posteriorly displaced (data not shown), indicating a general displacement of many or all nerve ring axons. However, no defects were observed in the ventral guidance of amphid axons in the amphid commissure (Figure 1G, Table 2), the HSN motor axons or the CAN axons. These phenotypes suggest a specific role for the *sax-7* and *sax-8* genes in the maintenance, but not the establishment, of nerve ring position.

Mutations in known guidance pathways disrupt ventral guidance in the amphid commissure

To supplement genetic screens for new genes involved in *C. elegans* nerve ring development, we investigated whether mutations in known genes disrupted the trajectories of amphid sensory axons. The *unc-6*/netrin secreted axon guidance molecule and its receptor, *unc-40*/DCC, are required for normal guidance of many *C. elegans* axons along the dorsoventral axis (Hedgecock *et al.*, 1990; Ishii *et al.*, 1992; Chan *et al.*, 1996). We found that in both *unc-6* and *unc-40* mutant animals, the ASI amphid axon sometimes failed to grow ventrally in the amphid commissure, and instead traveled directly to the nerve ring in a lateral position (Figure 2E; Table 3). In addition, other amphid axons labeled by DiI filling also exhibited ventral guidance defects (Figure 5), suggesting that, like *sax-3/robo*, *unc-6* and *unc-40* mutations disrupt the ventral guidance of multiple

amphid neuron types. In mutant animals in which ventral guidance occurred normally, amphid axons sometimes terminated prematurely while traveling dorsally in the nerve ring (Table 3; 17% defective in *unc-6(ev400)* n= 240, 11% defective in *unc-40(e271)* n=332 by DiI filling). We also examined animals mutant for UNC-5, an transmembrane receptor that mediates repulsion from UNC-6 in combination with UNC-40 (Hedgecock *et al.*, 1990; Leung-Hagesteijn *et al.*, 1992; Hamelin *et al.*, 1993). Few amphid defects were observed in *unc-5* mutants (Table 3; 1% defective in ventral guidance in *unc-5(e53)* by DiI filling, n=168).

Ventral guidance in the amphid commissure was also disrupted in *vab-1* mutants. DiI filling revealed a partially penetrant defect in which many amphid axons grew directly to the nerve ring in a lateral position, a defect qualitatively similar to the defects of *unc-6* and *unc-40* mutants (Figure 5). The *vab-1* gene encodes a *C. elegans* Eph receptor homolog expressed in neurons that project axons to the nerve ring (George *et al.*, 1998). *vab-1* mutants had a strong lateral axon phenotype in the ASI neuron, but no other ASI defects (Table 3). Amphid phenotypes were most severe in animals with the *vab-1(dx31)* deletion that removes the first four exons, but were also present in animals with the *vab-1(e2)* missense mutation that abolishes kinase activity (George *et al.*, 1998). *vab-1* mutations caused minimal defects in ventral guidance of the HSN axons (Table 4).

Like SAX-3/Robo, the VAB-1/Eph receptor also affects axon guidance at the *C. elegans* ventral midline. In half of *vab-1(e2)* and *vab-1(dx31)* mutant animals, the HSN axon aberrantly crossed and recrossed the ventral midline (Table 4). Likewise, *glr-1*-expressing interneuron axons sometimes failed to remain in the right ventral cord and aberrantly crossed over to the left side (Figure 3G, Table 4).

***sax-3/robo* functions in parallel to *vab-1* and *unc-6/unc-40* in ventral guidance of amphid axons**

sax-3, *unc-6*, *unc-40* and *vab-1* are all required for normal amphid axon trajectories; how do these molecules function together to guide axons ventrally in the amphid commissure? If these genes act in a single pathway, disrupting two genes should not cause a more severe defect than a complete loss of function in either one. Alternatively, if these genes act in parallel, then disrupting two genes together may cause a defect that is more severe than the defect in either single mutant.

The *vab-1(e2); sax-3(ky200)* double mutant was significantly more defective than animals lacking either *vab-1* or *sax-3* function (Figure 5A). Similarly, double mutant combinations between *sax-3* and either *unc-6* or *unc-40* were significantly more defective than animals with strong mutations in either *sax-3*, *unc-6* or *unc-40* (Figure 5B). By contrast, *unc-40; unc-6* double mutants were not enhanced compared to *unc-6* single mutants (Figure 5C), consistent with evidence that UNC-6 and UNC-40 participate in a single guidance pathway (Hedgecock *et al.*, 1990). These results establish that the guidance functions of SAX-3/Robo do not absolutely require VAB-1 Eph receptor or UNC-6/UNC-40 netrin signaling.

The ventral guidance of amphid axons was significantly more defective in *vab-1(e2); unc-6(ev400)* or *unc-40(e1430); vab-1(e2)* double mutants than in *unc-6* or *unc-40* single mutants (Figure 5C), indicating that the VAB-1 Eph receptor does not require UNC-6 or UNC-40 to execute guidance functions. However, the defects in these double mutants with the weak *vab-1* allele did not exceed those caused by the strong *vab-1(dx31)* allele alone, so UNC-6 could participate in either a subset of VAB-1 activities or in a separate pathway. Unfortunately, the lethality of double mutants precluded characterization of genetic combinations with strong loss of function *sax-3(ky123)* or *vab-1(dx31)* mutations.

***sax-3/robo* functions cell autonomously in ventral guidance of the AVM sensory axon**

The requirement for *sax-3/robo* in ventral guidance is consistent with two models: SAX-3 could act cell autonomously as a receptor on growing axons, or non-autonomously, either as a receptor in another pioneer axon or as a ligand on the substrate. Since amphid axons grow out in the amphid commissure bundle, their ventral guidance may be achieved through the combined action of axon-axon and axon-substrate interactions. Like amphid neurons, the AVM mechanosensory neuron has a cell body that is located on the lateral hypodermis and an axon that grows ventrally to the ventral midline; however, the AVM axon travels independently using only axon-substrate interactions. For this reason, we chose to examine the question of *sax-3* autonomy in the AVM neuron. AVM, like amphid neurons, relies on *sax-3* for its ventral axon guidance (Figure 6B,D) as well as *unc-6* and *unc-40* (Siddiqui, 1990; Chan *et al.*, 1996).

To determine the site of *sax-3* action for AVM ventral guidance, we expressed the *sax-3* cDNA from the *mec-7* promoter, which drives expression in six mechanosensory neurons, including AVM (Hamelin *et al.*, 1993). The *mec-7::sax-3* fusion rescued the AVM defects of *sax-3* mutants in two independent transgenic lines (Figure 6C,D), indicating that SAX-3 can function cell autonomously in AVM ventral guidance. This result does not rule out the possibility that SAX-3 could behave non-autonomously in other cell contexts, such as the nerve ring.

DISCUSSION

Identification of genes required for normal sensory axon trajectories

Mutations in eight *sax* genes disrupt the trajectories of sensory axons in the *C. elegans* nerve ring. *sax-3/robo* is required for two distinct guidance decisions in the amphid commissure and the nerve ring, while *sax-5*, *sax-9* and *unc-44* disrupt nerve ring axon extension and guidance. When amphid axons have completed their trajectories in the

nerve ring, the *sax-1*, *sax-2*, *sax-6*, *sax-7* and *sax-8* genes are required for the maintenance of nerve ring structure. In addition, mutations in the *sax-3*, *sax-5*, *sax-9* and *unc-44* genes disrupt axon guidance or cell migration in other neuron types, indicating that their function is not limited to the nerve ring. Most of the *sax* mutants were not defective for locomotion, and therefore would not have been isolated in previous screens for axon guidance mutants in a collection of behaviorally uncoordinated mutants.

***sax-3*, *vab-1* and *unc-6/unc-40* function in parallel for ventral axon guidance**

Characterization of SAX-3/Robo, VAB-1/Eph receptor and UNC-6/netrin, UNC-40/DCC function in the nerve ring revealed that these guidance systems are required to guide amphid sensory axons ventrally in the amphid commissure. Mutations in *sax-3*, *vab-1*, *unc-6*, and *unc-40* all disrupt ventral guidance of amphid axons, but cause relatively mild phenotypes individually. Double mutants are more severe, suggesting that the SAX-3/Robo, VAB-1/Eph receptor, and UNC-6/netrin, UNC-40/DCC pathways can function independently for ventral guidance, although these molecules may also share some functions. While the sequences of SAX-3/Robo, UNC-40/DCC and the VAB-1/Eph receptor suggest that they could act as guidance receptors in nerve ring axons, cell autonomy studies will be required to clearly establish the roles of these guidance molecules in the complex environment of the nerve ring.

The SAX-3/Robo immunoglobulin superfamily member functions cell autonomously in the AVM sensory neuron, consistent with a role as a receptor for ventral guidance. *sax-3* is expressed in amphid neurons as well as epidermal substrate cells during the time of amphid axon outgrowth in the embryo (Zallen *et al.*, 1998/Chapter 3). SAX-3 may act as a receptor for ventral guidance of amphid sensory neurons; alternatively, SAX-3 could function non-autonomously as a receptor in a nerve ring pioneer axon, as a ligand in an axon-substrate interaction, or in an earlier developmental

process (see below). The UNC-40 guidance receptor is widely expressed in neurons (Chan *et al.*, 1996). In the region of the nerve ring, its ligand UNC-6 is present in four neurons and two ventral CEP sheath cells that surround the amphid commissure, but is absent from the two dorsal CEP sheath cells (Wadsworth *et al.*, 1996). This expression pattern suggests a model in which UNC-6 secreted by the ventral CEP sheath cells may attract axons from the amphid commissure that express the UNC-40 receptor. In this model, UNC-6 could act either as a diffusible chemoattractant or as a local substrate for axon migration.

The VAB-1 Eph receptor is expressed in many head neurons but not in their epidermal substrate cells. In these neurons, its first developmental function is to direct the epidermal cell migrations that take place during ventral enclosure of the embryo (George *et al.*, 1998). *vab-1* and *sax-3* mutants share some epidermal abnormalities, including a partially-penetrant notched head phenotype. These defects are associated with lethality that is enhanced in *sax-3; vab-1*, *sax-3;unc-6/40* and *vab-1;unc-6/40* double mutants, suggesting that SAX-3, UNC-6 and UNC-40 may also affect epidermal morphogenesis.

We show here that *vab-1* mutations disrupt the ventral guidance of amphid axons. There are three possible explanations for this phenotype: VAB-1 and SAX-3 could mediate amphid axon guidance directly, amphid axon defects could arise indirectly as a consequence of abnormal epidermal migration, or, since physical interactions between neuroblasts are altered in *vab-1* mutants (George *et al.*, 1998), there could be changes in the neuronal substrates for axon migration. We favor the possibility that some effects of SAX-3 and VAB-1 are due to their actions in neurons. First, individual axons often exhibited guidance defects in *sax-3* and *vab-1* mutants even when the remainder of the nerve ring appeared normal. Second, in both *sax-3* and *vab-1* mutants, animals were observed with axon defects but no visible head morphogenesis phenotypes. Third, ventral guidance defects and anterior axon misrouting were not present in other notched-head mutants, such as *dpy-23* and *ina-1* (J.A.Z. and C.I.B., unpublished results). These

results do not support a model where head morphogenesis defects account for all axon defects in *sax-3* and *vab-1* mutants.

***sax-3*, *sax-5*, *sax-9* and *vab-1* affect axon crossover at the ventral midline**

Both *sax-3/robo* and the *vab-1* Eph receptor are required to prevent aberrant axon crossing in the ventral nerve cord at the *C. elegans* ventral midline (Zallen *et al.*, 1998/Chapter 3 and the present study), along with the new genes *sax-5* and *sax-9*. Axons from the left ventral cord can travel aberrantly on the right side in the absence of left cord pioneers (Durbin, 1987). However, axons from both the left cord (HSNL) and the right cord (HSNR and *glr-1::gfp*-labeled interneurons) cross the midline inappropriately in these mutants, indicating that these defects do not merely reflect an absence of the left cord. As in the nerve ring, aberrant midline crossover could represent direct defects in axon guidance or indirect consequences of ventral midline abnormalities. *Drosophila* Robo has been shown to function as a receptor on axons that prevents inappropriate crossing at the midline (Kidd *et al.*, 1998). In vertebrates and *Drosophila*, Robo proteins bind to Slit, a candidate ligand molecule that is secreted by midline cells (Brose *et al.*, 1999; Kidd *et al.*, 1999; Li *et al.*, 1999), suggesting that Robo may detect a localized midline repellent.

The finding that mutations in the VAB-1/Eph receptor lead to midline crossover defects suggests the possibility that Eph receptors may participate in axon guidance at the midline. Interestingly, a transmembrane ephrin is expressed at the ventral midline of the developing neural tube in vertebrates (Bergemann *et al.*, 1998). It is possible that the VAB-1/Eph receptor may interact with a conserved ephrin at the *C. elegans* ventral midline to prevent axons from crossing inappropriately.

***sax-1*, *sax-2*, *sax-6*, *sax-7* and *sax-8* function in nerve ring maintenance**

The genes required for nerve ring maintenance are distinct from those involved in early axon outgrowth and guidance. Five *sax* genes are specifically required for the

maintenance of axon morphology during larval stages. In *sax-1* and *sax-2* mutants, neurons initiate ectopic neurites that extend late in development. Although the pathfinding of embryonic axons proceeds normally, late-growing ectopic processes wander aberrantly into the region posterior to the nerve ring. These ectopic neurites may fail to grow into the nerve ring because molecules that direct early axon guidance, such as *sax-3*, are downregulated postembryonically (Zallen *et al.*, 1998/Chapter 3); alternatively, ectopic neurites could be indifferent to conventional guidance systems.

Posterior sensory axons are also present in mutants with abnormal sensory activity. These include mutations in *tax-2* and *tax-4*, subunits of a cyclic nucleotide-gated sensory channel, mutations that affect the structure of the amphid sensory cilia, and mutations that alter ion channel function (Coburn and Bargmann, 1996; Coburn *et al.*, 1998; Peckol *et al.*, 1999). *sax-1* and *sax-2* might participate in an activity-dependent pathway for maintaining axon morphology, or in an alternative pathway.

The *sax-7* and *sax-8* genes identify a distinct mechanism of nerve ring maintenance from *sax-1* and *sax-2*. In these mutants, the nerve ring is initially correctly positioned relative to the cell bodies in first larval stage animals, immediately following embryonic development. However, by the second larval stage these mutants begin to display an altered morphology, with the nerve ring appearing posteriorly displaced relative to the cell bodies of its contributing neurons. These mutants may provide information about the cell types and molecular pathways that maintain the position of the nerve ring bundle in the growing animal.

***sax* genes have distinct and overlapping roles in axon guidance, axon extension, axon initiation and cell migration**

The diverse phenotypes of *sax* mutant animals may reflect a versatility of proteins involved in morphogenesis. Mutations in *sax-5*, *sax-9* and *unc-44* disrupt axon guidance and extension of amphid sensory neurons and HSN motor neurons. Similarly, netrin

molecules promote both outgrowth and guidance of vertebrate commissural axons (Kennedy *et al.*, 1994; Serafini *et al.*, 1994). Therefore, a specific neuron type can display multiple responses to a single guidance cue. This overlap between guidance and extension responses could occur if components of the basic cytoskeletal machinery for axon extension are targets for regulation by axon guidance pathways.

unc-44 and *unc-33* mutants exhibited ectopic neurite defects in the HSN and PDE neurons, suggesting that these genes may regulate axon initiation in multiple neuron types (this work and Hedgecock *et al.*, 1985). Little is known about the mechanism of axon initiation and how it relates to axon guidance. UNC-44 is a *C. elegans* ankyrin, a protein that links transmembrane receptors to the actin cytoskeleton (Otsuka *et al.*, 1995) and UNC-33-related proteins may act downstream of receptors for the semaphorin guidance cue (Goshima *et al.*, 1995). Perhaps the localization of UNC-44, UNC-33 or other factors directs axon initiation to a single site in wild-type animals.

Mutations in the *sax-3*, *sax-5* and *sax-9* genes affected cell migration as well as axon pathfinding. All three mutations selectively disrupted the cell migration of the CAN neuron without affecting CAN axon outgrowth. A reciprocal requirement for *sax-5* and *sax-9* was observed in sensory neurons: mutations in these genes disrupted amphid axon trajectories while leaving amphid cell migrations intact. These genes may participate in axon guidance in one cellular context and cell migration in another. A parallel can be found in vertebrates, where ephrin guidance molecules direct the diverse processes of retinal axon guidance, neural crest cell migration and development of the vasculature (Krull *et al.*, 1997; Smith *et al.*, 1997; Wang and Anderson, 1997; Adams *et al.*, 1999).

The mechanisms by which guidance cues influence axon behavior in diverse ways are not understood, but may reflect differences in ligand presentation, receptor expression, or signal transduction. The characterization of multifunctional genes required for axon growth, guidance and maintenance should provide insight into the ways guidance systems operate in distinct cellular and molecular contexts.

Figure 1. Amphid axon trajectories in wild-type (A-C) and *sax* mutant animals (D-I), labeled by the *ceh-23::gfp* transgene.

(A) Schematic diagram of the anterior nervous system of *C. elegans*. Anterior is to the left, dorsal at top. Neurons and processes are indicated. The main process bundle is the nerve ring (arrow in B), with ~ 100 axons in a typical cross section (White *et al.*, 1986). Neurons that express the *ceh-23::gfp* transgene are shown in green. This lateral view shows one member of each bilaterally symmetric neuron pair. GFP expression is detected in the amphid sensory neurons ADF, ADL, AFD, ASE, ASG, ASH and AWC, each indicated by the last letter of its name. The BAG and AIY neurons in the head also express *ceh-23::gfp*. Most amphid axons first project ventrally through the amphid commissure to enter the nerve ring in a ventral position and then travel dorsally within the nerve ring to the dorsal midline. The ASE and AWC axons continue around the ring to terminate laterally on the other side. The ADL axon extends directly to the nerve ring in a lateral position and then branches, with the two branches extending within the nerve ring to the dorsal and ventral midlines, respectively.

(B) The *ceh-23::gfp* transgene labels amphid sensory neurons, shown here in a larval (L4) stage animal. GFP expression is detected in the cell bodies (excluded from the nucleus), axons and dendrites of labeled cells. The axons travel circumferentially in the nerve ring neuropil. Similar GFP expression is observed in all larval stages and the adult. Autofluorescence from the gut is present in the body of the animal. Scale bar = 10 μ m.

(C-I) Amphid neuron morphology in adult wild-type (C) or *sax* mutant animals (D-I).

(C) Wild-type amphid axons extend in the nerve ring; about half of the nerve ring can be

seen in this plane of focus. (D) An aberrant posteriorly-misdirected process in a *sax-2*

mutant. (E) An aberrant anteriorly-misdirected axon in a *sax-3(ky123)* mutant. (F)

Premature axon termination in the nerve ring in a *vab-3(ky112)* mutant. Most axons

terminate in a ventral position, while two axons terminate in more lateral positions. (G)

The nerve ring is displaced posteriorly relative to the amphid cell bodies in a *sax-7* mutant.

Several additional cells are now anterior to the nerve ring. (H) Anteriorly-displaced nerve ring in a *sax-3(ky123)* mutant. (I) Abnormal head morphology in a *sax-3(ky123)* mutant. Note that the cell bodies are in more anterior positions than in wild type.

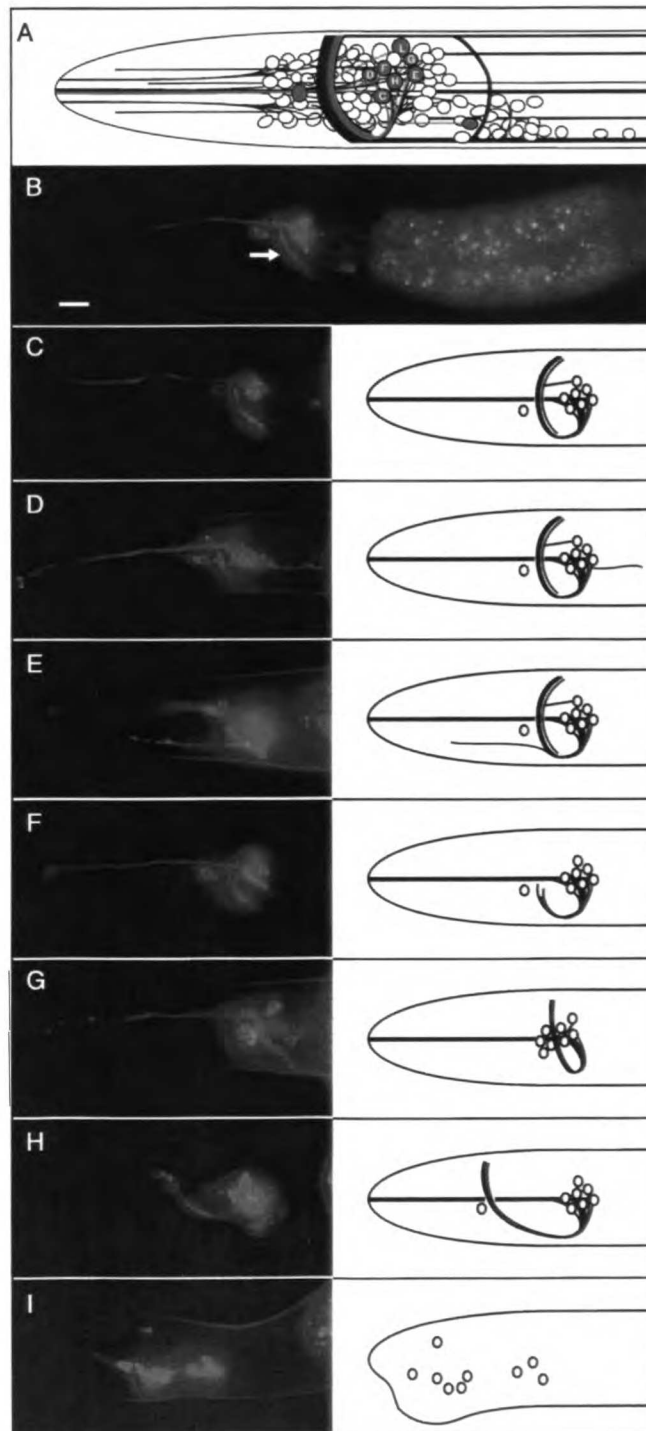


Figure 2. ASI axon trajectories in wild-type (A) and *sax* mutant animals (B-E), labeled by the *str-3::gfp* transgene. Anterior is to the left, dorsal at top. Scale bar = 10 μ m. (A) The wild-type ASI axon first projects ventrally to the ventral midline and then dorsally in the nerve ring. The ASI axon continues around the ring to terminate laterally on the opposite side; only one side of the animal is shown in these confocal images. (B) In a *sax-3(ky200)* mutant, the ASI axon fails to grow ventrally in the amphid commissure and extends directly to the nerve ring in a lateral position (arrow). In addition, the axons continues past the position of the nerve ring (arrowhead) and into the anterior head region. (C) In a *sax-5(ky118)* mutant, the ASI axon terminates prematurely (arrow). (D) In a *sax-2(ky216)* mutant, the primary axon extends normally in the nerve ring. In addition, an ectopic neurite (arrow) travels in a posterior direction. (E) In an *unc-40(ev271)* mutant, the ASI axon grows directly to the nerve ring in a lateral position (arrow).

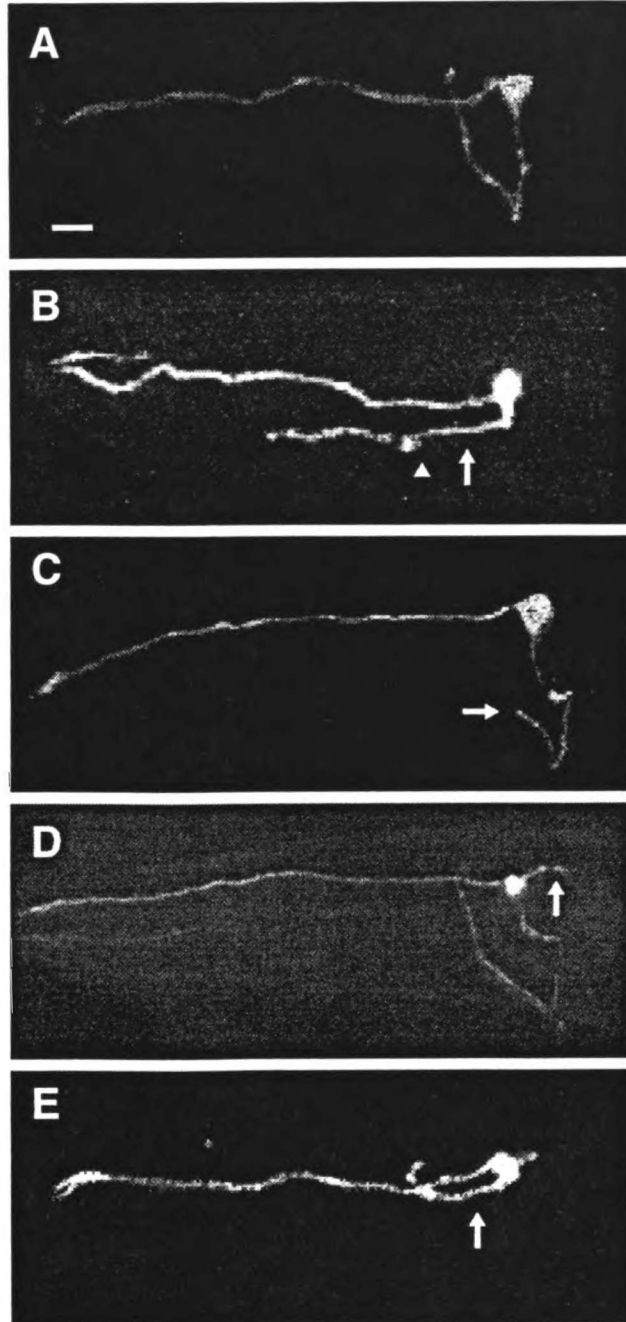


Figure 3. HSN and interneuron axon trajectories in wild-type (A,D,F) and *sax* mutant animals (B,C,E,G), labeled with antibodies to serotonin (A-E) or the *glr-1::gfp* transgene (F,G). Anterior is to the left, lateral view (A-C) or ventral view (D-G). Scale bar = 10 μ m. (A) HSN morphology in a wild-type animal. The HSN cell body is located in the midbody. The HSN axon (arrows) extends ventrally to the vulva (arrowhead), where it forms a branch and extends anteriorly in the ventral nerve cord. (B) In a *sax-5(ky118)* mutant, the HSN axon first grows ventrally, then wanders and branches extensively in the vicinity of the vulva (arrowhead) without reaching the ventral cord. (C) In an *unc-44(ky110)* mutant, three axons (arrows) project from the HSN cell body. One axon extends ventrally as in wild type, but terminates prematurely at the vulva. Additional axons grow in aberrant lateral positions in anterior and posterior directions. The anteriorly-directed axon wanders dorsally and posteriorly before terminating. (D) In a wild-type ventral view, the two HSN axons travel on opposite sides of the ventral midline, shown here immediately anterior to the vulva (out of view at right). (E) In a *sax-5(ky118)* mutant, the HSN axons cross and recross the midline, often traveling together on one side of the ventral cord (arrows). (F) In a wild-type ventral view, eleven interneuron axons travel on the right side of the ventral midline (arrowhead = vulva). (G) In a *vab-1(dx31)* mutant, these axons aberrantly cross over to the left side of the ventral cord (arrows).

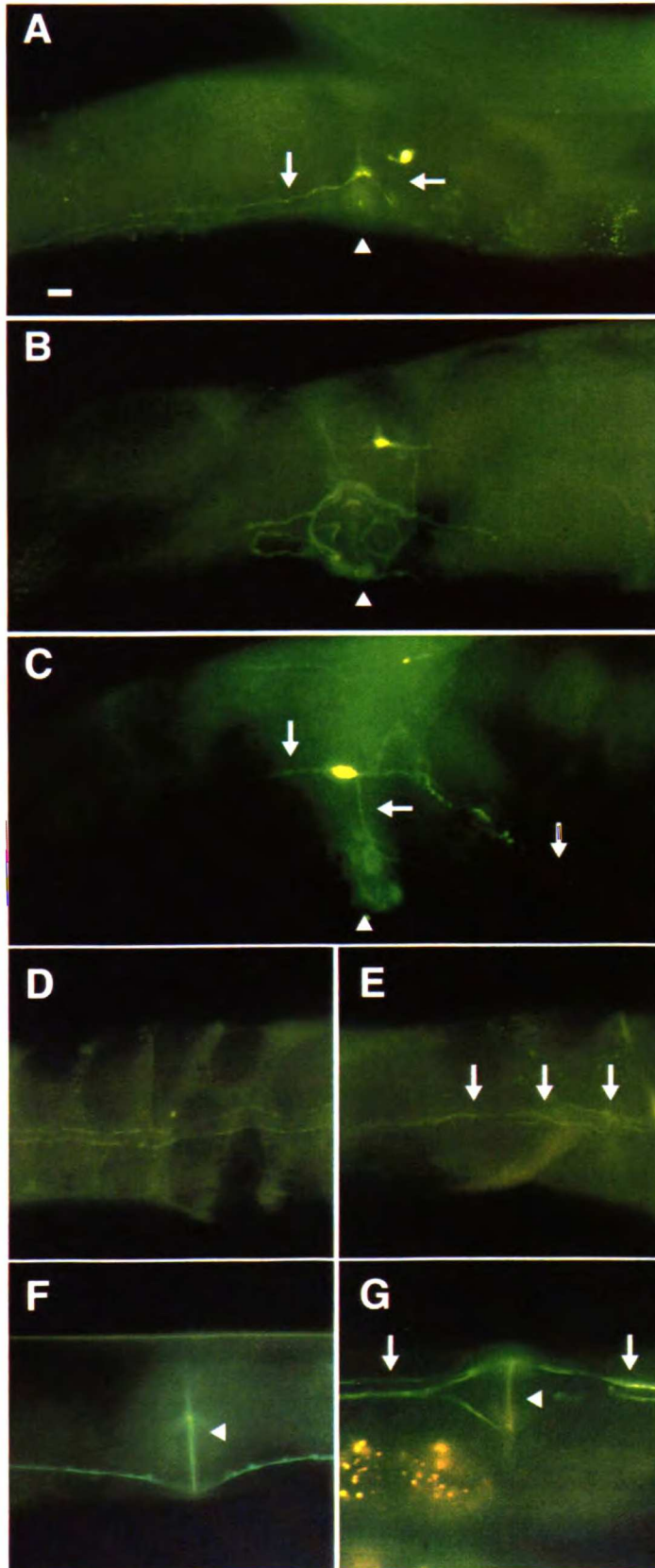


Figure 4. CAN neuron positions in wild-type (A) and *sax* mutant animals (B,C), labeled with the *ceh-23::gfp* transgene. Anterior is to the left, dorsal at top. (A) CAN morphology in a wild-type animal. The CAN cell body migrates posteriorly from the head to its final position in the midbody of the animal (arrow). One CAN axon travels anteriorly to the head in a lateral position, while the other travels posteriorly to the tail (not shown). The nerve ring in the head of the animal is marked with an arrowhead. (B) The CAN cell body is observed in a more anterior position in a *sax-3(ky123)* mutant (arrow). The posterior CAN axon is unaffected, although it leaves the plane of focus in this photograph. The anterior CAN axon travels to the head as in wild type. (C) The CAN cell body is observed in the head of a *sax-5(ky118)* mutant. The posterior CAN axon is unaffected. It was not possible to score the anterior CAN axon.

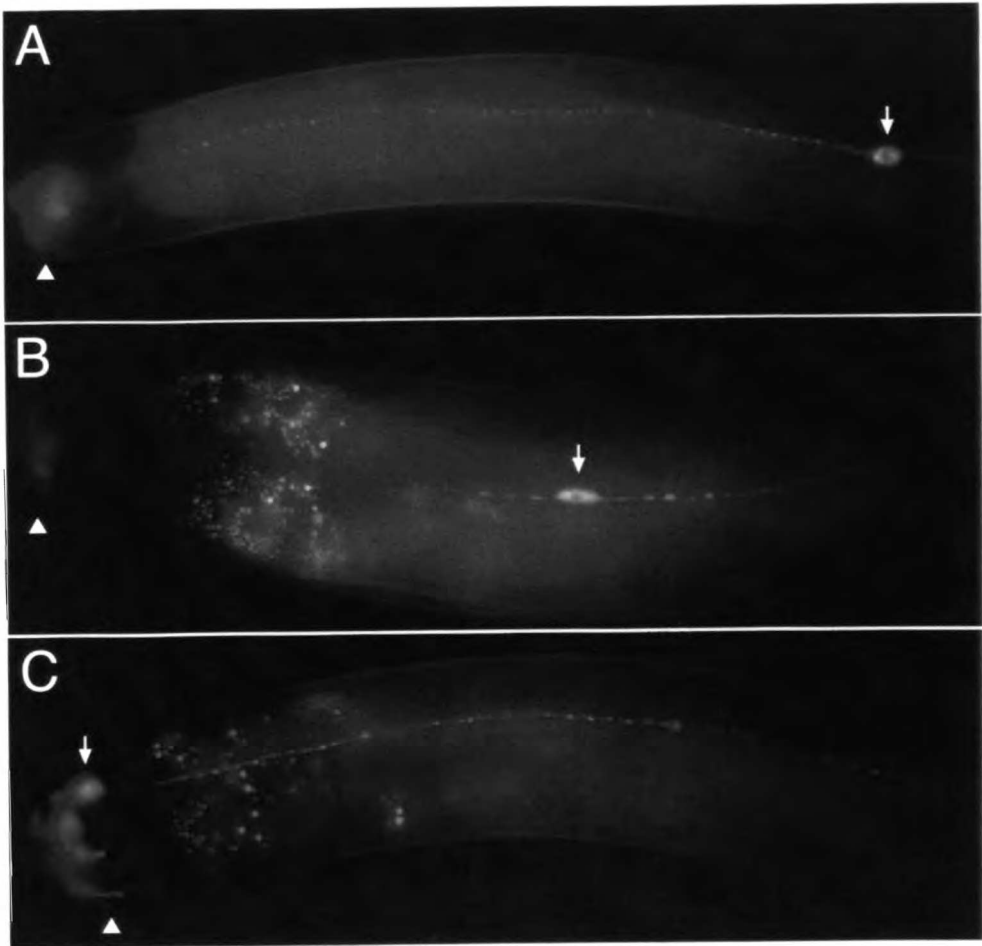


Figure 5. Amphid ventral guidance defects in *sax-3*, *vab-1*, *unc-6* and *unc-40* single and double mutants, detected by the fluorescent dye DiI. Error bars show the standard error of proportion. Percent defective represents percent of amphids in which at least half of the axons followed an aberrant lateral trajectory, n = 108-346 amphids. (A) *sax-3 vab-1* double mutants. Double asterisks indicate double mutants that are significantly more defective than mutants with the strongest loss of function in either single gene ($p < 0.001$, Chi-square test). (B) *sax-3 unc-6/unc-40* double mutants. Double asterisks indicate double mutants that are significantly more defective than mutants with a complete loss of *unc-6* or *unc-40* function ($p < 0.001$) and mutants with the strongest loss of *sax-3* function ($p \leq 0.016$). (C) *vab-1 unc-6/unc-40* double mutants. Single asterisks indicate double mutants that are significantly more defective than mutants with a complete loss of *unc-6* or *unc-40* function ($p < 0.001$) or mutants with the partial loss of function *vab-1(e2)* mutation ($p < 0.001$).

Figure 6. The AVM ventral guidance defect in *sax-3* mutants is rescued cell autonomously. AVM morphology was scored in adult and L4 animals using a *mec-4::gfp* transgene (Figure 6A). Anterior is to the left, dorsal at top. Scale bar = 10 μ m. (A) AVM morphology in a wild-type animal. The AVM axon (arrow) grows ventrally to the ventral midline and then turns anteriorly in the ventral cord (out of the plane of focus). The ALMR neuron (arrowhead in all panels) also expresses *mec-4::gfp*. (B) In a *sax-3(ky123)* mutant, the AVM axon (arrow) fails to grow ventrally and instead extends anteriorly in a lateral position. (C) In a *sax-3(ky123)* mutant with a *mec-7::sax-3* transgene driving *sax-3* expression specifically in six cells including AVM, the AVM axon (arrow) grows ventrally as in wild type. (D) AVM ventral guidance defects in *sax-3(ky123)* mutants and two independent *sax-3(ky123); mec-7::sax-3* transgenic lines. Percent defective represents the percent of AVM neurons. Error bars show the standard error of proportion. Lines 1 and 2 were significantly different from *sax-3(ky123)* (Line 1 $p < 0.001$, Line 2 $p = 0.02$, Chi-square test). The AVM rescue was specific, as the *sax-3* amphid axon guidance defects were not rescued by the *mec-7::sax-3* transgene (*sax-3(ky123)* 66% defective n=105 amphids, Line 1 65% defective n=65, Line 2 62% defective n=63).

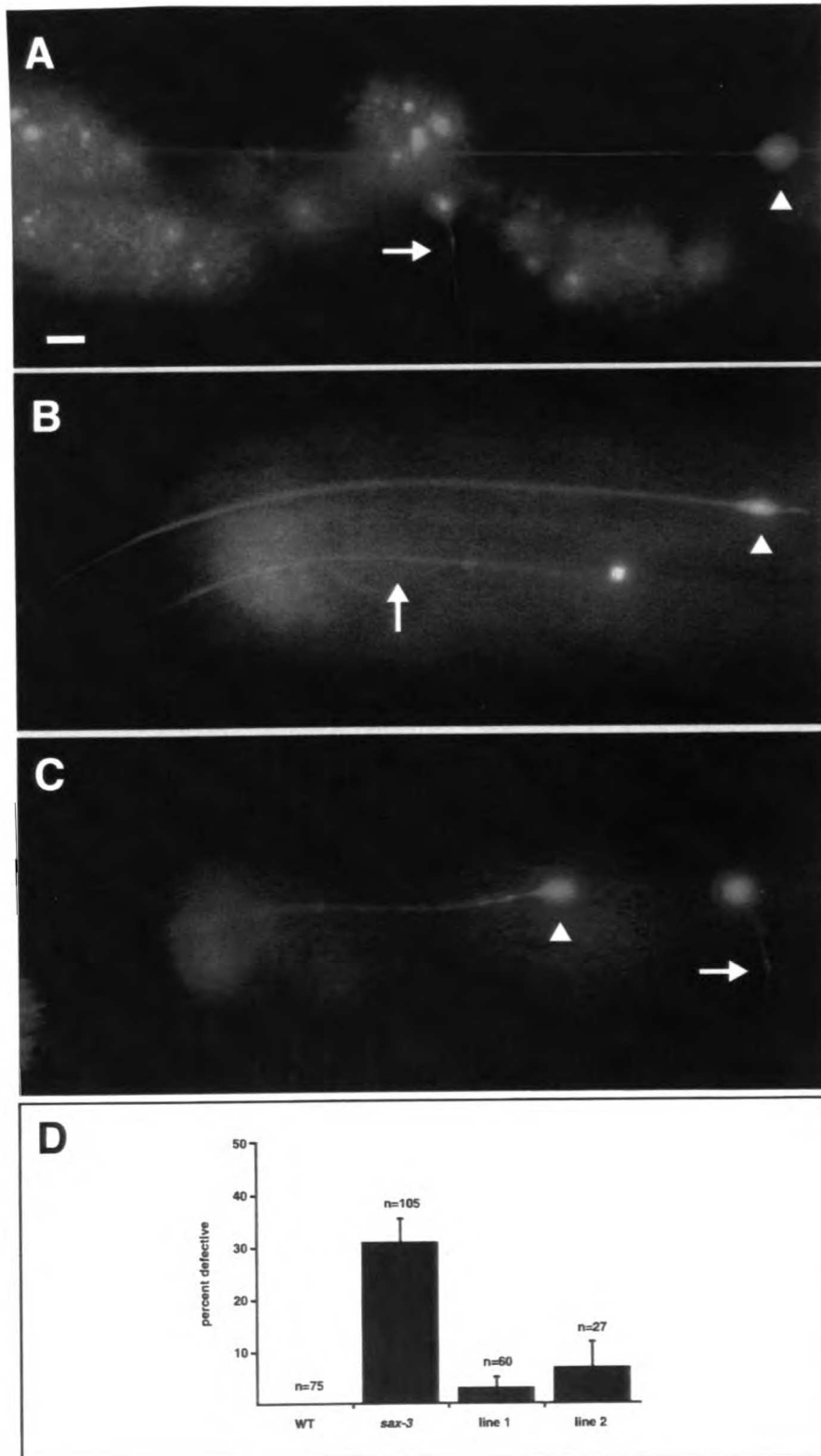


Table 1. Genes required for normal amphid axon trajectories.

Gene (alleles)	Linkage Group	Movement
Posteriorly-misdirected axons		
<i>sax-1(ky211)</i> ¹	X	wild-type
<i>sax-2(ky216)</i> ¹	III	wild-type
<i>sax-6(ky214)</i> ¹	I	wild-type
<i>sax(ky213)</i> ²		wild-type
Anteriorly-misdirected axons		
<i>sax-3(ky123, ky198, ky200¹, ky203)</i>	X	mild kinker and coiler Unc
Premature axon termination		
<i>sax-5(ky118)</i>	IV	kinker Unc
<i>unc-33(ky255)</i>	IV	immobile Unc
<i>unc-44(ky110, ky115, ky116, ky186, ky256, ky257)</i>	IV	immobile Unc
<i>unc-76(ky258)</i>	V	immobile Unc
Altered nerve ring placement		
<i>sax-7(ky146)</i>	IV	wild-type
<i>sax-8(ky188, ky199, ky201)</i>	III	wild-type
Multiple defects		
<i>sax-9(ky212, ky218)</i> ¹	IV	mild kinker Unc

¹ *sax-1*, *sax-2*, *sax-3(ky200)*, *sax-6* and *sax-9* mutants were temperature sensitive. Unless otherwise noted, these mutants were scored at 25°C. All other mutants were scored at 20°C.

² The *sax(ky213)* mutant phenotype was too weak for linkage mapping.

Table 2. Amphid axon defects in sax mutants.

Genotype	Wild type	Termination	Defasciculation	Anterior process	Anterior nerve ring ¹	Posterior process	Posterior nerve ring ¹	n
wild type	100%							300
posterior processes								
sax-1(ky211) 20°C	76%					24%		130
sax-1(ky211) 25°C	36%					64%		190
sax-2(ky216) 20°C	89%					11%		103
sax-2(ky216) 25°C	54%					46%		134
sax-6(ky214)	80%					20%		376
sax(ky213)	92%					8%		95
anterior processes								
sax-3(ky123) ^{2,3}	16%		25%	13%	60%		9%	55
axon termination								
sax-5(ky118)	7%	81%		2%		48%		42
unc-44(ky116)		90%		7%		90%		30
altered nerve ring placement								
sax-7(ky146)	4%			2%			94%	50
sax-8(ky201) ²	41%						59%	29
multiple defects								
sax-9(ky212) ²	67%	11%	16%	4%		13%		45






Amphid axon phenotypes were characterized in adults with the *ceh-23::gfp* marker. Schematic drawings show the head of the animal. Anterior is to the left, dorsal at top. n = number of animals scored. Mutants characterized at multiple temperatures are indicated. Animals with more than one phenotype were scored in multiple categories, so percentages do not always add up to 100%.

¹ In these mutants, all amphid axons were found in an abnormal location with respect to their cell bodies.

² All alleles of sax-3, sax-8 and sax-9 had similar amphid defects.



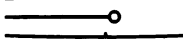

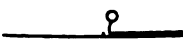

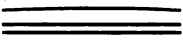

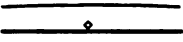

³ Axons were scored only when the amphid cell bodies were correctly positioned.

Table 3. Axon defects in the ASI amphid neurons.

						n
	Wild type	Axon termination	Lateral axon	Anterior axon	Ectopic neurite	
WT	100%					300
<i>sax-1(ky211)</i>	55%				45%	267
<i>sax-2(ky216)</i>	26%				74%	364
<i>sax-3(ky200) 20°C</i>	97%	3%				104
<i>sax-3(ky200) 25°C</i>	20%	14%	23%	59%		132
<i>sax-5(ky118)</i>	1%	99%				300
<i>unc-6(ev400)</i>	71%	12%	17%			386
<i>unc-40(e1430)</i>	84%	10%	6%			300
<i>unc-40(e271)</i>	91%	4%	5%			300
<i>unc-40(n324)</i>	90%	3%	7%			314
<i>unc-5(e53)</i>	99%		1%			622
<i>vab-1(dx31)</i>	41%		59%			41

Amphid axon phenotypes were characterized in adults using the *str-3::gfp* marker. Schematic drawings show the head of the animal. Anterior is to the left, dorsal at top. n = number of neurons scored. Mutants scored at multiple temperatures are indicated. Animals with more than one phenotype were scored in multiple categories, so percentages do not always add up to 100%.

Table 4. Ventral guidance and midline crossover defects in *sax* mutants.

	WT	<i>sax-5</i>	<i>sax-9</i> ³	<i>vab-1</i> ³	<i>unc-44</i> ³
Wild-type HSN (lateral view)		100%	6%	85%	99%
Defects in ventrally-directed growth axon wandering/branching			26%	9%	30%
lateral axon ¹			3%	5%	1%
Defects in anteriorly-directed growth termination of anterior axon			37%		54%
posterior axon ²			57%	5%	84%
Ectopic axons			3%		57%
	n = 70	n = 35	n = 97	n = 185	n = 37
Wild-type HSN (ventral view)		98%	38%	68%	49%
Axon crossover		2%	62%	32%	51%
	n = 63	n = 34	n = 31	n = 126	ND
Wild-type <i>glr-1::GFP</i> (ventral view)		100%	96%		97%
Axon crossover			4%	8% ⁴	3%
	n = 121	n = 85	ND	n = 100	n = 75

Axon phenotypes were scored in adults stained with anti-serotonin antibodies (HSN motor neurons) or the *glr-1::gfp* marker (ventral cord interneurons). Schematic drawings show the central third (top and bottom panels) or anterior third (middle panel) of the animal. Anterior is to the left. Animals with more than one phenotype were scored in multiple categories, so numbers do not always add up to 100%. n = number of neurons (top panel), axon segments (middle panel) or animals (bottom panel) scored.


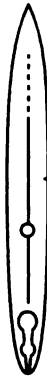
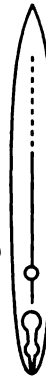
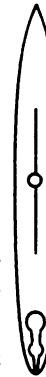
¹ The lateral axon category included axons that grew in anterior or posterior directions.

² The posterior axon category included axons that grew in ventral or lateral positions.

³ Alleles scored were *sax-9(ky212)*, *vab-1(e2)* (HSN), *vab-1(dx31)* (*glr-1::gfp*), *unc-44(ky116)* (HSN) and *unc-44(ky145)* (*glr-1::gfp*). Similar HSN defects were observed in *vab-1(dx31)*, *unc-44(e362)* and *unc-44(ky110)*.

⁴ The *vab-1(dx31)* *glr-1::gfp* crossover defect differs significantly from wild type (p=0.005, Chi-square test).

Table 5. CAN cell migration and axon outgrowth defects in *sax* mutants.

	WT	<i>sax-3</i> ²	<i>sax-5</i>	<i>sax-9</i> ²	<i>unc-44</i> ²
wild-type CAN					
>1/2 normal migration distance ³	100% ¹	10%	51%	52%	100%
					
≤1/2 normal migration distance ³		37%		3%	
					
axon termination		53%	49%	45%	
					
		post. 4%	post. 6%		ant. 100% post. 100%
	n = 100	n = 30	n = 67	n = 31	n = 31

CAN axon outgrowth and cell migration phenotypes were characterized in adults with the *ceh-23::gfp* transgene. Schematic drawings show the entire animal. Anterior is to the left, dorsal at top. n = number of neurons scored.

No CAN cell migration or axon outgrowth defects were observed in *sax-1*, *sax-2*, *sax-6*, *sax-7* or *sax-8* mutants.

¹The wild-type strain used for comparison was the *ceh-23::gfp* strain *kyls4*. *kyls4* control animals exhibited low penetrance CAN cell displacement, with 3/100 neurons migrating approximately 3/4 of the normal distance.

Therefore, CAN neurons were only scored as defective if the cell migrated less than 2/3 of the normal distance.

²Alleles scored were *sax-3(ky123)*, *sax-9(ky212)* and *unc-44(ky116)*. *sax-9(ky218)* and *unc-44(ky110)* caused similar defects.

³In animals with CAN cell migration defects, the posterior CAN axon was almost always longer than or equal to its wild-type length: *sax-3* (96%, n=30), *sax-5* (94%, n=67) and *sax-9* (100%, n=31).

Chapter Three

The conserved immunoglobulin superfamily member SAX-3/Robo
directs multiple aspects of axon guidance in *C. elegans*

The Conserved Immunoglobulin Superfamily Member SAX-3/Robo Directs Multiple Aspects of Axon Guidance in *C. elegans*

Jennifer A. Zallen, B. Alexander Yi,
and Cornelia I. Bargmann*

Howard Hughes Medical Institute
Programs in Developmental Biology,
Neuroscience, and Genetics
Department of Anatomy
The University of California
San Francisco, California 94143-0452

Summary

The *C. elegans sax-3* gene encodes a predicted transmembrane protein with five immunoglobulin domains and three fibronectin type III repeats that is closely related to *Drosophila* Robo. Mutations in *sax-3* lead to repeated midline crossing by ventral cord axons that normally do not cross the midline after they join the ventral cord, a phenotype similar to that of *robo* mutants. *sax-3* is also required for guidance of some axons to the ventral cord, implicating this gene in two different types of guidance events. A *sax-3::GFP* fusion gene is expressed in developing neurons during axon outgrowth, and *sax-3* function is required at the time of axon guidance, suggesting that this gene mediates cell interactions during guidance decisions.

Introduction

Developing axons navigate through complex environments using highly conserved guidance cues and receptors (Keynes and Cook, 1995; Goodman, 1996; Tessier-Lavigne and Goodman, 1996). These pathways are particularly well-defined in the vertebrate spinal cord and its invertebrate equivalents, the ventral nerve cord of *C. elegans* and the ventral CNS of *Drosophila melanogaster*. In all cases, diffusible axon guidance molecules of the netrin/UNC-6 family attract axons from peripheral locations to the ventral midline where the major nerve cord forms (Hedgecock et al., 1990; Ishii et al., 1992; Kennedy et al., 1994; Serafini et al., 1994, 1996; Harris et al., 1996; Mitchell et al., 1996; Wadsworth et al., 1996). Attraction to netrin/UNC-6 is mediated by the DCC/UNC-40/*frazzled* family of receptors, which encode predicted transmembrane proteins with four immunoglobulin domains and six fibronectin type III domains (Chan et al., 1996; Keino-Masu et al., 1996; Kolodziej et al., 1996).

Axon guidance away from the ventral midline can also be mediated by netrin/UNC-6 cues through chemorepellent effects on axons that express receptors in the UNC-5 family (Hedgecock et al., 1990; Hamelin et al., 1993). UNC-5 receptors are transmembrane molecules with two immunoglobulin domains and two thrombospondin type 1 domains (Leung-Hagstestijn et al., 1992);

like UNC-40/DCC/*frazzled* receptors, their intracellular regions do not include known catalytic domains.

In both vertebrates and invertebrates, axons that arrive at the ventral midline receive additional guidance cues that govern their organization. Midline axons are divided into two discrete longitudinal bundles that flank the midline bilaterally. In vertebrates and in *Drosophila*, most axons cross the midline before joining one of these two longitudinal bundles. Genetic studies in *Drosophila* have implicated two antagonistic genes, *roundabout* (*robo*) and *commis sureless* (*comm*), in guidance across the midline (Seeger et al., 1993). In *comm* mutants, axons remain in longitudinal bundles instead of crossing the midline in commissures, indicating that this molecule promotes midline crossing. *comm* encodes a novel transmembrane protein that is expressed on midline cells and some neurons (Tear et al., 1996). In *robo* mutants, the opposite phenotype is observed: the commissures are thickened and longitudinal bundles are diminished, suggesting that axons aberrantly cross the ventral midline instead of remaining in their normal longitudinal positions (Seeger et al., 1993). Thus, *robo* activity normally inhibits midline crossing. In chick, the ability of axons to join the correct bundle requires two transmembrane immunoglobulin domain-containing proteins, axonin-1/TAG-1 and NrCAM (Stoeckli and Landmesser, 1995; Stoeckli et al., 1997). Axonin-1 is present on axons that cross the midline and NrCAM is present on midline cells. If the interaction between these two molecules is blocked, axons are unable to cross the midline and stall on the ipsilateral side, a result similar to that observed in *Drosophila comm* mutants.

The *C. elegans* ventral nerve cord also has left and right longitudinal bundles, but unlike the vertebrate and *Drosophila* midlines, the *C. elegans* ventral nerve cord is asymmetric (White et al., 1976, 1986). Although most of the neurons that contribute longitudinal axons to the nerve cord have cell bodies in bilaterally symmetric pairs, the right ventral nerve cord contains about 40 axons, while the left ventral nerve cord in the central body contains only four axons (Figure 1A). These two axon bundles are separated by an epidermal protrusion called the hypodermal ridge. Thus, most neurons whose cell bodies are on the left have axons that cross over to the right side, while axons from most cell bodies on the right remain ipsilateral. In *C. elegans*, midline crossing is only observed when an axon first joins the ventral nerve cord, usually at the anterior or posterior end of the nerve cord.

Two types of neurons contribute to the organization of the ventral nerve cord. The AVG neuron is an unpaired neuron whose axon runs along the right ventral nerve cord. When it is killed, ventral nerve cord axons are defasciculated and some motor axons extend aberrantly in the left ventral nerve cord, although longitudinal interneuron axons remain on the right (Durbin, 1987). The PVPR axon is required for the formation of the left ventral nerve cord. When PVPR is killed, all axons join the right nerve cord (Durbin, 1987). Thus, the right-hand bias of the nerve cord is preserved even in the absence of these pioneer neurons.

* To whom correspondence should be addressed.

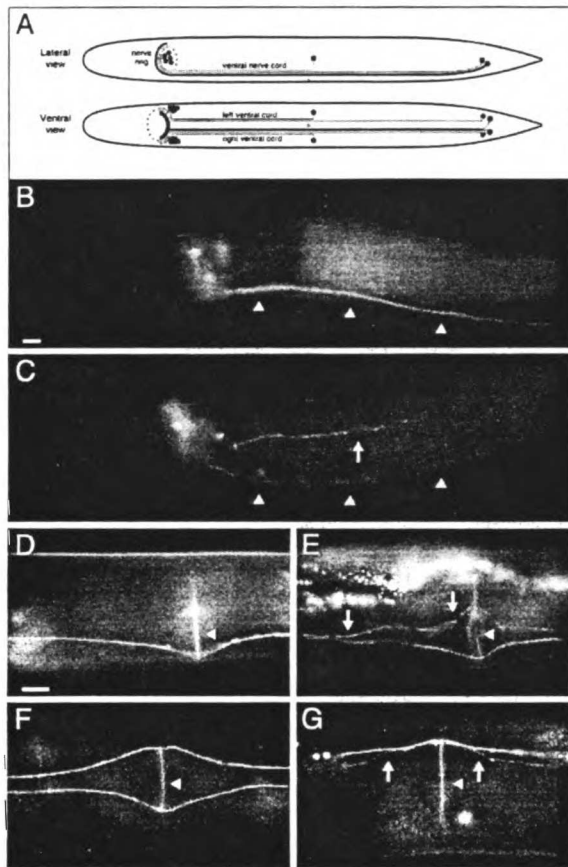


Figure 1. Disrupted Guidance of Interneuron Axons to and within the Ventral Nerve Cord of *sax-3* Mutants

(A) Organization of the ventral nerve cord of *C. elegans*. Interneurons with axons that extend in the right ventral cord are shown in blue. Axons from cell bodies on the right side of the animal travel in the right ventral cord without crossing the ventral midline, while many axons from cell bodies on the left side cross the midline to join the right ventral cord. The HSN motor neuron pair in the midbody is shown in red, and the PVQ interneuron pair in the tail is shown in green. Both neuron pairs send axons ventrally to the midline and then anteriorly to the head without crossing the midline. Not shown are the two other axons in the left ventral cord, the ~30 other axons in the right ventral cord, and the ~90 other axons in the nerve ring.

(B-E) Axons from the AVA, AVB, AVD, AVE, AVG, and PVC interneurons extend in the ventral nerve cord and express the *glr-1::GFP* transgene. (B) In wild-type animals (lateral view), these axons are restricted to the ventral nerve cord (arrowheads). (C) In *sax-3* mutants (lateral view), some axons extend aberrantly in a lateral position (arrow) but most reach the ventral nerve cord (arrowheads, not in focus). (D) In wild-type animals (ventral view), all axons are right of the ventral midline (defined by the vulva, arrowhead). (E) In a *sax-3(ky123)* mutant (ventral view), some axons cross the midline and extend in the left ventral nerve cord (arrows; arrowhead defines the vulva).

(F and G) Axons from the two PVQ interneurons extend in the ventral nerve cord and express *sra-6::GFP*. (F) In wild-type animals (ventral view), each axon is restricted to the ipsilateral nerve cord (the midline is marked by the vulva, labeled with an arrowhead in all panels). (G) In a *sax-3(ky123)* mutant animal (ventral view), the PVQ axons cross the midline at multiple positions. Here both axons (arrows) run on the left side of the vulva. Anterior is at left in all panels.

Scale bars = 10 μ m.

We describe here the effects of the *sax-3* gene in the ventral nerve cord. In *sax-3* mutants, most longitudinal axons in the ventral cord extend to their full length, but the left-right asymmetry of the ventral cord is disrupted so that many longitudinal axons extend on the incorrect side of the nerve cord. A single mutant axon can cross the midline many times along its trajectory. Thus, *sax-3* acts to establish the asymmetry of the ventral nerve cord. In addition, *sax-3* activity is required to guide axons to the ventral midline; in mutant animals, some ventral cord axons are found in aberrant lateral positions. These functions of *sax-3* allow it to act in concert with the *unc-6/netrin* pathway to recruit axons to the ventral nerve cord. *sax-3* encodes a predicted transmembrane molecule that is similar to the *Drosophila robo* gene product (Kidd et al., 1998a [this issue of *Cell*]), identifying a new conserved family of cell surface molecules involved in axon guidance.

Results

Mutations in *sax-3* Disrupt Axon Guidance in the Ventral Nerve Cord

The two primary axon bundles in *C. elegans* are the nerve ring in the head and the ventral nerve cord along the midline of the body. Most *C. elegans* neurons extend axons into at least one of these axon bundles (White et al., 1976, 1986). Four mutations in the *sax-3* gene were identified in a screen for mutations that affect the formation of the nerve ring (J. A. Z. and C. I. B., unpublished data). In these mutants, the nerve ring was found in an aberrant anterior position and many nerve ring axons were misrouted. While these defects are dramatic, they are difficult to analyze because little is known about the formation of the nerve ring during development. Therefore, we examined the function of *sax-3* in the better-understood ventral nerve cord. These studies were con-

Table 1. Axon Defects in Ventral Cord Interneurons in *sax-3* Mutants

	WT	<i>sax-3(ky123)</i>
Wild type (ventral view)	100%	80%
Axon crossover		20%
	n = 53	n = 60
Wild type (lateral view)		39%
Lateral axons	short <= vulva ¹	<1%
	> vulva ¹	55%
Premature termination	short <= vulva ¹	19%
		1%
	n = 122	n = 31

Axon phenotypes were scored in adults with the *glr-1::GFP* marker, which labels the following interneurons with axons in the ventral nerve cord: AVA, AVB, AVD, AVE, AVG, and PVC. Schematic drawings show the central third (top panel) or anterior third (bottom panel) of the animal. The vulva is indicated by a diamond. n = number of animals scored. Animals with more than one phenotype were scored in multiple categories, so percentages do not always add up to 100%. Nerve ring axon phenotypes were not scored.

¹ <= vulva, axons terminated before or at the vulva, a landmark halfway between the head and the tail. > vulva, axons terminated after passing the vulva. These refer to aberrant lateral axons in the lateral axon category and ventral cord axons in the premature termination category.

ducted with the mutation *sax-3(ky123)*, which is predicted to cause a strong loss of function based on its nerve ring phenotype (J. A. Z. and C. I. B., unpublished data) and the molecular lesion associated with it (see below).

To examine the overall structure of the ventral nerve cord, we made use of a *glr-1::GFP* transgene (Maricq et al., 1995). This gene is expressed at high levels in 11 neurons with axons in the ventral nerve cord. In wild-type animals, all of these axons are found in the right ventral nerve cord, and a single axon bundle is visible at the ventral side of the animal (Figures 1B and 1D). In *sax-3* mutants, two types of defects were observed. First, in over half of the animals one or more axons from head neurons were located in lateral positions instead of the ventral nerve cord (Figure 1C; Table 1). It was not possible to determine whether the same cells were affected in all animals. Infrequent termination of axons within the ventral nerve cord was also observed. In *sax-3* mutants, the cell bodies of the *glr-1::GFP*-expressing neurons were present in normal number and in the appropriate body region. Since no axons in the head normally follow the lateral trajectories observed in *sax-3* mutants, they appear to have a defect in guidance and not in neuronal cell fate determination.

Second, in *sax-3* mutants the *glr-1*-expressing axons within the ventral nerve cord were not restricted to the right-hand side but were instead found on both the right and left sides of the nerve cord (Figure 1E; Table 1). This unusual disorganization was most apparent at the vulva, where the left and right ventral cords are widely separated. In rare cases, the entire bundle of axons ran on the left instead of the right side; more often, a small

number of axons crossed the midline at some point in their trajectory. Except for these crossover events, the *glr-1*-expressing neurons were tightly fasciculated with one another, as they are in wild-type animals. Thus, *sax-3* functions both in the guidance of *glr-1::GFP*-expressing axons to the ventral midline and in their restriction to the right ventral nerve cord.

Single Axons Cross the Midline Multiple Times in *sax-3* Mutant Ventral Nerve Cords

To examine the behavior of single axons in *sax-3* mutants in greater detail, we made use of a transgene that labels a single pair of ventral cord axons. The two PVQ neurons have cell bodies in the tail and axons that travel the length of the ventral nerve cord: the PVQR axon in the right cord and the PVQL axon in the left cord. The PVQ axons in wild-type animals normally grow along the ventral midline without crossing it. An *sra-6::GFP* transgene is expressed in the PVQ axons and in no other axons in the ventral nerve cord (Troemel et al., 1995; Figure 1F). This transgene was introduced into *sax-3* mutants to characterize the morphology of the PVQ axons.

In *sax-3* mutants, the PVQ axons extended to their full length in the ventral nerve cord but repeatedly crossed the ventral midline (Figure 1G). One or more crossovers were observed in 55% of *sax-3(ky123)* mutant animals, compared to 5% of wild-type animals (n = 60 each). These defects at the ventral midline resemble those of the *Drosophila robo* mutant, where there is increased axon crossing of the ventral midline (Seeger et al., 1993). Individual animals displayed from one to six apparent crossover events throughout the length of the ventral nerve cord. The examination of single PVQ axons demonstrated that the midline crossing events were superimposed on a mostly normal longitudinal trajectory.

Similar crossover phenotypes were observed in the axons of the two serotonergic HSN motor neurons, visualized with antibodies to serotonin. In the wild type, each HSN motor neuron sends an axon ventrally to the midline and then anteriorly to the head without crossing the midline (Figure 2A). In *sax-3* mutants, the HSN axons were able to cross and recross the ventral midline (Figure 2B; Table 2; data not shown).

The HSN axon also had defects in the initial ventrally directed component of its outgrowth in *sax-3* mutants. In wild-type animals, the HSN axon grows ventrally to the nerve cord either immediately at the cell body or shortly anterior of the cell body (Figure 2C). In *sax-3* mutants, a high proportion of HSN axons traveled laterally for long distances before reaching the ventral nerve cord, either in an anterior direction or in an aberrant posterior direction (Figures 2D and 2E; Table 2). Thus, as was observed for the ventral cord interneurons, *sax-3* plays two roles in the guidance of the HSN motor neurons: it is required for growth along the epidermis to the ventral nerve cord and for selection of the ipsilateral nerve cord during anterior growth.

In summary, mutations in *sax-3* caused defects in axon guidance to the ventral nerve cord and disrupted the asymmetry between the right and left ventral nerve

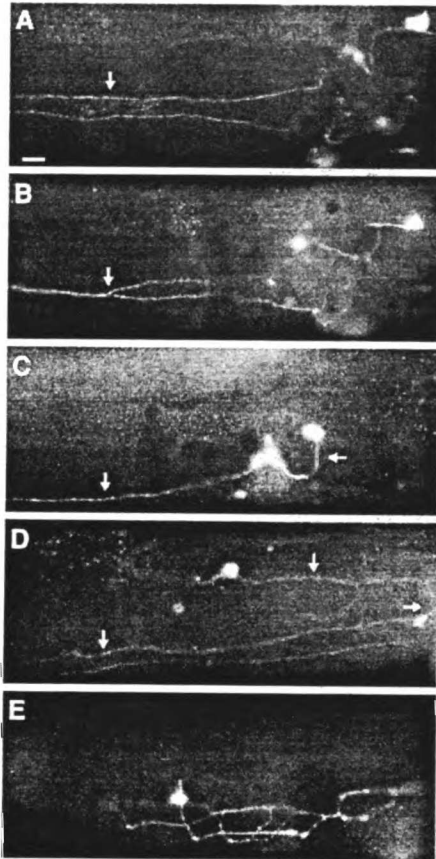


Figure 2. Disrupted Guidance of HSN Motor Neuron Axons to and within the Ventral Nerve Cord of *sax-3* Mutants

(A) Wild-type HSN morphology in a *sax-3(ky200ts)* animal raised at the permissive temperature, stained with anti-serotonin antibodies (ventrolateral view). The HSN motor axons do not cross the ventral midline (arrow).
 (B) Axon crossover defect in a *sax-3(ky200ts)* animal raised at the restrictive temperature (ventrolateral view). One HSN axon crosses the midline to join the axon on the other side (arrow).
 (C) Wild-type HSN axon in a *sax-3(ky200ts)* mutant grown at the permissive temperature (lateral view). The HSN axon (arrows) extends to the ventral midline soon after leaving the HSN cell body.
 (D and E) abnormal HSN axons in a *sax-3(ky198)* animal (D) and a *sax-3(ky200ts)* animal grown at the restrictive temperature (E). Some axons eventually reach the ventral nerve cord after long anterior or posterior detours (D), while others wander aimlessly in lateral regions (E). One HSN axon is marked with arrows in (D); the contralateral HSN axon is also visible, since this animal is slightly tilted. Anterior is at left in all panels. Scale bar = 10 μ m.

corde. These mutant phenotypes and the nerve ring defects in *sax-3* mutants suggest that *sax-3* functions to establish the major axon bundles of *C. elegans*.

SAX-3 Is a Member of the Immunoglobulin Superfamily

sax-3 was cloned using a combination of genetic mapping and transformation rescue of its mutant phenotype. Briefly, *sax-3* mapped to the X chromosome between the gene *fax-1* and the polymorphism *stP40*. Cosmid clones and subclones covering this region were assayed for rescue of the *sax-3* nerve ring axon phenotype (Figure 3A). cDNA clones for *sax-3* were isolated from the *C. elegans* EST project (a generous gift of Yuji Kohara), by screening a mixed-stage cDNA library (a generous gift of Bob Barstead) and by RT-PCR (see Experimental Procedures). These clones represented three alternatively spliced *sax-3* isoforms differing by nine amino acids in their cytoplasmic domains. The longest *sax-3* isoform was predicted to encode a 1273 amino acid protein (Figure 3B).

sax-3 encodes a novel transmembrane protein in the immunoglobulin superfamily. The SAX-3 protein was predicted to contain a hydrophobic signal sequence, an extracellular domain containing five immunoglobulin-like domains and three fibronectin type III repeats (amino acids 31–837), a transmembrane domain (amino acids 876–896), and a large cytoplasmic domain (Figures 3A and 3B). SAX-3 shares this modular structure with the *Drosophila* DRobo1 protein and with Robo homologs identified in *Drosophila* and vertebrates (Kidd et al., 1998a). SAX-3 is 35% identical to DRobo1 and 37% identical to hRobo1 in the extracellular domain. Despite lower conservation in the cytoplasmic domains, there are three conserved cytoplasmic motifs across all homologs (described in Kidd et al., 1998a). Another vertebrate protein, CDO, shares the five immunoglobulin domain/three fibronectin type III domain structure with SAX-3 and the Robo proteins, but is significantly less similar to the SAX-3/Robo family (Kang et al., 1997).

To confirm that this open reading frame represented the *sax-3* gene, we identified the mutations in the four *sax-3* alleles (Figures 3A and 3B). *sax-3(ky123)* deleted the signal sequence and the first exon of the gene, *sax-3(ky200ts)* was a proline to serine substitution in amino acid 37 of the first Ig domain, *sax-3(ky198)* disrupted a splice acceptor site before the seventh exon, and *sax-3(ky203)* introduced a stop codon that truncates the protein immediately after the transmembrane domain. Three of the mutations were G→A transition mutations, while the fourth mutation was a small deletion, consistent with the types of lesions induced by the chemical mutagen EMS. All four were recessive alleles and exhibited a similar spectrum of defects (J. A. Z. and C. I. B., unpublished data) consistent with their causing a loss of gene function.

sax-3::GFP Is Expressed Transiently in Neurons during Axon Outgrowth

To gain insight into *sax-3* expression, we generated a transgene in which the upstream regions and most of the *sax-3* coding region, including all large introns, were fused to an artificial transmembrane domain and the green fluorescent protein (GFP) reporter gene (Figures 3A and 3B). This transgene does not include all of *sax-3*, so it may not fully reflect transcriptional and posttranscriptional controls on *sax-3* expression. The *sax-3::GFP*

Table 2. Axon Defects in HSN Motor Neurons in *sax-3* Mutants

	WT	<i>sax-3(ty200ts)</i> 20° C	<i>sax-3(ty200ts)</i> 25° C	<i>sax-3(ty123)</i>
Wild-type HSN (ventral view)	100%	58%	8%	
Axon crossover		44%	91%	ND
		n = 79	n = 46	
Wild-type HSN (lateral view)	100%	88%	71%	40%
Defects in ventrally-directed growth axon wandering/branching			6%	8%
lateral axon ¹		3%	21%	36%
Defects in anteriorly-directed growth posterior axon ²		2%	7%	18%
	n = 55	n = 102	n = 154	n = 25

HSN axon phenotypes were characterized in adults stained with anti-serotonin antibodies. Schematic drawings show the anterior third (top panel) or central third (bottom panel) of the animal. Anterior is to the left. Animals with more than one phenotype were scored in multiple categories, so numbers do not always add up to 100%. n = number of neurons (bottom panel) or axon segments (top panel) scored (see Experimental Procedures).

¹ The lateral axon category included axons that grew in anterior or posterior directions.

² The posterior axon category included axons that grew in ventral or lateral positions.

transgene exhibited complex and dynamic expression. The fusion gene was expressed in most or all neurons at high levels as well as some hypodermal and muscle cells. In most neurons, *sax-3::GFP* expression was transient, peaking during the period of axon outgrowth.

sax-3::GFP expression was observed at highest levels in the embryo, particularly during the initial period of axon outgrowth at 350–400 min of development (comma stage, Figure 4A). The nerve ring and ventral nerve cords are formed within 1–2 hr of this time (Durbin, 1987). At the comma stage, the reporter gene is expressed at high levels in the anterior embryo, including most developing neurons of the nerve ring, and in a swath of ventral cells that includes the developing motor neurons of the ventral nerve cord and posterior neurons such as PVQ. A lower level of expression was observed in epidermal cells. Earlier in embryogenesis (200–400 cell stage; 200–300 min of development) *sax-3::GFP* was expressed in all epidermal cells at a low level. Later in embryogenesis (3-fold stage, >500 min of development), *sax-3::GFP* was expressed in the muscles that extend from the nerve ring to the anterior tip of the head. The early epidermal expression followed by later neuronal expression is similar to the expression of Robo protein in the *Drosophila* embryo (Kidd et al., 1998a).

By the first larval stage, the *sax-3::GFP* transgene was no longer expressed in most sensory neurons but persisted in motor neurons in the head including RMD, RMG, SMD, SIA, and SIB neurons; projection interneurons in the head and tail, including AVA, AVB, PVC, AVD, PVQ, and ALA neurons; and the sensory OLQ neurons (Figure 4B). This neuronal expression diminished slowly throughout postembryonic development. During the first

larval stage, *sax-3::GFP* expression continued in head muscles and appeared in muscles along the body wall, with ventral muscles expressing more strongly than dorsal muscles and anterior muscles expressing more strongly than posterior muscles (Figure 4B–4D). This expression persisted until the adult stage. Epidermal expression was rarely observed in larval stages.

Despite the general extinction of neuronal expression in larvae, *sax-3::GFP* expression appeared in the HSN motor neurons during the second larval stage. At this time, the HSN neurons begin to extend an axon from their lateral cell bodies toward the ventral midline (Figures 4C and 4D). The *sax-3::GFP* marker revealed an elaborate growth cone leading the HSN axon ventrally during the second larval stage (Figure 4C); the axon reaches the ventral nerve cord around the third larval stage (Figure 4D). *sax-3::GFP* expression continued in HSN during the fourth larval stage, when the HSN axon grows anteriorly to the head, and decreased in the adult stage after the completion of HSN axon outgrowth. *sax-3::GFP* expression in the adult included the motor neurons, interneurons, and sensory neurons listed above as well as postembryonic ventral cord motoneurons, some interneurons from the tail, and head, body wall, and vulval muscles.

SAX-3 Is Required at the Time of Axon Guidance

sax-3::GFP is expressed in neurons and in embryonic epidermis, consistent with a direct requirement for SAX-3 during axon guidance or an earlier role for SAX-3 in epidermal patterning events. One way to distinguish between these possibilities is to provide *sax-3* activity at different times during development. To ask when *sax-3*

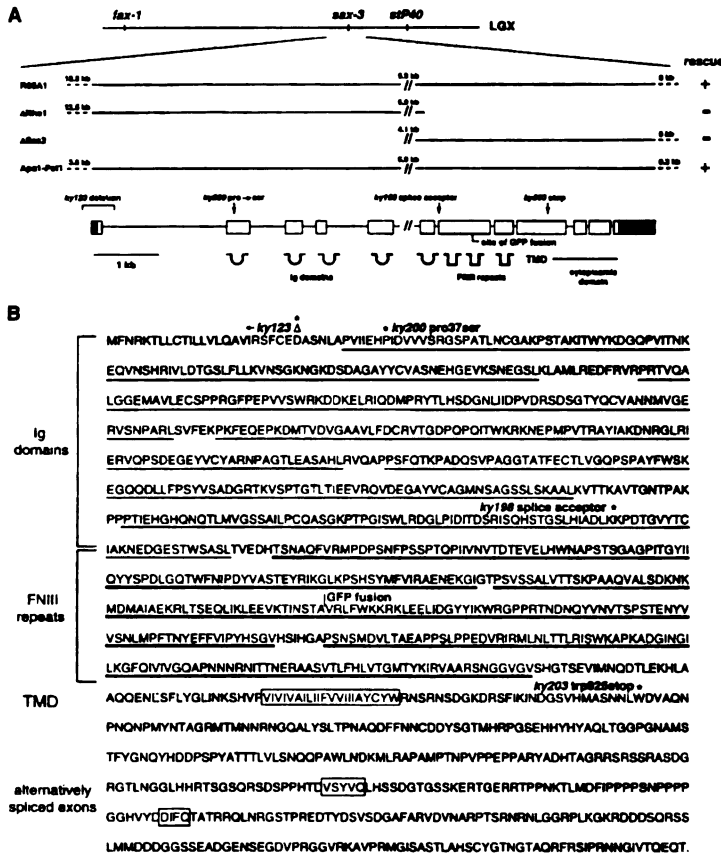


Figure 3. Molecular Analysis of *sax-3*

(A) Genetic map position and rescue of *sax-3* with cosmid clones and subclones, showing the genomic organization of the *SAX-3* coding region with sites of mutations and the site of the *sax-3::GFP* fusion marked. Exons are indicated by open boxes, and 5' and 3' untranslated regions by filled boxes.

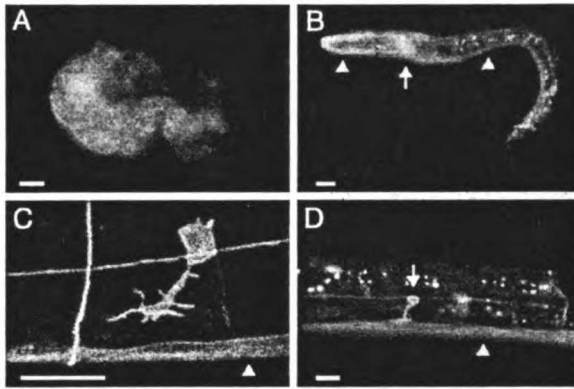
(B) Predicted protein sequence of *SAX-3*. Immunoglobulin domains are underlined, fibronectin type III domains are underlined in bold, and the predicted transmembrane domain and alternatively spliced exons are boxed. Asterisks denote sites of *sax-3* mutations, and the site of *GFP* fusion is indicated.

activity was required, we conducted temperature shift experiments with a temperature-sensitive allele, *sax-3(ky200ts)*. We examined three phenotypes: the formation of the nerve ring, which takes place in the embryo; the ventral outgrowth of the HSN axon, which takes place in the L2 stage; and the longitudinal growth of the HSN axon, which takes place in the L4 stage. All of these defects were more severe in *sax-3(ky200ts)* animals grown at 25°C than at 20°C (Figure 5; Table 2).

Temperature shift experiments with *sax-3(ky200ts)* animals indicated that *SAX-3* is required at different times in different neurons, correlating with the time of

their axon extension and guidance. *sax-3* activity was required embryonically for nerve ring axon guidance (Figure 5A). Animals raised at the permissive temperature during embryogenesis exhibited wild-type nerve ring axon morphology irrespective of the temperature they encountered in larval stages. Animals raised at the restrictive temperature in the embryo were mutant even if they were shifted to the permissive temperature immediately after embryogenesis. This embryonic requirement for *sax-3* function correlates with the time of axon extension into the nerve ring.

Additional temperature shift experiments revealed a



(C) is a confocal image obtained by Tim Yu; all other images are taken using conventional fluorescence microscopy. Anterior is at left and dorsal is up in all panels. Scale bars = 10 μ m.

Figure 4. Expression of *sax-3::GFP*

(A) Comma stage embryo. The anterior cells that express *sax-3::GFP* include developing neurons and epidermal cells. The ventral cells in the midbody are the ventral motor neuron precursors. Much weaker expression is observed in the lateral epidermal cells. (B) L1 stage larva. Expression is high in head motor neurons and interneurons (arrow). Muscles of the head and ventral body also express the transgene (arrowheads). Epidermal expression is absent by this time. No expression is observed in the immature HSN motor neurons. (C) L2 stage larva. The HSN motor neuron is extending a growth cone toward the ventral midline and expresses *sax-3::GFP* at high levels. Arrowhead denotes muscle expression. (D) L3 stage larva. The HSN axon has reached the ventral midline, but is not yet extending along the longitudinal bundles (arrow). The ventral muscles also express *sax-3::GFP* (arrowhead).

similar embryonic requirement for *sax-3* in the outgrowth of the PVQ axon, which grows longitudinally in the ventral nerve cord during embryogenesis. Only the temperature before the L1 stage was important for the midline crossing phenotype of the PVQ axon (data not shown).

Guidance of the HSN axon in later larval stages required postembryonic *sax-3* activity (Figures 5B and 5C). For the guidance of the HSN axon to the ventral midline, *sax-3* activity was most important during the L2 and L3 stages (Figure 5B). This requirement for *sax-3* coincides with the time that the HSN axon contacts the ventral midline and expresses *sax-3::GFP*, implicating *sax-3* function at the time of HSN guidance. By contrast, the patterning of epidermal cells and the axon outgrowth of all neurons in the ventral nerve cord other than the HSN take place in the embryo and L1 stages.

The midline crossing defect of the HSN axon had a more complicated temperature dependence (Figure 5C). Shifts to the permissive temperature demonstrated that *sax-3* activity provided as late as the L4 stage of development can rescue the HSN axon crossover defect. At this late time the HSN axon has reached the ventral midline and begun longitudinal outgrowth, indicating that *sax-3* activity prevents midline crossing during the time that the HSN axon extends in the longitudinal nerve cords. *sax-3* activity supplied in the adult could not repair the HSN midline crossing defect, indicating that *sax-3* cannot rescue HSN axons after they have crossed the midline. In the converse experiment, shifting animals to the restrictive temperature in the L1 stage or later did not result in excess midline crossing. These results indicate that *sax-3* activity either in the embryo or at the time of HSN outgrowth can prevent aberrant crossing of the ventral midline. One possible interpretation of these results is that HSN axons in the L4 stage can follow a normal uncrossed nerve cord in a wild-type environment (established in the embryo) without *sax-3* activity, but they require *sax-3* activity to extend in an abnormal nerve cord without crossing the midline.

Discussion

sax-3 mutants are defective in the axon guidance of neurons throughout the *C. elegans* nervous system, and SAX-3 is predicted to be a transmembrane protein in the immunoglobulin superfamily. SAX-3 could act either as a ligand or a receptor mediating cell interactions, or a receptor for cell-substrate interactions. The expression of *sax-3::GFP* in developing neurons suggests that SAX-3 acts as a receptor. Most strikingly, the induction of *sax-3::GFP* in the HSN correlates precisely with the onset of HSN axon outgrowth and with the temperature-sensitive period for ventral guidance of the HSN axon. A receptor function for SAX-3 is also suggested by its similarity to *Drosophila* Robo, which is expressed on the growth cones of developing axons (Kidd et al., 1998a). SAX-3 and the Robo family members have a five immunoglobulin/three fibronectin type III domain organization and substantial sequence similarity that identifies them as a new subfamily within the immunoglobulin superfamily.

SAX-3 is involved in the guidance of axons to the ventral nerve cord, the second largest axon bundle in *C. elegans*; in *sax-3* mutant animals, axons failed to navigate ventrally to the midline and instead traveled aberrantly in lateral positions. SAX-3 was also required for the proper organization of axons within the ventral nerve cord. In wild-type animals, the smaller left bundle and the larger right bundle of the ventral cord remain entirely separate throughout their trajectories as they extend in parallel along the length of the body (White et al., 1976, 1986). Mutations in *sax-3* disrupted the integrity of these bundles, allowing axons to cross repeatedly between the left and right sides of the ventral cord. However, the same axons were still able to extend normally in a longitudinal direction. Thus, the defect in *sax-3* mutants represents a defect in guidance rather than extension of ventral axons.

The repeated midline crossing and the associated loss

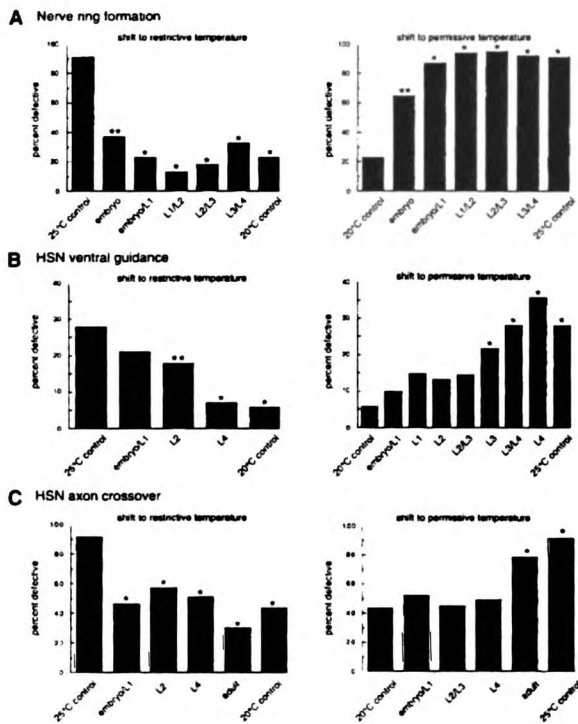


Figure 5. *sax-3* Activity Is Required at Different Times for Different Axon Guidance Events

Single asterisks denote values different from the left-hand control value at $p < 0.01$ (see Experimental Procedures). Double asterisks denote values different from both the 20°C and 25°C control values at $p < 0.02$.

(A) Temperature dependence of nerve ring formation in the *sax-3(ky200ts)* allele. All postembryonic shifts to the restrictive temperature were significantly different from the 25°C control ($\chi^2 > 65$, $p < 0.001$). All postembryonic shifts to the permissive temperature were significantly different from the 20°C control ($\chi^2 > 73$, $p < 0.001$). Embryonic temperature shifts were significantly different from both the 25°C control ($\chi^2 > 14$, $p < 0.001$) and the 20°C control ($\chi^2 > 7$, $p < 0.01$).

(B) Temperature dependence of ventral guidance of the HSN motor axons. Shift to the restrictive temperature in the embryo/L1 stage revealed no significant difference from the 25°C control ($\chi^2 = 1$, $p > 0.05$). However, shift to the restrictive temperature in the L2 stage partially rescued HSN ventral guidance, differing from both the 25°C control ($\chi^2 = 6.6$, $p = 0.01$) and the 20°C control ($\chi^2 = 6.1$, $p = 0.014$). Animals shifted to the restrictive temperature in the L4 stage were more completely rescued (L2 vs. L4 $\chi^2 = 5.9$, $p = 0.015$). In the converse experiment, shifts to the permissive temperature at any time before the L3 stage completely rescued HSN ventral guidance, with no significant difference from the 20°C control ($\chi^2 < 3$, $p > 0.05$). However, shifting to the permissive temperature in the L3 stage or later was not able to rescue the ventral defect of the HSN axon, differing from the 20°C control at $\chi^2 > 9$, $p < 0.01$.

(C) Temperature dependence of longitudinal guidance of the HSN motor axons. Shifts to

the permissive temperature up to the L4 stage rescued the HSN crossing defect (all larval shifts to the permissive temperature were indistinguishable from the 20°C control and differed from the 25°C control at $\chi^2 > 11$, $p < 0.001$). Conversely, shifts to the restrictive temperature up to the L4 stage did not result in midline crossing defects (all larval shifts to the restrictive temperature were statistically indistinguishable from the 20°C control and differed from the 25°C control at $\chi^2 > 11$, $p < 0.01$). Animals shifted in the adult stage were indistinguishable from animals that had not been shifted at all ($\chi^2 < 1.9$, $p > 0.05$) and significantly different from animals raised at the temperature to which they had been shifted ($\chi^2 > 11$, $p < 0.01$).

of ventral nerve asymmetry in *sax-3* mutants are unique mutant phenotypes in *C. elegans*. Nine genes that affect the extension of axons in the ventral nerve cord have been identified in previous mutant screens (*unc-14*, *-33*, *-34*, *-44*, *-51*, *-71*, *-73*, *-76*, and *vab-8*). In all cases, mutant axons terminate prematurely at a high frequency but maintain a strong bias of axons toward the right ventral cord (McIntire et al., 1992; Wightman et al., 1996). Seven other genes that do affect ventral cord asymmetry have activities that are opposite to *sax-3*; mutations in *unc-3*, *-30*, *-42*, *-115*, *fax-1*, *enu-1*, and *unc-61/netrin* reduce the number of axons in the left ventral cord (Wadsworth et al., 1996; Wightman et al., 1997). Cell ablation experiments have revealed an essential role for the PVPR neurons in establishing the left ventral nerve cord (Durbin, 1987); mutants with missing left nerve cords may be defective in PVPR function or the ability of other neurons to recognize PVPR.

The ventral cord crossover phenotypes of *sax-3* mutants are highly reminiscent of the phenotypes of *Drosophila robo* mutants (Seeger et al., 1993), a result that

is especially striking given the dissimilarity of the *Drosophila* and *C. elegans* ventral nerve cords. In *Drosophila*, most axons cross the midline once before projecting longitudinally. In *robo* mutants, the small fraction of axons that normally remain ipsilateral cross the midline, and axons that normally cross the midline once are thought to cross multiple times because of the dramatic thickening of mutant commissures (Seeger et al., 1993). In contrast to the extensive and symmetric arrangement of crossovers in the normal *Drosophila* CNS, *C. elegans* axons normally do not cross at all after they join the ventral nerve cord. However, in *sax-3* mutants the PVQ axon can cross the *C. elegans* midline multiple times, indicating that *robo* and *sax-3* both act to promote longitudinal fascicle integrity and prevent midline crossing. The sequence similarity between *sax-3* and *robo* (Kidd et al., 1998a) reveals a deep molecular homology in the organization of these different ventral nerve cords.

In *Drosophila* and vertebrates, the left and right longitudinal axon tracts are kept separate in part by a repulsive activity of the midline (Myers and Bastiani, 1993;

Seeger et al., 1993; Stoeckli and Landmesser, 1995; Stoeckli et al., 1997). *Drosophila* Robo has been hypothesized to act as a receptor for the putative midline repellent (Kidd et al., 1998a). From our studies in the *C. elegans* ventral nerve cord, we cannot distinguish whether *sax-3* acts to promote growth along the longitudinal fascicles or to prevent growth across the midline. The ligand (or receptor) for SAX-3 could be an attractive molecule on axons, a repulsive molecule on the hypodermal ridge, or both. However, other *C. elegans* mutants with defasciculated nerve cords do not exhibit extensive midline crossing, indicating that decreased access to other axons does not drive midline crossing by default (McIntire et al., 1992). Moreover, in *sax-3* mutants most *glr-1*-expressing axons in the ventral nerve cord fasciculate normally when they are not crossing the midline, indicating that *sax-3* does not disrupt all cell-cell recognition in the ventral cord. One suggestive result implicating *sax-3* in midline repulsion is that *sax-3* activity provided in the L4 stage can prevent HSN midline crossing. At this stage, the earlier axons in the left ventral nerve cord (PVPR and PVQL) have completed their outgrowth; the HSN axon typically fasciculates with these axons on the left side (Garriga et al., 1993). Animals raised at the restrictive temperature during embryogenesis have extensive PVQ crossover defects and possibly PVP crossover defects as well. However, if *sax-3* activity is provided beginning in the L4 stage, the HSN axon does not aberrantly cross the midline. In this context, the left HSN axon presumably had a choice between aberrantly crossing the midline along with its normal neighbors or remaining on the left side without its longitudinal neighbors. Since it remained on the left side in a *sax-3*-dependent fashion, *sax-3* is more strongly implicated in a midline interaction than in fasciculation with specific ventral cord axons.

In addition to its role at the ventral midline, our results also suggest a role for *sax-3* in other guidance events. In particular, *sax-3* was required for guidance of the HSN axon from the lateral HSN cell body to the ventral midline. The HSN axon migrates over epidermis to reach the ventral nerve cord, guided by interactions with epidermal cells but not by other axons or egg-laying muscles (Garriga et al., 1993). In animals that lack SAX-3, up to half of HSN axons travel long distances in lateral positions before reaching the midline. These axons migrate along nerve bundles and hypodermal regions that are normally barren of HSN axon outgrowth.

SAX-3 may cooperate with different adhesion or guidance molecules in different cell contexts. SAX-3 acts together with UNC-6/netrin to guide the HSN axon to the ventral nerve cord. Mutations in *sax-3* also affect cell migrations, including the posteriorly directed migration of the CAN neurons and the anteriorly directed migration of the HSN neurons (J. A. Z. and C. I. B., unpublished data). These cell migrations are affected in similar ways by the *C. elegans* α integrin gene *ina-1* (Baum and Garriga, 1997), but they are not affected by *unc-6*. Thus, in cell migration SAX-3 may act in concert with integrin-mediated adhesion pathways and possibly a *frizzled* pathway as well (S. Clark and C. I. B., unpublished data). *sax-3* also participates in other guidance events that are less well understood (J. A. Z. and C. I. B., unpublished

data), including its requirement for proper placement of the nerve ring, the major circumferential axon bundle in the head of the animal (White et al., 1986).

sax-3 affects many types of guidance and cell recognition events (J. A. Z. and C. I. B., unpublished data) and one possibility is that SAX-3 might act as a ligand or a receptor in different contexts. Cell-associated cues can be bidirectional: for example, transmembrane members of the Eph immunoglobulin domain-tyrosine kinase family can function either as receptors for transmembrane or GPI-linked ephrin ligands or as ligands for transmembrane ephrins (Friedman and O'Leary, 1996; Holland et al., 1996; Drescher et al., 1997). A more diverse set of SAX-3 functions is plausible if it acts as a multifunctional axon guidance molecule.

Sequential induction of different guidance molecules could also contribute to the regulated integration of guidance cues. It is intriguing that another molecule with five immunoglobulin domains and three fibronectin type III domains, the CDO protein, is regulated by multiple receptor systems (Kang et al., 1997). CDO is transcriptionally repressed by tyrosine kinase signaling pathways, which are known to influence axon guidance. In addition, the CDO protein is posttranscriptionally down-regulated when cells lose contact with their substrate. Similarly, the activity of *Drosophila* Robo may be inhibited by the action of Commissureless (Comm), a transmembrane protein that is required for axons to cross the midline (Seeger et al., 1993; Tear et al., 1996; Kidd et al., 1998b). Conceptually similar events occur during lymphocyte adhesion, where activation of one type of adhesion molecule, such as a lectin, permits the subsequent engagement of an integrin receptor (Luscinskas et al., 1994). Regulation of SAX-3 activity by other types of guidance systems could provide spatial and temporal precision to a broadly acting cell recognition system.

Experimental Procedures

Strains and Genetics

Wild-type animals were *C. elegans* variety Bristol, strain N2. Strains were maintained using standard methods (Brenner, 1974). Animals were grown at 20°C except for the *sax-3(ky200)* strain, which was grown at either 20°C or 25°C, as noted. Some strains were provided by the Caenorhabditis Genetic Center.

sax-3 mutant alleles were isolated by EMS mutagenesis (J. A. Z. and C. I. B., unpublished data). The nerve ring axon defect of *sax-3(ky123)* was mapped to LGX under the *mnDp57* duplication. Three-factor mapping was conducted to further localize *sax-3* on LGX. 8/12 *unc-20 non-lon-2* recombinants and 6/9 *lon-2 non-unc-20* recombinants were mutant for *sax-3*. 20/20 *lon-2 non-dpy-23* recombinants were mutant for *sax-3*. 15/15 *lon-2 non-lin-18 unc-78* recombinants and 5/6 *lon-2 lin-18 non-unc-78* recombinants were mutant for *sax-3*. 36/39 *lon-2 non-fax-1* recombinants segregated *sax-3*.

The *stP40* restriction fragment length polymorphism that differs between the Bristol strains RW7000 and N2 was used to further map *sax-3*. Recombinants were isolated from *sax-3(ky123) lon-2(e648)/RW7000* heterozygotes, and 2/6 *sax-3 non-lon-2* recombinants and 15/16 *lon-2 non-sax-3* recombinants segregated the *stP40* polymorphism. These mapping data placed *sax-3* between *fax-1* and *stP40* on LGX.

Germline Transformation

Transgenic strains were created as previously described (Mello et al., 1991). Multiple lines from each injection were characterized for rescue of the nerve ring phenotype. Cosmids spanning the region between *fax-1* and *stP40* were injected at 10 ng/ μ l in pools of 4-5

cosmids using the dominant pRF4 *rol-6(su1006)* plasmid at 100 ng/ μ l as a co-injection marker. Cosmids from the rescuing pool were injected individually at 30 ng/ μ l, identifying R06A1 as the single rescuing cosmid. An ApaI-PstI subclone of R06A1 rescued the *sax-3* mutant phenotype at 10–30 ng/ μ l. This subclone contained 3.8 kb upstream of the start codon, the entire *sax-3* open reading frame, the *sax-3* 3' UTR, and 0.2 kb of downstream sequence.

cDNA Isolation and Allele Sequencing

27 partial *sax-3* cDNAs were isolated by screening approximately 5×10^5 plaques of a mixed stage *C. elegans* cDNA library at high stringency (Barstead and Waterston, 1989) with the yk142c5 cDNA probe (a gift from Y. Kohara). Nine cDNAs were sequenced in their entirety and the rest partially sequenced. The longest cDNA represented amino acid 459 to the 3' end of the gene with a 3' UTR of 562 nucleotides. Of ten cDNAs sequenced across the alternatively spliced exons, four contained both exons, four contained the first but not the second exon, and two did not contain either exon.

The 5' end of the *sax-3* coding region was identified by RT-PCR from wild-type N2 RNA prepared by Trizol extraction (GIBCO), using primers from the *sax-3* coding region and the *C. elegans* splice leader SL1. The *sax-3* sequence was confirmed and its genomic organization determined by aligning the cDNA with the reported genomic sequence from the *C. elegans* genome sequencing consortium (Sulston et al., 1992).

To identify the mutations in the four *sax-3* alleles, the open reading frame and splice junctions of the mutant alleles were amplified using the Expand PCR kit (Boehringer Mannheim) from genomic DNA preparations of the mutant strains. PCR fragments were sequenced on one strand using the *fmo1* sequencing kit (Promega). Mutations were confirmed by sequencing the complementary strand on a separately amplified PCR fragment.

DNA manipulations were performed according to standard protocols (Sambrook et al., 1989).

Characterization of Neuronal Morphology

Axons visualized with integrated GFP transgenes were scored in living adult animals. Nerve ring axons were visualized with an integrated *ceh-23::GFP* transgene (strain CX2627, *kyls4 X*; J. A. Z. and C. I. B., unpublished data). Ventral cord axons were visualized with an integrated *glr-1::GFP* transgene (strain CX2835, *kyls29 X*) (Maricq et al., 1995). The PVQ interneurons were visualized with an integrated *sra-6::GFP* transgene (strain CX3350, *kyls39 I*, integrated by David Kwan) (Troemel et al., 1995). Animals were mounted on 2.5% agarose pads containing 5 mM sodium azide or in buffer solution containing 5 mM sodium azide.

HSN motor neuron morphology was examined by staining fixed adult animals with antibodies to serotonin as previously described (Desai et al., 1988). Quantitation of HSN phenotypes was conducted on mutant strains that did not contain a GFP transgene. For the HSN axon crossover phenotype (Table 2, top panel), penetrance calculations represent the number of crossover events per half-length of the HSN trajectory, since the complete HSN trajectory in the ventral cord could not be scored in every animal. For the HSN ventrally directed and anteriorly directed outgrowth (Table 2, bottom panel), penetrance calculations represent the percent of neurons with defects. Animals were visualized by fluorescence microscopy. Photographs were scanned into a computer graphics file using a Nikon Scanner and assembled using the Adobe Photoshop program. Figures 1B and 1C show animals that were fixed for 1 hr at 4°C in 4% paraformaldehyde to reduce background autofluorescence (a modified version of the first step of the anti-serotonin antibody staining protocol [Desai et al., 1988]).

sax-3 Expression Analysis

A translational *sax-3::GFP* fusion was constructed by cloning a blunt ApaI-EagI fragment from the ApaI-PstI R06A1 rescuing subclone in frame into the SmaI site of the GFP expression vector pPD95.75 (A. Fire, et al., personal communication). This construct contained the 3.8 kb of *sax-3* upstream sequence present in the rescuing subclone, the first 667 amino acids of the *sax-3* open reading frame, including the five Ig domains and the first FNIII domain, as well as the first six introns. The *sax-3::GFP* transgene was

injected at 100 ng/ μ l into *lin-15(n765ts)* X mutant animals using a *lin-15(+)* plasmid at 30 ng/ μ l as a co-injection marker (Huang et al., 1994). Transformants were maintained by picking animals rescued for the *lin-15* multivulval phenotype. The *sax-3* expression pattern was assessed in variably mosaic animals that contained the *sax-3::GFP* plasmid as unstable extrachromosomal DNA.

The transgenic line in which expression was analyzed appeared to have mostly normal morphology of *sax-3::GFP*-expressing cells. However, disruption of neuronal morphology was observed in some animals.

Temperature Shift Experiments

Animals grown at 20°C were synchronized by collecting embryos laid by adults over a 3–5 hr time period. Animals grown at 25°C were synchronized by washing off adults and larvae from a plate, leaving behind unhatched eggs, which were transferred to a new plate for subsequent temperature shifts. Nerve ring phenotypes were scored using the *ceh-23::GFP* transgene. HSN phenotypes were scored by staining with anti-serotonin antibodies. Animals were fixed as adults at a time point at least 24 hr after they were shifted to a new temperature. Between 30 and 365 animals were scored at all data points, except the embryo/L1 shifts in Figure 5C ($n = 13$ and 21); an average of around 100 animals were scored per data point. Data points were compared to the control using the χ^2 statistic and the Primer of Biostatistics program (Stanton A. Glantz, McGraw-Hill Publishers).

Acknowledgments

We are grateful to Tom Kidd and Corey Goodman for insightful discussions, sharing results before publication, and their analysis of the *SAX-3* and Robo sequences. We thank Shannon Grantner, Luqin Tong, and Yongmei Zhang for excellent technical support; Tim Yu for generating the confocal images of *sax-3::GFP*; Yuji Kohara for a partial *sax-3* cDNA; Bob Barstead for the mixed-stage cDNA library; David Kwan for integrating the *sra-6::GFP* transgene; Bruce Wightman and Paul Baum for mapping markers; and Gian Garriga, Katja Brose, Tim Yu, Zemer Gitai, Erni Peckol, Noelle L'Etolle, and Erik Lundquist for critiques of the manuscript. This work was supported by the Howard Hughes Medical Institute. J. A. Z. is an NSF predoctoral fellow, and C. I. B. is an Assistant Investigator of the Howard Hughes Medical Institute.

Received October 20, 1997; revised November 24, 1997.

References

- Barstead, R.J., and Waterston, R.H. (1989). The basal component of the nematode dense-body is vinculin. *J. Biol. Chem.* 264, 10177–10185.
- Baum, P.D., and Garriga, G. (1997). Neuronal migrations and axon fasciculation are disrupted in *ina-1* integrin mutants. *Neuron* 19, 51–62.
- Brenner, S. (1974). The genetics of *Caenorhabditis elegans*. *Genetics* 77, 71–94.
- Chan, S.S., Zheng, H., Su, M.W., Wilk, R., Killeen, M.T., Hedgecock, E.M., and Culotti, J.G. (1996). UNC-40, a *C. elegans* homolog of DCC (Deleted in Colorectal Cancer), is required in motile cells responding to UNC-6 netrin cues. *Cell* 87, 187–195.
- Desai, C., Garriga, G., McIntire, S.L., and Horvitz, H.R. (1988). A genetic pathway for the development of the *Caenorhabditis elegans* HSN motor neurons. *Nature* 336, 638–646.
- Drescher, U., Bonhoeffer, F., and Müller, B.K. (1997). The Eph family in retinal axon guidance. *Curr. Opin. Neurobiol.* 7, 75–80.
- Durbin, R.M. (1987). Studies on the development and organization of the nervous system of *Caenorhabditis elegans*. PhD thesis, University of Cambridge, Cambridge, England.
- Friedman, G.C., and O'Leary, D.D. (1996). Eph receptor tyrosine kinases and their ligands in neural development. *Curr. Opin. Neurobiol.* 6, 127–133.
- Garriga, G., Desai, C., and Horvitz, H. (1993). Cell interactions control

- the direction of outgrowth, branching and fasciculation of the HSN axons of *Caenorhabditis elegans*. *Development* 117, 1071-1087.
- Goodman, C.S. (1996). Mechanisms and molecules that control growth cone guidance. *Annu. Rev. Neurosci.* 19, 341-377.
- Hamein, M., Zhou, Y., Su, M., Scott, I., and Culotti, J. (1993). Expression of the UNC-5 guidance receptor in the touch neurons of *C. elegans* steers their axons dorsally. *Nature* 364, 327-330.
- Harris, R., Sabatelli, L.M., and Seeger, M.A. (1996). Guidance cues at the *Drosophila* CNS midline: identification and characterization of two *Drosophila* Netrin/UNC-6 homologs. *Neuron* 17, 217-228.
- Hedgecock, E.M., Culotti, J.G., and Hall, D.H. (1990). The *unc-5*, *unc-6*, and *unc-40* genes guide circumferential migrations of pioneer axons and mesodermal cells on the epidermis in *C. elegans*. *Neuron* 4, 61-85.
- Holland, S.J., Gale, N.W., Mbaruku, G., Yancopoulos, G.D., Henkemeyer, M., and Pawson, T. (1996). Bidirectional signaling through the EPH-family receptor Nuk and its transmembrane ligands. *Nature* 383, 722-725.
- Huang, L.S., Tzou, P., and Sternberg, P.W. (1994). The *lin-15* locus encodes two negative regulators of *Caenorhabditis elegans* vulval development. *Mol. Biol. Cell* 5, 395-412.
- Ishii, N., Wadsworth, W.G., Stern, B.D., Culotti, J.G., and Hedgecock, E.M. (1992). UNC-6, a laminin-related protein, guides cell and pioneer axon migrations in *C. elegans*. *Neuron* 9, 873-881.
- Kang, J.S., Gao, M., Feinleib, J.L., Cotter, P.D., Guadagno, S.N., and Krauss, R.S. (1997). CDO: an oncogene-, serum-, and anchorage-regulated member of the Ig/fibronectin type III repeat family. *J. Cell Biol.* 138, 203-213.
- Keino-Masu, K., Masu, M., Hinck, L., Leonardo, E.D., Chan, S.S., Culotti, J.G., and Tessier-Lavigne, M. (1996). *Deleted in Colorectal Cancer (DCC)* encodes a netrin receptor. *Cell* 87, 175-185.
- Kennedy, T.E., Serafini, T., de la Torre, J.R., and Tessier-Lavigne, M. (1994). Netrins are diffusible chemotropic factors for commissural axons in the embryonic spinal cord. *Cell* 78, 425-435.
- Keynes, R., and Cook, G.M. (1995). Axon guidance molecules. *Cell* 83, 161-169.
- Kidd, T., Brose, K., Mitchell, K.J., Fetter, R.D., Tessier-Lavigne, M., Goodman, C.S., and Tear, G. (1998a). Roundabout controls axon crossing of the CNS midline and defines a novel subfamily of evolutionarily conserved guidance receptors. *Cell* 92, this issue, 205-215.
- Kidd, T., Russell, C., Goodman, C.S., and Tear, G. (1998b). Dosage-sensitive and complementary functions of Roundabout and Commissureless control axon crossing of the CNS midline. *Neuron* 20, 25-33.
- Kolodziej, P.A., Timpe, L.C., Mitchell, K.J., Fried, S.R., Goodman, C.S., Jan, L.Y., and Jan, Y.N. (1996). *frizzled* encodes a *Drosophila* member of the DCC immunoglobulin subfamily and is required for CNS and motor axon guidance. *Cell* 87, 197-204.
- Leung-Hagsteyn, C., Spence, A.M., Stern, B.D., Zhou, Y., Su, M.W., Hedgecock, E.M., and Culotti, J.G. (1992). UNC-5, a transmembrane protein with immunoglobulin and thrombospondin type 1 domains, guides cell and pioneer axon migrations in *C. elegans*. *Cell* 71, 289-299.
- Luscinskas, F.W., Kansas, G.S., Ding, H., Pizcueta, P., Schlieffenbaum, B.E., Tedder, T.F., and Gimbrone, M.A.J. (1994). Monocyte rolling, arrest and spreading on IL-4-activated vascular endothelium under flow is mediated via sequential action of L-selectin, beta 1-integrins, and beta 2-integrins. *J. Cell Biol.* 125, 1417-1427.
- Maricq, A.V., Peckol, E., Driscoll, M., and Bargmann, C.I. (1995). Mechanosensory signaling in *C. elegans* mediated by the GLR-1 glutamate receptor. *Nature* 378, 78-81.
- McIntire, S.L., Garriga, G., White, J., Jacobson, D., and Horvitz, H.R. (1992). Genes necessary for directed axonal elongation or fasciculation in *Caenorhabditis elegans*. *Neuron* 8, 307-322.
- Mello, C.C., Kramer, J.M., Stinchcomb, D., and Ambros, V. (1991). Efficient gene transfer in *C. elegans*: extrachromosomal maintenance and integration of transforming sequences. *EMBO J.* 10, 3959-3970.
- Mitchell, K.J., Doyle, J.L., Serafini, T., Kennedy, T.E., Tessier-Lavigne, M., Goodman, C.S., and Dickson, B.J. (1996). Genetic analysis of Netrin genes in *Drosophila*: netrins guide CNS commissural axons and peripheral motor axons. *Neuron* 17, 203-215.
- Myers, P.Z., and Bastiani, M.J. (1993). Growth cone dynamics during the migration of an identified commissural growth cone. *J. Neurosci.* 13, 127-143.
- Sambrook, J., Fritsch, E.F., and Maniatis, T. (1989). *Molecular Cloning: A Laboratory Manual*. (Cold Spring Harbor, NY: Cold Spring Harbor Press).
- Seeger, M., Tear, G., Ferrer-Marco, D., and Goodman, C.S. (1993). Mutations affecting growth cone guidance in *Drosophila*: genes necessary for guidance toward or away from the midline. *Neuron* 10, 409-426.
- Serafini, T., Kennedy, T.E., Galke, M.J., Mirzayan, C., Jessell, T.M., and Tessier-Lavigne, M. (1994). The netrins define a family of axon outgrowth-promoting proteins homologous to *C. elegans* UNC-6. *Cell* 78, 409-424.
- Serafini, T., Colamarino, S.A., Leonardo, E.D., Wang, H., Bedington, R., Skarnes, W.C., and Tessier-Lavigne, M. (1996). Netrin-1 is required for commissural axon guidance in the developing vertebrate nervous system. *Cell* 87, 1001-1014.
- Stoeckli, E.T., and Landmesser, L.T. (1995). Axonin-1, Nr-CAM, and Ng-CAM play different roles in the *in vivo* guidance of chick commissural neurons. *Neuron* 14, 1165-1179.
- Stoeckli, E.T., Sonderegger, P., Pollerberg, G.E., and Landmesser, L.T. (1997). Interference with axonin-1 and NrCAM interactions unmasks a floor-plate activity inhibitory for commissural axons. *Neuron* 18, 209-221.
- Sulston, J., Du, Z., Thomas, K., Wilson, R., Hillier, L., Staden, R., Halloran, N., Green, P., Thierry-Mieg, J., Qiu, L., et al. (1992). The *C. elegans* genome sequencing project: a beginning. *Nature* 356, 37-41.
- Tear, G., Harris, R., Sutaria, S., Kilomanski, K., Goodman, C.S., and Seeger, M.A. (1996). *commissureless* controls growth cone guidance across the CNS midline in *Drosophila* and encodes a novel membrane protein. *Neuron* 16, 501-514.
- Tessier-Lavigne, M., and Goodman, C.S. (1996). The molecular biology of axon guidance. *Science* 274, 1123-1133.
- Troemel, E.R., Chou, J.H., Dwyer, N.D., Colbert, H.A., and Bargmann, C.I. (1995). Divergent seven transmembrane receptors are candidate chemosensory receptors in *C. elegans*. *Cell* 83, 207-218.
- Wadsworth, W.G., Bhatt, H., and Hedgecock, E.M. (1996). Neuroglia and pioneer neurons express UNC-6 to provide global and local netrin cues for guiding migrations in *C. elegans*. *Neuron* 16, 35-46.
- White, J.G., Southgate, E., Thomson, J.N., and Brenner, S. (1976). The structure of the ventral nerve cord of *Caenorhabditis elegans*. *Phil. Transact. R. Soc. Lond. B* 275, 327-48.
- White, J.G., Southgate, E., Thomson, J.N., and Brenner, S. (1986). The structure of the nervous system of the nematode *Caenorhabditis elegans*. *Phil. Transact. R. Soc. Lond. B* 314, 1-340.
- Wightman, B., Clark, S.G., Taskar, A.M., Forrester, W.C., Maricq, A.V., Bargmann, C.I., and Garriga, G. (1996). The *C. elegans* gene *vab-8* guides posteriorly directed axon outgrowth and cell migration. *Development* 122, 671-682.
- Wightman, B., Baran, R., and Garriga, G. (1997). Genes that guide growth cones along the *C. elegans* ventral nerve cord. *Development* 124, 2571-2580.

GenBank Accession Number

The GenBank accession number for *sax-3* is AF041053.

Chapter Four

Neuronal cell shape and neuritogenesis are regulated by the Ndr kinase SAX-1,
a member of the Orb6/COT-1/Warts serine/threonine kinase family

Abstract

The *C. elegans sax-1* gene is required to prevent excessive neuronal cell spreading and neurite outgrowth. Neuronal cell bodies in *sax-1* mutants appear expanded and irregular, whereas normal cells are compact and spherical. Mutant neurons also extend ectopic neurites in addition to axonal and dendritic projections, suggesting a defect in cell polarity. *sax-1* encodes a serine/threonine kinase in the Ndr family that is related to Orb6 (*S. pombe*), Warts/Lats (*Drosophila*) and COT-1 (*Neurospora*) kinases that function in cell shape regulation. These kinases are distantly related to Rho kinases, but lack Rho binding domains. Dominant negative mutations in the *C. elegans* RHOA GTPase caused cell shape defects similar to those of *sax-1* mutants, suggesting that GTPase signaling may also affect neuronal cell shape. In some sensory neurons, sensory activity regulates neurite formation in a pathway that involves the UNC-43 calcium/calmodulin-regulated kinase. SAX-1 acts in parallel to this activity-dependent pathway, but an *unc-43* gain of function mutation can partially suppress *sax-1* mutant defects, suggesting that these two pathways may converge on common targets in the regulation of neuronal morphology.

Introduction

Cell morphology is determined by the intrinsic properties of a cell and its interactions with other cells, diffusible factors and the extracellular matrix. Neurons adopt particularly complex morphologies: a typical neuron has a defined cell body, a branched or unbranched axon, and one or more dendrites. In recent years, substantial progress has been made in understanding the extrinsic cues that regulate axon guidance and branching (Tessier-Lavigne and Goodman, 1996; Mueller, 1999; Wang *et al.*, 1999), but less is known about the intrinsic determinants of cell structure. For example, polarized epithelial

and neuronal cells utilize common molecules to establish distinct subcellular compartments (Kaech *et al.*, 1998; Rongo *et al.*, 1998); however, it is not understood how these molecules create distinct morphologies in different cell types. Furthermore, neurons differentiate single or multiple axonal and dendritic processes, but the mechanisms that determine the number and site of neurite initiation are unknown.

Regulation of the actin cytoskeleton by Rho family GTPases is a critical determinant of cell morphology (Hall, 1994). Gain of function and dominant negative experiments in mammalian cells and *Drosophila* implicate Cdc42 in the formation of filopodia, Rac in membrane ruffling, and both Cdc42 and Rac in axon outgrowth (Ridley *et al.*, 1992; Luo *et al.*, 1994; Kozma *et al.*, 1995; Nobes and Hall, 1995; Luo *et al.*, 1997). By contrast, Rho is implicated in contractile events such as stress fiber formation and neurite retraction (Paterson *et al.*, 1990; Ridley and Hall, 1992; Gebbink *et al.*, 1997). These GTPases exert their activity through binding and regulating multiple targets, including actin-binding proteins and several classes of kinases (Tapon and Hall, 1997).

Rho GTPase is specifically implicated in the regulation of stable properties of cell shape, perhaps by regulating the activity of Rho kinases. The Rho kinase family includes Rho kinase (Leung *et al.*, 1995; Ishizaki *et al.*, 1996; Matsui *et al.*, 1996), LET-502 (Wissmann *et al.*, 1997), Genghis Khan (Luo *et al.*, 1997), Citron (Di Cunto *et al.*, 1998; Madaule *et al.*, 1998) and MRCK (Leung *et al.*, 1998). These proteins share a related kinase catalytic domain as well as domains that allow GTPase association. Mutations in the *C. elegans* LET-502 kinase prevent the epidermal cell shape changes that drive embryonic elongation, while mutations in Genghis Khan disrupt actin structures in the *Drosophila* egg chamber (Luo *et al.*, 1997; Wissmann *et al.*, 1997). These phenotypes, together with functional studies in cultured cells (Leung *et al.*, 1996; Amano *et al.*, 1997; Ishizaki *et al.*, 1997), implicate Rho kinases in the regulation of cell morphology.

Members of a distinct family of serine/threonine kinases, including Orb6, COT-1 and Warts/Lats, are required for the regulation of cell morphology in diverse organisms;

mutations in these kinases cause aberrant cell growth and spreading (Yarden *et al.*, 1992; Justice *et al.*, 1995; Xu *et al.*, 1995; Verde *et al.*, 1998). Kinases in the Orb6/COT-1/Warts family are closely related to Rho kinases in the kinase catalytic domain but lack Rho-binding motifs. The pathways that regulate these kinases are unknown; however, Orb6 may function downstream of the Pak1/Shk1 kinase (Verde *et al.*, 1998), which functions together with the Cdc42 GTPase in morphological regulation (Marcus *et al.*, 1995; Otilie *et al.*, 1995). Studies of an expressed sequence tag (EST) in *C. elegans* led to the identification of Ndr, a new member of the Orb6/COT-1/Warts kinase family that is conserved in *C. elegans*, *Drosophila* and humans (Millward *et al.*, 1995). However, the *in vivo* function of the Ndr kinases is not known.

A screen for mutants with altered neuronal morphology in *C. elegans* identified mutations in the *sax-1* gene (Zallen *et al.*, submitted/Chapter 2). Here we show that *sax-1* encodes the *C. elegans* Ndr kinase, a member of the Orb6/COT-1/Warts family. *sax-1* mutants exhibit defects in neuronal cell shape and polarity: cells appear expanded and irregular instead of compact and spherical, and they initiate ectopic neurites in addition to the normal axon and dendrite. Cell shape defects are also caused by dominant negative mutations in the *C. elegans* RHOA GTPase, in a pathway that functions at least partly in parallel to SAX-1. In sensory neurons, ectopic neurites are also caused by mutations that disrupt neuronal activity (Coburn and Bargmann, 1996; Coburn *et al.*, 1998; Peckol *et al.*, 1999). We find that the activity-dependent pathway for neurite outgrowth is mediated by the UNC-43 calcium/calmodulin-dependent protein kinase II (CaMKII) and functions in parallel with the SAX-1 kinase to regulate neuronal morphology.

Materials and Methods

Strains and genetics

Wild-type animals were *C. elegans* variety Bristol, strain N2. Strains were maintained using standard methods (Brenner, 1974). Animals were grown at 20°C or 25°C, as indicated. Some strains were provided by the *Caenorhabditis* Genetic Center.

sax-1 and *sax-2* mutant alleles (Zallen *et al.*, submitted/Chapter 2) were outcrossed twice by *kyIs4* X; *him-5(e1490)* V, once by *kyIs4* X and once by N2. Axon defects detected by the *ceh-23::gfp kyIs4* transgene were followed to map *sax-1(ky211)* to LGX. 5/5 *lon-2* non *lin-18 unc-78* recombinants and 2/4 *lon-2 lin-18* non-*unc-78* recombinants were mutant for *sax-1*. 2/7 *lon-2* non-*fax-1* recombinants were mutant for *sax-1*.

The stP40 restriction fragment length polymorphism that differs between the Bristol strains RW7000 and N2 was used to further map *sax-1*. Recombinants were isolated from *unc-20(e112ts) sax-1(ky211) lon-2(e648)/RW7000* heterozygotes. 0/3 *unc-20 sax-1* non-*lon-2* recombinants and 2/2 *unc-20* non-*sax-1 lon-2* recombinants segregated the stP40 polymorphism. 0/2 *lon-2 sax-1* non-*unc-20* recombinants segregated the stP40 polymorphism and 3/3 *lon-2* non *sax-1 unc-20* recombinants segregated the stP40 polymorphism. These mapping data placed *sax-1* to the left of *lin-18* and to the right or close on the left of stP40 on LGX.

Germline Transformation

Transgenic strains were created as described (Mello *et al.*, 1991). Multiple lines from each injection were characterized for rescue of the nerve ring phenotype in a *sax-1(ky211) kyIs4* X strain. Cosmids spanning the region between stP40 and *lin-18* were injected at 10 ng/μl each in pools of 4-5 cosmids using the dominant pRF4 *rol-6(su1006)* plasmid at 100 ng/μl as a coinjection marker. Cosmids from the rescuing pool were injected individually at 30 ng/μl with pRF4. Rescue activity of the R11G1 cosmid was retained in a 17 kb SacII-NarI subclone of the R11G1 cosmid cloned into the SacII-ClaI sites of pBSKII+ (pJAZ 19, injected at 30 ng/μl) and a 7.7 kb SacII-XhoI subclone of the R11G1 cosmid cloned into the SacII-XhoI sites of pBSKII (pJAZ29, injected at 50 ng/μl). The

sax-1 deleted rescuing construct was digested with *BalI* and religated, removing 1 kb of genomic sequence that deletes conserved kinase domains V (part), VIa, VIb and VII (part) and breaks within an intron, which is predicted to disrupt *sax-1* splicing. The *BalI* deleted construct (pJAZ30) was injected at 30 ng/μl with pRF4.

cDNA isolation and allele sequencing

A high-stringency screen of 5×10^5 plaques of a mixed stage *C. elegans* cDNA library (Barstead and Waterston, 1989) identified 15 full-length *sax-1* cDNAs and 1 partial cDNA with the *cm11b8* cDNA as a probe (a generous gift from R. Waterston). Six cDNAs were fully sequenced and the rest partially sequenced. The *sax-1* sequence was confirmed and its genomic organization determined by aligning the cDNA with reported genomic sequence from the *C. elegans* Sequencing Consortium. The cDNAs were flanked by a 38 bp 5' UTR and a 335 bp 3' UTR and a polyA tail.

The *sax-1(ky211)* mutation was identified by sequencing the *sax-1* open reading frame and splice junctions from genomic DNA amplified using the Expand PCR kit (Boehringer Mannheim). PCR fragments were sequenced on one strand using the *fmol* sequencing kit (Promega). The mutation was confirmed by sequencing a separately-amplified PCR fragment.

The *sdg-1* transcript was identified by fully sequencing five expressed sequence tags from the *C. elegans* EST database (a generous gift from Y. Kohara). The longest cDNA represented a partial cDNA fragment containing the 3' 712 amino acids of *sdg-1* in addition to the 3' UTR, which ranged from 171 to 335 bp in the five ESTs. The 5' end of *sdg-1* was identified by RT-PCR from wild-type N2 RNA prepared by Trizol extraction (GIBCO) using 3' primers from the predicted *sdg-1* coding region in combination with a 5' primer to the *C. elegans* SL2 spliced leader sequence. No transcripts were identified with 5' primers to the *sax-1* cDNA or the SL1 spliced leader sequence. The SL2-spliced *sdg-1* transcript encodes a predicted protein of 811 amino acids. An additional, in-frame

sdg-1 exon upstream of the SL2 splice junction was present in one of the five cDNAs; however, the 5' end of this transcript was not detected by RT-PCR.

Characterization of neuronal morphology

Axons visualized with integrated *gfp* transgenes were scored in living adult animals, except for larval animals scored in Figure 2. The ASER neuron was visualized with the *gcy-5::gfp* transgene (Yu *et al.*, 1997) in the integrated strain *kyIs164 II*. The ASJ neuron pair was visualized in Figures 1 and 2 and Table 1 with a *tax-2Δ::gfp* transgene (Coburn and Bargmann, 1996) as an integrated strain (*kyIs150 IV*; Peckol *et al.*, 1999). *tax-2Δ::gfp* labels ASJ along with the AWB, AWC, ASG, ASI and ASK amphid neuron pairs. The AWC neuron type was visualized with an integrated *str-2::gfp* transgene (*kyIs140 I*; Dwyer *et al.*, 1998). Transgenes were integrated by trimethylpsoralen and ultraviolet radiation and outcrossed 3 - 7 times.

To visualize ASJ neurons in the absence of a *gfp* transgene (Figure 4G, Figure 5), adult animals were exposed to 15 μg/ml DiI in M9 buffer for 1.5 hours to label ASJ along with the ADL, ASH, ASI, ASK and AWB amphid neuron pairs. Penetrance calculations of ASJ defects scored by DiI staining and the *tax-2Δ::gfp* transgene differed by up to 20%; however, consistent genetic interactions were observed when animals were scored by the same method (Figure 5 and data not shown).

Animals were scored as having ectopic neurite defects if at least one neuron had an ectopic thin or thick process that was longer than the diameter of the cell body (n = animals scored). Ectopic neurites emerged directly from the cell body in *sax-1* and *sax-2* mutants and grew posteriorly along the lateral body wall. *tax-4* mutants also exhibited ventral axon defects in ASJ (Peckol *et al.*, 1999). that were not included in this analysis. In Table 1, neurons were scored as defective in cell shape if the mutant cell body appeared at least twice the size of a wild-type cell body. In Figure 6, neurons were scored as defective in cell shape if the cell body was expanded compared to wild-type neurons, but not

necessarily to twice its normal size. This difference in scoring underestimated the defects in Table 1 but revealed an increase in expressivity at high temperature.

Statistical analysis was conducted using Primer of Biostatistics software (Stanton A. Glantz, McGraw-Hill publishers) and Kaleidograph. Confocal images were acquired using LaserSharp Acquisition Version 2.1A software (BioRad), an Optiphot-2 microscope (Nikon) and the Laser Scanning Confocal Imaging System MRC-1024 (BioRad). Epifluorescence images were acquired using an Axioplan 2 (Zeiss) and assembled using Adobe Photoshop.

***sax-1* expression analysis**

A full-length translational SAX-1::GFP fusion was constructed by cloning an intronic GFP flanked by splice acceptor and donor sites (ppD103.75, a generous gift from Andy Fire) cut with EcoRV into the blunted AflII site in the last intron of the SacII-XbaI *sax-1* genomic fragment in a pBSKII+ backbone. The SAX-1::GFP transgene (pJAZ31) was injected at 50 ng/μl into a *lin-15(n765ts)* mutant using 30 ng/μl of the pJM23 *lin-15* plasmid as a coinjection marker (Huang *et al.*, 1994). To assess whether the SAX-1::GFP tag was functional, SAX-1::GFP was injected at 100 ng/μl into *sax-1(ky211) X* and *sax-1(ky491) X* mutant animals with pRF4. The *sax-1* expression pattern was characterized in variably mosaic animals that contained the SAX-1::GFP plasmid as unstable extrachromosomal DNA. Amphid sensory neurons were scored for rescue by DiI-filling of transgenic animals.

To analyze the subcellular localization of the SAX-1::GFP translational fusion, the SAX-1::GFP (pJAZ31) construct was remade by cloning the intronic GFP (ppD103.75) cut with ClaI (blunted) and SalI (blunted) into the blunted AflII site in the last intron of a SacII-XbaI *sax-1* genomic fragment in a pBSKII+ backbone, to produce the pJAZ33 intermediate. A SalI-ApaL1 fragment of pJAZ33 was cloned into the *sta-1::sax-1* fusion

(pJAZ22) in two steps. The *sta-1::sax-1::gfp* fusion (pJAZ35) was injected at 100 ng/μl into wild-type N2 animals with pRF4 and ASJ morphology was scored by DiI filling.

The *sdg-1* open reading frame immediately 3' of *sax-1* was tagged by cloning a PCR fragment containing GFP flanked with AatII sites in frame into the unique AatII site of the pJAZ19 plasmid, 20 amino acids before the predicted stop codon. The SDG-1::GFP transgene (pJAZ12) was injected at 30 ng/μl into the *lin-15(n765ts)* X strain using pJM23 as a coinjection marker.

Isolation of a *sax-1* deletion mutant

A *sax-1* deletion mutation was isolated by PCR as described (Dernburg *et al.*, 1998). A deletion library of 10⁶ genomes was constructed using the EMS mutagen for half and UV/TMP for half of the library. First round PCR was conducted with the JAZ211 and JAZ34 primers and second round PCR was conducted with the JAZ210 and JAZ36 primers to amplify a 3 kb fragment containing the *sax-1* kinase domain. A 1.7 kb deletion band was identified in a pool from the EMS part of the library and sequenced. A single animal homozygous for the deletion was isolated after three rounds of sib selection. The *sax-1(ky491)* X deletion mutant was outcrossed once by N2 and once by *lon-2(e678)* X.

***sax-1* cell autonomy**

The *sta-1::gfp* construct contained a 3 kb fragment of the *sta-1* promoter (cosmid R09F10 nucleotides 24398 - 27397) engineered by PCR to contain a 5' Sph1 site and a 3' BamH1 site and cloned into the corresponding sites of the ppD95.77 GFP vector (a generous gift from A. Fire). The *gcy-5* constructs contained a 2.7 kb fragment upstream of the *gcy-5* start codon engineered by PCR to contain a 5' Sph1 site and a 3' BamH1 site and cloned into the corresponding sites of the pPD95.75 vector (a generous gift from A. Fire). The promoter-GFP fusions were used to make the following *sax-1* cDNA expression constructs.

A Kpn1 site was engineered immediately upstream of the *sax-1* cDNA start codon by PCR. The complete *sax-1* cDNA was cut at the 5' Kpn1 site and the 3' Nae1 site in the *sax-1* 3' UTR. The *sax-1* cDNA was joined to the downstream *unc-54* 3' UTR (cut with EcoR1 and blunted) and the upstream *sta-1* or *gcy-5* promoters (cut with Kpn1). *gcy-5::sax-1* was injected at 50 ng/μl into the *sax-1(ky491) X; kyls164 II* strain with pRF4. *sta-1::sax-1* was injected at 50 ng/μl with *sta-1::sax-1* at 50 ng/μl and pRF4 into the *sax-1(ky491) X* strain and the *sax-1(ky491) X; kyls164 II* strain. In all cases, ASE rescue was assessed by *gcy-5::gfp* expression and ASJ rescue by DiI filling.

Results

Mutations in *sax-1* and *sax-2* disrupt neuronal cell shape

sax-1 and *sax-2* were identified in a screen for mutations that disrupt the morphology of amphid chemosensory neurons (Zallen *et al.*, submitted/Chapter 2). In *sax-1* and *sax-2* mutant animals, the embryonic extension and guidance of amphid axons was normal, producing a bipolar neuron with one dendrite that connects to the tip of the nose and one axon that grows circumferentially in the nerve ring neuropil (Figure 1). However, neuronal cell bodies appeared expanded and irregular in shape (Figure 1B,C,E,F), and some amphid neurons had an ectopic neurite in addition to the normal dendrite and axon (Figure 1H,I). These ectopic neurites extended posteriorly from the cell body for up to 25 μm and ranged in diameter from 0.1 μm to about 1 μm; a normal axon is 75 μm long and 0.1 μm in diameter.

Characterization of *sax-1* and *sax-2* mutants with cell-specific GFP markers revealed defects in cell shape and neurite growth in several chemosensory neurons, including the AWC, ASE and ASJ amphid neurons (Figure 1, Table 1). These three

sensory neuron types exhibited a range of phenotypes, with primarily cell shape defects in the AWC and ASE neurons and ectopic neurites in the ASJ neurons (Figure 1). Despite striking defects in AWC morphology, *sax-1* and *sax-2* mutant animals generated nearly wild-type chemotaxis responses to attractive odorants detected by AWC (Figure 2A), suggesting that these morphological defects do not eliminate AWC function.

sax-1 and *sax-2* mutations also disrupted the morphology of some non-sensory neuron types. Ectopic neurites were observed in *glr-1::gfp*-expressing interneurons and altered cell shape and ectopic neurites were observed in the CAN neurons (Zallen *et al.*, submitted/Chapter 2). In other respects, *sax-1* and *sax-2* mutant animals appeared morphologically and behaviorally normal, with no obvious defects in locomotion or egg laying.

***sax-1* and *sax-2* are required for the maintenance of neuronal morphology**

The ectopic neurite phenotypes of *sax-1* and *sax-2* mutants are reminiscent of defects caused by mutations that disrupt the electrical activity of sensory neurons, which result in late-onset neurite growth during larval and adult stages (Peckol *et al.*, 1999). To determine whether *sax-1* and *sax-2* also affect a late developmental process, we examined the ectopic neurite defects in the ASJ sensory neurons at different larval stages. Although ASJ axon guidance is completed in the embryo, the ectopic neurites in *sax-1* and *sax-2* mutants increased in severity throughout the four larval stages and continued to appear in adults (Figure 2B). Unlike ectopic neurites, the cell shape defects in *sax-1* and *sax-2* mutants were not observed in mutants with defects in sensory activity and have not been previously described in *C. elegans*. The AWC cell shape defects also increased in severity between the first and second larval stages (Figure 2C). Therefore, *sax-1* and *sax-2* are required to repress neurite outgrowth, and to some extent cell spreading, during larval and adult development.

We previously reported that the overall amphid neuron defects of *sax-1* and *sax-2* mutants are more severe at higher temperatures (Zallen *et al.*, submitted/Chapter 2). Therefore, we examined whether individual neuron types were susceptible to temperature changes. The ASJ ectopic neurite defect was temperature-sensitive in the two *sax-1* alleles and the single *sax-2* allele (Table 1, Figure 5). In addition, AWC and ASE cell shape defects were temperature-sensitive in some *sax-1*, but not *sax-2*, mutants (Table 1).

***sax-1* encodes a serine/threonine protein kinase**

The location of the *sax-1* gene was mapped with respect to genetic markers and physical polymorphisms. *sax-1* mapped to chromosome X between the stP40 polymorphism and the *lin-18* gene and cosmid pools covering this region were injected into the *sax-1(ky211)* strain. The R11G1 cosmid and its subclones rescued the *sax-1* mutant defects (Figure 3A).

Sequence information from the *C. elegans* Sequencing Consortium predicted that the smallest rescuing subclone contained a serine/threonine kinase. A 1 kb deletion within the predicted kinase domain completely abolished rescuing activity (Figure 3A). To confirm that this gene was disrupted in *sax-1* mutant animals, we sequenced *sax-1(ky211)* and identified a G to A transition mutation in a predicted splice acceptor site. The transcript produced by the *sax-1* locus was identified by screening a mixed-stage *C. elegans* cDNA library (Barstead and Waterston, 1989) using a probe from the cm11b8 cDNA (a generous gift from R. Waterston). The fifteen full-length cDNAs isolated define a 1.8 kb primary transcript that encodes a predicted protein of 467 amino acids. An additional two amino acids were present at the eleventh splice acceptor site in one of fifteen clones. The *sax-1* transcript was contained within the 7.7 kb rescuing subclone, with 1.9 kb of upstream sequence and 2.4 kb of downstream sequence (Figure 3A).

sax-1 encodes a protein with homology to serine/threonine protein kinases, including the eleven highly conserved motifs that constitute the catalytic domain (Hanks *et al.*, 1988). The SAX-1 kinase belongs to a family of serine/threonine kinases that is conserved from yeast to humans (Figure 3B,C). SAX-1 is most closely related to the Ndr kinases (Millward *et al.*, 1995), with 62% amino acid identity to human Ndr and 60% identity to *Drosophila* Ndr. Certain features distinguish Ndr kinases from other serine/threonine kinases, including a conserved N-terminal region and a 34-45 amino acid spacer between kinase motifs VII and VIII. Several close relatives of Ndr possess these features, including *S. pombe* Orb6, *Neurospora* COT-1 and *Drosophila* Warts/Lats (Yarden *et al.*, 1992; Justice *et al.*, 1995; Xu *et al.*, 1995; Verde *et al.*, 1998). However, the Ndr kinases form distinct class: *C. elegans* has both *sax-1*/Ndr and a Warts/Lats homolog, and *Drosophila* has an Ndr kinase as well as Warts/Lats.

SAX-1 is related to Rho kinases (Figure 3C), with 35% amino acid identity and 52% amino acid similarity to human p160^{ROCK}/ROK β . However, Rho kinases lack the SAX-1 spacer region between kinase subdomains VII and VIII, possess divergent N-termini and contain an additional C-terminal region that mediates Rho association (Leung *et al.*, 1995; Fujisawa *et al.*, 1996).

Immediately 3' of the predicted *sax-1* gene lies a second predicted open reading frame that contains C1 and C2 type lipid-binding motifs (*C. elegans* sequencing consortium). C1 cysteine-rich domains are found in members of the protein kinase C (PKC) family (Nishizuka, 1984) and Rho kinases (Leung *et al.*, 1995; Ishizaki *et al.*, 1996; Matsui *et al.*, 1996). Some C1 domains have been shown to coordinate zinc and associate with phorbol esters and diacylglycerol (DAG) (Ono *et al.*, 1989; Ahmed *et al.*, 1991). The C2 domain is also present in PKC and has been shown to bind calcium (Davletov and Sudhof, 1993). To test whether these downstream exons could encode alternative exons of *sax-1*, we sequenced five expressed sequence tags (kindly provided by Y. Kohara) and identified the full-length transcript by reverse-transcriptase PCR (RT-

PCR). None of these cDNAs contained *sax-1* sequences; instead, a transcript predicted to encode an 811 amino acid protein was trans-spliced to the SL2 spliced leader sequence (Figure 3A), a property of *C. elegans* genes that are located downstream in an operon (Zorio *et al.*, 1994). We named this transcript *sdg-1*, for *sax-1* downstream gene. The *sdg-1* coding region was not required for *sax-1* rescue (Figure 3A). Therefore, *sax-1* and *sdg-1* appear to encode distinct protein products that may belong to a common operon, although it is possible that they are also included in a single transcript that was not detected by RT-PCR.

Isolation of a candidate *sax-1* null mutation

The *sax-1(ky211)* mutation is predicted to disrupt *sax-1* splicing, and may cause a partial or complete loss of gene function. To obtain a null allele of *sax-1*, we used a PCR-based strategy to isolate a deletion mutant from a library of 10⁶ EMS- or UV-TMP-mutagenized animals (Materials and Methods). The *sax-1(ky491)* mutation represented a 1.3 kb deletion of genomic sequence that removed 152 bp of coding region, including conserved domains IV, V and VIA of the *sax-1* kinase region. This deletion disrupted the *sax-1* open reading frame and is predicted to encode a truncated gene product containing only three of the eleven conserved kinase domains. Therefore, *sax-1(ky491)* is a candidate null allele. The *sax-1(ky491)* deletion mutation caused defects similar to those caused by the *sax-1(ky211)* allele (Table 1; Figure 1E, 2A and 5B), indicating that the partially penetrant, temperature sensitive defects in the ASJ and ASE neurons represent the *sax-1* null phenotype.

A SAX-1::GFP translational fusion is broadly expressed in neurons, hypodermis, and muscle

To determine the pattern of *sax-1* expression, we inserted a *gfp* reporter flanked by splice sites into the final *sax-1* intron, 15 amino acids before the stop codon. The SAX-1::GFP fusion contained all exons, introns and 5' regulatory regions present in the rescuing *sax-1* subclone. SAX-1::GFP rescued the ASJ defects of *sax-1(ky211)* and *sax-1(ky491)* mutant animals (Figure 3A). We examined SAX-1::GFP expression in larval and adult animals, since *sax-1* mutants exhibited defects that continued to worsen during these stages. SAX-1::GFP was detected in multiple cell types, including neurons that contribute axons to the nerve ring (Figure 4A), hypodermal cells, including lateral seam cells (Figure 4B), and muscle, where SAX-1::GFP displayed a punctate subcellular localization (Figure 4C).

To further characterize the *sax-1* operon, we inserted the GFP in a translational fusion near the 3' end of the *sax-1* downstream gene, *sdg-1*, in a fusion containing all *sdg-1* exons and introns and upstream (7.5 kb) and downstream (4.6 kb) sequences. SDG-1::GFP was expressed in muscle cells, including body wall, vulval and head muscles (Figure 4D), but was not detected in hypodermis. Within muscles, SDG-1::GFP displayed a punctate localization, as did SAX-1::GFP. SDG-1::GFP was also expressed faintly in axons in the nerve ring (Figure 4E).

***sax-1* functions cell autonomously to regulate cell shape**

Since SAX-1::GFP is broadly expressed, we wanted to determine whether SAX-1 functions cell autonomously in amphid sensory neurons to regulate amphid cell shape and neurite outgrowth. We used the *gcy-5* promoter (Yu *et al.*, 1997) to drive *sax-1* expression in the right ASE neuron. Expressing *gcy-5::sax-1* in ASER was able to fully rescue the ASER defects of *sax-1* null mutant animals (Figure 4G), indicating that SAX-1 can function cell autonomously to regulate ASER cell shape. However, the ASJ ectopic neurite defects were also partially rescued in these animals (Figure 4G). These results are

consistent with two models: SAX-1 could function cell autonomously in ASER and non-autonomously in ASJ, or the *gcy-5* promoter may be expressed at a low level in ASJ, allowing partial ASJ rescue.

To determine whether SAX-1 can function cell autonomously in ASJ to repress neurite outgrowth, we used an independent promoter to express SAX-1 in ASJ but not ASE. The promoter for the predicted seven transmembrane domain receptor *sta-1* drives expression in the two ASJ sensory neurons and pharyngeal muscle (Y. Zheng and C. I. B., unpublished results). Expression of the *sax-1* cDNA from the *sta-1* promoter fully rescued the ectopic neurite defects in the ASJ neurons of *sax-1(ky491)* null mutant animals, but did not rescue the ASER defects (Figure 4G). To determine whether rescuing activity was due to *sax-1* expression in ASJ or in pharyngeal muscle, we coinjected the *sta-1::sax-1* transgene and a *sta-1::gfp* fusion to form an unstable extrachromosomal array whose site of expression can be monitored by *gfp* fluorescence. Mosaic animals with *gfp* expression in ASJ but not in the pharyngeal muscle were rescued for the ASJ defects (14 of 15 mosaic animals rescued). *sax-1* expression in ASJ is sufficient for ASJ rescue, indicating that SAX-1 can function cell autonomously in ASJ to regulate neurite outgrowth.

To examine the subcellular localization of SAX-1, we expressed a SAX-1::GFP translational fusion from the *sta-1* promoter in the ASJ neurons of *sax-1* null mutant animals. The *sta-1::SAX-1::GFP* fusion rescued the ASJ ectopic neurite defects of *sax-1* mutants (three independent transgenic lines: 10-12% defective, n=46-80, each line significantly rescued at $p < 0.001$ compared to control *sax-1(ky491)* animals: 61% defective, n=218). In larval and adult animals, SAX-1::GFP fluorescence was detected throughout the ASJ cell body, including the nucleus and the cytoplasm, and occasionally in the proximal axon and dendrite (Figure 4F).

The UNC-43 calcium/calmodulin-dependent kinase and the TAX-4 sensory transduction channel regulate neurite outgrowth in parallel to SAX-1

The SAX-1-related human Ndr kinase is activated by calcium (Millward *et al.*, 1998) and calcium-dependent kinases such as the calcium/calmodulin-dependent kinase II (CaMKII) have been implicated in the regulation of neuronal morphology. Disruption of CaMKII function in *Drosophila* motor neurons leads to increased axon branching (Wang *et al.*, 1994) and inhibition of CaMKII function in *Xenopus* tectal neurons causes increased dendrite branching (Wu and Cline, 1998). *C. elegans* has a single predicted CaMKII homolog encoded by the *unc-43* gene (Reiner *et al.*, submitted). To determine whether CaMKII is involved in the regulation of cell morphology in *C. elegans*, we examined amphid sensory neurons in *unc-43* mutants. Both the null *unc-43(n1186lf)* mutation and the gain of function *unc-43(n498gf)* mutation caused occasional ectopic neurites in the ASJ (Figure 5A) and ASE neurons (13% defective in *unc-43(lf)*, n=194; 3% defective in *unc-43(gf)*, n=159), but no cell shape defects.

The *unc-43* mutant phenotypes resemble those observed in mutants with altered sensory transduction or electrical activity. For example, animals defective in the TAX-4 cGMP-gated ion channel exhibit ectopic neurite outgrowth in the ASE and ASJ neurons in larval stages, but no defect in cell shape (Coburn and Bargmann, 1996; Komatsu *et al.*, 1996; Coburn *et al.*, 1998). To investigate whether the UNC-43 CaMKII functions in an activity-regulated pathway in *C. elegans* sensory neurons, we constructed double mutant combinations between the *tax-4* null mutation and loss- or gain-of-function *unc-43* alleles. The ASJ defects in the *tax-4; unc-43(lf)* double mutant were not enhanced compared to the *tax-4* single mutant (Figure 5A), suggesting that UNC-43 functions in a TAX-4 pathway. The *tax-4; unc-43(gf)* double mutant was significantly suppressed for the *tax-4* ASJ defects, indicating that the UNC-43 kinase acts downstream of the TAX-4 sensory channel. However, *tax-4* null mutants were substantially more defective than *unc-43* null

mutants (Figure 5A), suggesting that TAX-4 carries out additional, UNC-43-independent functions.

To determine whether SAX-1 participates in an activity-dependent pathway, we generated double mutants defective in both *sax-1* and *tax-4*. ASJ neurons in the *sax-1*; *tax-4* double mutant display significantly more severe ectopic neurite defects than a null mutant in either gene (Figure 5B), indicating that these genes function in two distinct pathways that suppress neurite outgrowth.

UNC-43, like TAX-4, functions in parallel to the SAX-1 kinase. The ASJ neurons in the *sax-1*; *unc-43(lf)* double mutant were significantly more defective than in a null mutant in either gene, indicating that SAX-1 and UNC-43 operate in parallel pathways (Figure 5C). Interestingly, the *sax-1*; *unc-43(gf)* double mutant was suppressed compared to the *sax-1* single mutant at 25°C, suggesting that increased activity of the UNC-43 kinase can partially compensate for decreased SAX-1 kinase activity.

sax-1 and *sax-2* mutants have similar defects in neurite outgrowth and cell shape. The ASJ defects in *sax-1*; *sax-2* double mutants were no more severe than in either single mutant (Figure 5D), indicating that these genes act in the same genetic pathway.

The *C. elegans* RHOA GTPase can influence amphid cell shape and neurite outgrowth

Rho GTPases regulate cell morphology in mammalian cell culture and budding and fission yeast (Paterson *et al.*, 1990; Matsui and Toh-E, 1992; Ridley and Hall, 1992; Yamochi *et al.*, 1994) and Rho kinases have been identified as candidate Rho effectors (Leung *et al.*, 1996; Amano *et al.*, 1997; Ishizaki *et al.*, 1997). Since SAX-1 belongs to a kinase superfamily that includes the Rho kinases, we investigated the role of the *C. elegans* RHOA GTPase in sensory neurons. RHOA shares 87% identity with vertebrate RhoA GTPases (Chen and Lim, 1994), and is expressed in nerve ring neurons during larval stages, consistent with a possible function at the same time as SAX-1 (Chen and

Lim, 1994). Use of RNA interference (RNAi) to disrupt *rhoA* function caused embryonic lethality (E. A. Lundquist and C. I. B., unpublished observations), precluding a straightforward loss-of-function analysis. Therefore, we generated mutations in conserved residues in the *rhoA* open reading frame that are predicted to confer dominant negative (*rhoA^{T19N}*) or gain of function (*rhoA^{Q63L}*) properties (Feig and Cooper, 1988; Bourne *et al.*, 1991). Wild-type *rhoA*, *rhoA^{T19N}* and *rhoA^{Q63L}* were expressed from the *gcy-5* promoter (Yu *et al.*, 1997) to drive expression in the ASER amphid neuron in late embryo, larval and adult animals.

The *rhoA^{T19N}* allele, which is predicted to reduce endogenous *rhoA* function, caused ASER cell shape defects (Figure 6B,F) that resembled those of *sax-1* mutant animals (Figure 6C). Minimal defects were caused by expression of *rhoA* or *rhoA^{Q63L}* (Figure 6F). These results indicate that RHOA, or a related GTPase, can function in amphid sensory neurons to regulate cell shape. A distinct mutation in the GTP-binding domain, *rhoA^{D13T}*, also caused cell shape defects (Figure 6F), indicating that both *rhoA^{T19N}* and *rhoA^{D13T}* can function as dominant negative alleles. Interestingly, increased *sax-1* activity modified the cell shape phenotype caused by dominant negative *rhoA*. *sax-1* expression in ASER from a high copy *gcy-5::sax-1* transgene partially suppressed the defects caused by *rhoA^{D13T}* (Figure 6C,F), while a high copy transgene containing the *gcy-5* promoter alone had no effect (Figure 6F).

ASER morphology is influenced by at least three genes: *sax-1*, *tax-4* and *rhoA*. To explore how these genes interact, we expressed *rhoA*, *rhoA^{T19N}* or *rhoA^{Q63L}* alleles in *sax-1* and *tax-4* mutant backgrounds. Increased *rhoA* activity through expression of high-copy *rhoA* or *rhoA^{Q63L}* transgenes partially suppressed the cell shape defects in the ASER neurons of *sax-1* null mutant animals (Figure 6G). By contrast, expression of the *rhoA^{T19N}* dominant negative allele had no effect (Figure 6G). Increased *rhoA* activity through expression of the *rhoA^{Q63L}* allele, but not *rhoA^{T19N}*, also partially suppressed the ectopic neurite defects of *tax-4* null mutants (Figure 6H). Therefore, increased RHOA

activity inhibited both the cell shape defects caused by loss of the SAX-1 pathway and the aberrant neurite outgrowth caused by loss of the TAX-4 pathway.

Discussion

C. elegans sax-1 mutants are defective in the maintenance of cell shape and polarity in amphid sensory neurons, while other morphogenetic processes, such as cell migration and axon guidance, occur normally in the same neurons. *sax-1* encodes a serine/threonine kinase related to the *Drosophila* and human Ndr kinases (Millward *et al.*, 1995) in a kinase family that includes *S. pombe* Orb6, *Neurospora* COT-1 and *Drosophila* Warts/Lats. Orb6, COT-1 and Warts/Lats are all required *in vivo* for normal cell shape (Yarden *et al.*, 1992; Justice *et al.*, 1995; Xu *et al.*, 1995; Verde *et al.*, 1998). Therefore, SAX-1 and its Ndr kinase homologs may participate in an evolutionarily conserved mechanism for the regulation of cell morphology.

The *sax-1* mutant defects are selective: dendrites and axons of amphid sensory neurons appear morphologically and in some cases functionally normal in *sax-1* mutants, suggesting that their defects are limited to cell body structure. Mutant neurons expand to produce an irregularly-shaped cell body and ectopic axon-like processes. These defects could reflect an underlying failure of cytoskeletal contractility in *sax-1* mutants. *sax-1* mutant defects become more severe as animals mature, suggesting an ongoing requirement for SAX-1 kinase activity in the maintenance of cell morphology. The fission yeast Orb6 kinase is similarly required for cell shape maintenance; arrested elongate cells become spherical when *orb-6* function is disrupted (Verde *et al.*, 1995). *Drosophila warts/lats* mutants also exhibit selective cell shape defects, where epidermal cells undergo aberrant expansion in their apical regions but retain the septate and adherens junctions characteristic of polarized cells (Justice *et al.*, 1995). Therefore, SAX-1 and its related kinases may

define pathways for the regulation of specific aspects of cell shape. Warts/Lats and Orb6 play an additional role in cell division (Justice *et al.*, 1995; Xu *et al.*, 1995; Verde *et al.*, 1998; St. John *et al.*, 1999), but we have not observed cell proliferation defects in *sax-1* mutants (data not shown).

SAX-1 functions in parallel to an activity-dependent pathway mediated by the TAX-4 sensory channel and the UNC-43 calcium/calmodulin-regulated kinase

The SAX-1 kinase functions together with an activity-dependent pathway in the maintenance of sensory neuron morphology. Ectopic neurites form late in development in mutants with abnormal sensory activity resulting from defects in sensory transduction, ion channel function, or development of the dendritic sensory endings (Coburn and Bargmann, 1996; Coburn *et al.*, 1998; Peckol *et al.*, 1999). Double mutant analysis indicates that the sensory transduction channel TAX-4 functions upstream of the UNC-43 calcium/calmodulin-regulated kinase II (CaMKII) in a common pathway affecting sensory neuron morphology. While this interaction may not be direct, it is possible that ion flux through the native TAX-4 channel, which is permeable to calcium (Komatsu *et al.*, 1999), could activate calcium-regulated effectors such as the UNC-43 CaMKII (Hanson and Schulman, 1992), in a pathway that allows neuronal morphology to respond to sensory activity.

CaMKII has been implicated in the activity-dependent regulation of neuronal morphology in other animals. In *Xenopus* tectal neurons, inhibition of CaMKII function leads to increased dendrite branching while CaMKII activation decreases dendrite branching (Wu and Cline, 1998), in a process that responds to activity via the NMDA glutamate receptor (Constantine-Paton *et al.*, 1990). Disruption of CaMKII function in *Drosophila* motor neurons leads to increased axon branching (Wang *et al.*, 1994) a defect

also observed in ion channel mutants with altered motor neuron activity (Budnik *et al.*, 1990). These results suggest that CaMKII may share conserved functions with activity-dependent pathways in worms, flies and vertebrates.

The SAX-1 kinase functions in parallel to the TAX-4/UNC-43 pathway in the regulation of sensory neuron morphology; *sax-1; tax-4* and *sax-1; unc-43* double mutants are significantly more defective than the individual single mutants. The human Ndr kinase is regulated by calcium through a domain that is conserved in SAX-1 (Millward *et al.*, 1998). This observation raises the possibility that both kinases could be regulated by neuronal activity, with UNC-43 responding to calcium influx regulated by sensory input from the environment and SAX-1 responding to calcium from another source, such as the synapse. Alternatively, these two pathways may represent activity-dependent (TAX-4 and UNC-43) and activity-independent (SAX-1) mechanisms for the maintenance of sensory neuron morphology.

Interestingly, a gain of function mutation in the UNC-43 CaMKII can suppress the ectopic neurite defects caused by loss of SAX-1, even though SAX-1 and UNC-43 appear to function in parallel. This result is consistent with a model where two independent pathways suppress neurite outgrowth, and increased activity of one pathway can partially compensate for decreased activity of the other. Alternatively, the SAX-1 and TAX-4 pathways could converge on a common downstream target. CaMKII proteins have been shown to phosphorylate a number of substrates *in vitro*, including the myosin regulatory light chain involved in actin-mediated contractility (Tan *et al.*, 1992). SAX-1/Ndr targets are unknown, but the related Rho kinase can phosphorylate myosin light chain on the same site phosphorylated by CaMKII, leading to activation of its ATPase activity (Edelman and Cunningham, 1990; Amano *et al.*, 1996). Furthermore, Rho kinase has been shown to phosphorylate and inactivate myosin light chain phosphatase (Kimura *et al.*, 1996; Wissmann *et al.*, 1997), which is predicted to increase the levels of active phosphorylated myosin. Phosphorylated myosin can regulate actin assembly and inhibit

neurite extension (Tan *et al.*, 1992; Wang *et al.*, 1996). Therefore, it is possible that the SAX-1 and UNC-43 kinases could influence cell morphology through the phosphorylation of targets that regulate myosin function.

A possible role for RHOA GTPase in regulating neuronal morphology

Disruption of the *C. elegans* SAX-1 kinase causes sensory neuron cell bodies to adopt an expanded and irregular morphology and leads to aberrant neurite initiation and growth. In cultured mammalian neurons, the RhoA GTPase has similar functions: dominant negative RhoA^{N19} promotes cell flattening and neurite extension, while gain of function RhoA^{V14} causes cell rounding and decreased neurite extension (Gebbinck *et al.*, 1997). Consistent with the effects of Rho in mammalian cells, the putative dominant negative *rhoA*^{T19N} allele causes expanded and irregular cell morphology in *C. elegans* chemosensory neurons. Conversely, increased *rhoA* activity partially suppressed *sax-1* and *tax-4* mutant defects in cell shape and neurite extension. RhoA signaling may inhibit the formation of ectopic neurites and cell spreading; alternatively, high level expression of mutant *rhoA* alleles could titrate out components required for the regulation of other proteins. Since RNA interference (RNAi) of *rhoA* resulted in early embryonic lethality, it is not straightforward to generate a simple loss of function phenotype to distinguish between these models (E. Lundquist and C. I. B., unpublished). However, mutations in other GTPase pathways, such as the *C. elegans* MIG-2 GTPase or the UNC-73 Dbp-homology exchange factor (Zipkin *et al.*, 1997; Steven *et al.*, 1998) do not cause cell shape defects in ASER (our data not shown), indicating that the effects of RHOA expression on cell shape are selective among GTPases.

Although kinases in the Orb6/COT-1/Warts family are related to Rho kinases, they lack the Rho-binding domain, along with other domains in the Rho kinase C-terminus that are proposed to have signaling or regulatory functions. It is possible that SAX-1 and Rho kinases can phosphorylate shared or similar targets, but are regulated by different

upstream pathways. These results are consistent with the results of double mutant analysis between *sax-1*, *tax-4*, and *rhoA* alleles: the ability of *rhoA* expression to affect cell shape in a *sax-1* null mutant implies that SAX-1 cannot be the sole target of RHOA action. However, Orb6 overexpression partially rescues the cell shape defects caused by a mutation in the Cdc42-regulated Pak1/Shk1 kinase and Orb6 localization is disrupted in a *pak1/shk1* mutant, suggesting that the Orb6 kinase may function downstream of GTPase signaling (Verde *et al.*, 1998). Therefore, it is possible that SAX-1-related kinases in the Orb6/COT-1/Warts family, like the related Rho kinases, may also function in a GTPase signaling pathway.

SAX-1 and the regulation of neuronal cell shape and polarity

The mechanisms by which cellular asymmetries are established and communicated throughout the cytoplasm are not well understood, although rigid, polar, and extensive cytoskeletal structures provide an ideal framework for directed membrane and organelle traffic. The SAX-1-related Orb6 kinase colocalizes with cortical actin structures at the growing tips of *S. pombe* cells (Verde *et al.*, 1998). Human Ndr kinase localizes primarily to the nucleus in cultured cells, but a subpopulation of hNdr protein is present at the cell periphery (Millward *et al.*, 1995); these two localized populations could have related or distinct activities. A functional SAX-1::GFP fusion is localized throughout the cell body of the ASJ sensory neurons, consistent with a requirement in either the cytoplasm or the nucleus.

In one model, activation of SAX-1 kinase activity by upstream signals such as calcium entry or localized GTPase signaling could stabilize actin-membrane contacts and help to maintain rigid properties of cell shape. In the absence of these stable contacts, neuronal cells that are normally spherical due to internal rigidity may relax to produce expanded, irregular morphologies. The specialized cytoskeletal structures that promote extension of normal axons and dendrites might make them immune to a general loss of

rigidity in the cell body of *sax-1* mutants. A similar model could account for the epithelial cell expansion in *Drosophila warts/lats* mutants. A loss of internal structure in *S. pombe* cells growing in suspension could cause them to collapse from a rigid rod-like shape into a sphere. The difference between a cell spreading defect in *Drosophila* and *C. elegans* as opposed to collapse in *S. pombe* may be due to the presence of an extracellular matrix substrate for spreading. The identification and characterization of other components of the SAX-1 pathway, such as SAX-2, may provide insight into the molecular mechanisms that maintain cell shape and polarity and their regulation in the context of a developing neuron.

Figure 1. Morphological defects in amphid sensory neurons of *sax-1* and *sax-2* mutants. Neuronal morphology was characterized with integrated transgenes that express GFP in AWC (top row), ASER (middle row) and ASJ (bottom row, indicated by closed arrowheads). All panels show a lateral view of one side of the animal. Anterior is to the left, dorsal at top. Scale bar = 10 μ m. Panels show wild-type (A,D,G), *sax-1(ky211)* (B,H), *sax-1(ky491)* (E) and *sax-2(ky216)* (C,F,I) animals. The AWC and ASE neurons exhibited expanded and irregular cell shape defects in *sax-1* and *sax-2* mutants. The ASJ neurons produced ectopic, posteriorly-misdirected neurites (arrows in H and I) in addition to an apparently wild-type axon in the nerve ring (open arrowheads in G, H and I).

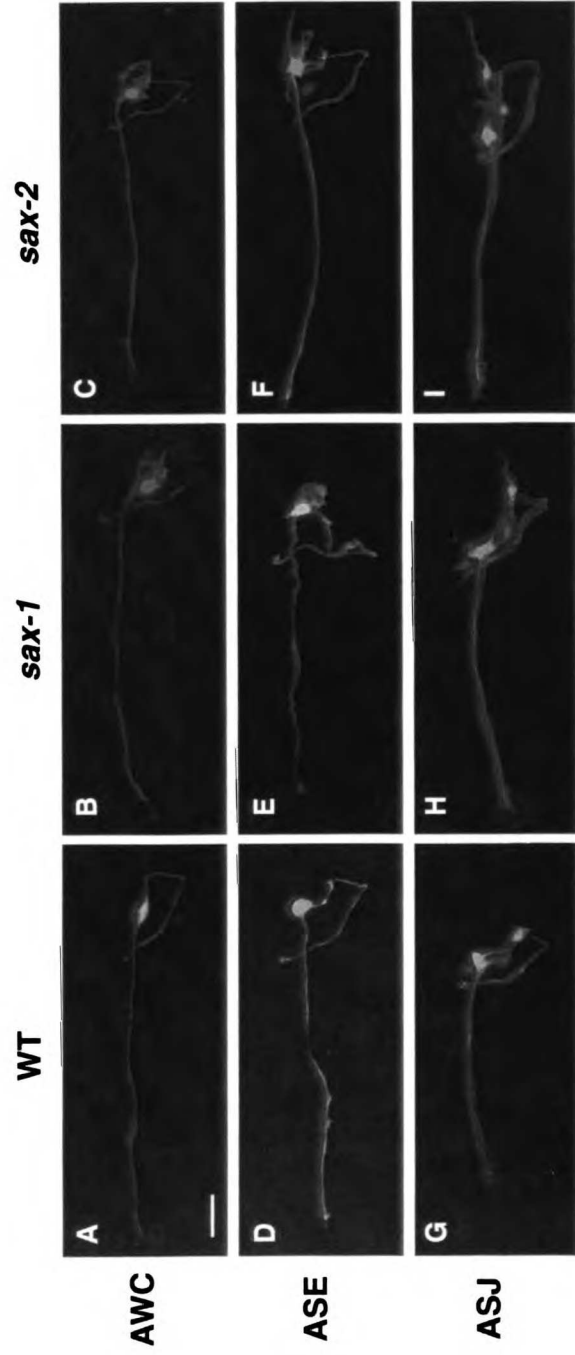


Figure 2. *sax-1* and *sax-2* morphological defects appear late in development and do not lead to severe behavioral defects. A. *sax-1* and *sax-2* mutants generate chemotaxis responses to attractive odorants detected by the AWC sensory neurons. Wild-type animals are represented by black bars, *sax-1(ky211)* by dark gray bars, *sax-1(ky491)* by light gray bars and *sax-2(ky216)* by white bars. Animals were tested for chemotaxis to three attractive odorants sensed by AWC: benzaldehyde (1/200 dilution in ethanol), isoamyl alcohol (1/100 dilution) and 2-butanone (1/1000 dilution). Chemotaxis assays were conducted as described (Bargmann *et al.*, 1993). A chemotaxis index of 1 indicates complete attraction, while a chemotaxis index of 0 indicates no response. Error bars indicate the standard error of the mean, based on 5 - 7 independent assays performed on ~100 animals in each assay. While *sax-1* and *sax-2* mutant animals were extremely defective in AWC morphology (Table 1), mutant animals were only slightly defective in AWC-mediated chemotaxis.

B., C. ASJ ectopic neurite defects increase in severity during larval and adult stages in *sax-1* and *sax-2* mutants. Animals were scored at each of the four larval stages (L1-L4) and as one-day or three-day old adults. Error bars indicate the standard error of proportion, n= 47 - 246 animals scored for each data point. Asterisks indicate populations that were significantly more defective than animals at the previous developmental stage at $p < 0.01$ (Chi-square test). For ASJ neurons in *sax-1* mutants (B), L3 differs from L2 at $p = 0.007$; young adult differs from L4 at $p = 0.003$; old adult differs from young adult at $p = 0.002$. For ASJ neurons in *sax-2* mutants (B), L3 differs from L2 at $p < 0.001$; young adult differs from L4 at $p = 0.002$; old adult differs from young adult at $p < 0.001$. For AWC neurons in *sax-2* mutants (C), L2 differs from L1 at $p < 0.001$.

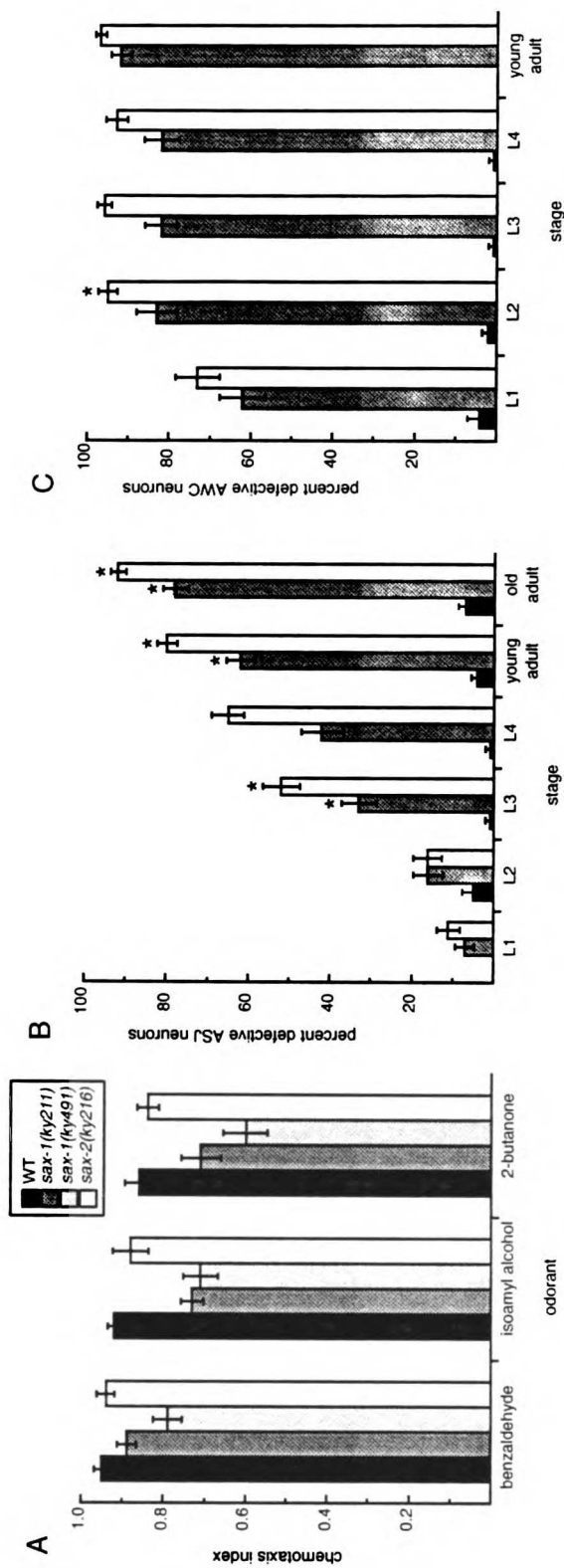
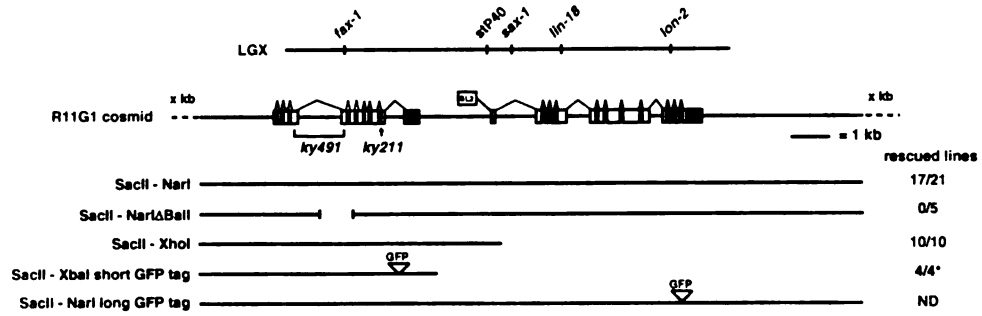


Figure 3. *sax-1* encodes a serine/threonine kinase. A. The *sax-1* mutation mapped to LGX between the stP40 and *lin-18* markers. *sax-1* mutant defects were rescued by the R11G1 cosmid and specific cosmid subclones. The exon/intron structure of the *sax-1* genomic region is shown; exons are open boxes, 5' and 3' untranslated regions are closed boxes and introns are lines. Rescued lines indicate the number of independent transgenic *sax-1(ky211)* lines whose amphid defects were rescued by the specified plasmid (see Materials and Methods). The asterisk indicates that 2/2 *sax-1(ky211)* transgenic lines were rescued and 2/2 *sax-1(ky491)* transgenic lines were rescued.

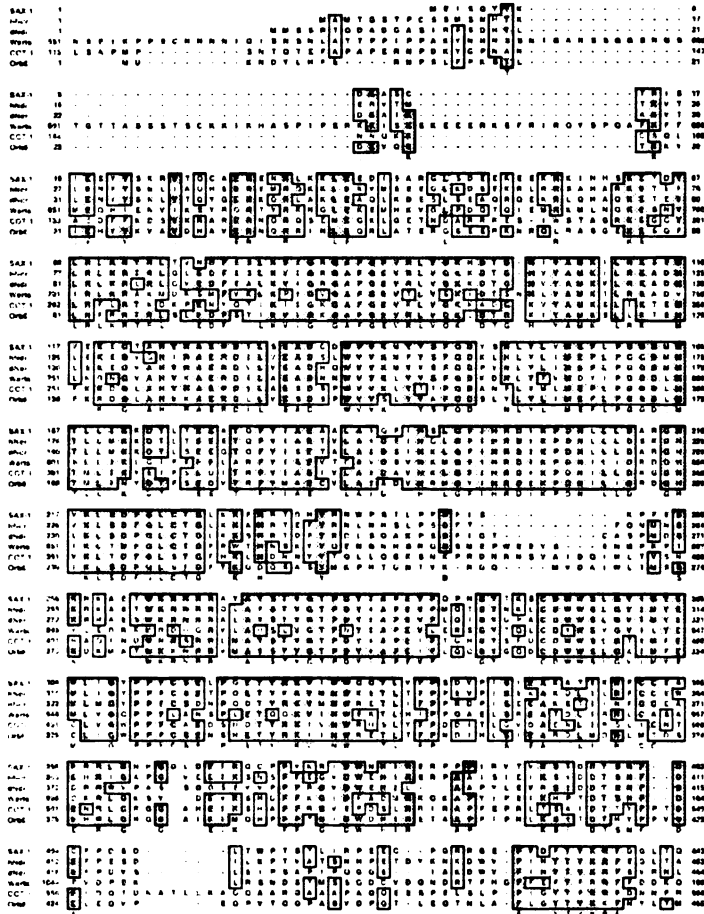
B. Alignment of the SAX-1 protein sequence with sequences of the human and *Drosophila* Ndr kinases (hNdr and dNdr), *Drosophila* Warts/Lats, *Neurospora* COT-1 and *S. pombe* Orb6.

C. Phylogenetic tree indicating the relationship between the kinase catalytic domains of SAX-1 other serine/threonine kinases (phylip program).

A.



B.



C.

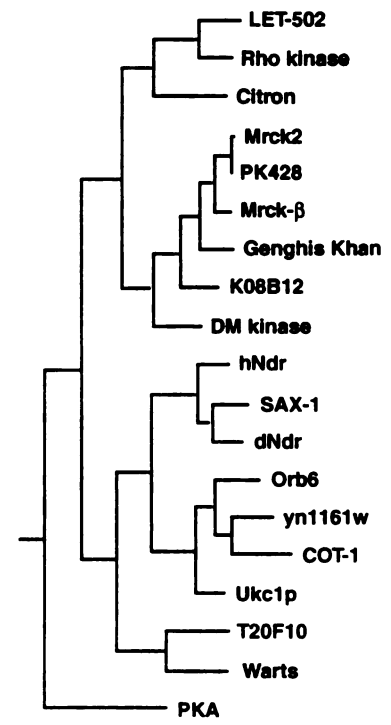


Figure 4. SAX-1::GFP expression and site of action. SAX-1::GFP (A,B,C,F) and SDG-1::GFP (D,E) expression are shown in larval (B,F) and adult (A,C,D,E) animals. All panels show a lateral view of one side of the animal. Anterior is to the left, dorsal at top. Scale bars = 10 μ m. (A) SAX-1::GFP is expressed in lateral ganglion neurons in the head of the animal (arrowhead) that contribute axons to the nerve ring (arrow). (B) SAX-1::GFP labels lateral seam cells in the epidermis. (C) SAX-1::GFP displays a punctate localization in muscle, shown here in body wall muscle in the midbody of the animal. (D) SDG-1::GFP also exhibits a punctate localization in muscle, shown here in head muscles. (E) SDG-1::GFP is expressed faintly in axons of the nerve ring (arrow), as well as pharyngeal muscle (arrowhead). (F) The *sta-1::sax-1::gfp* fusion was detected throughout the cell body of the ASJ neuron type (arrowhead) and occasionally in the proximal axon and dendrite (arrow). G. SAX-1 functions cell autonomously in the ASJ and ASE amphid neurons. ASJ phenotypes are represented by black bars and ASE phenotypes by white bars. Error bars indicate the standard error of proportion, n = 46 - 307 animals scored for each data point. Expression of the *sta-1::gfp* transgene in ASJ rescued the ASJ defects of *sax-1(ky491)* mutants (four independent transgenic lines) but not the ASE defects (two independent transgenic lines). Expression of the *gcy-5::sax-1* transgene in ASE rescued the ASE defects of *sax-1(ky491)* mutants (four independent transgenic lines) and partially rescued the ASJ defects (two independent transgenic lines). All rescued lines were significantly different from *sax-1(ky491)* animals ($p < 0.001$, Chi-square test).

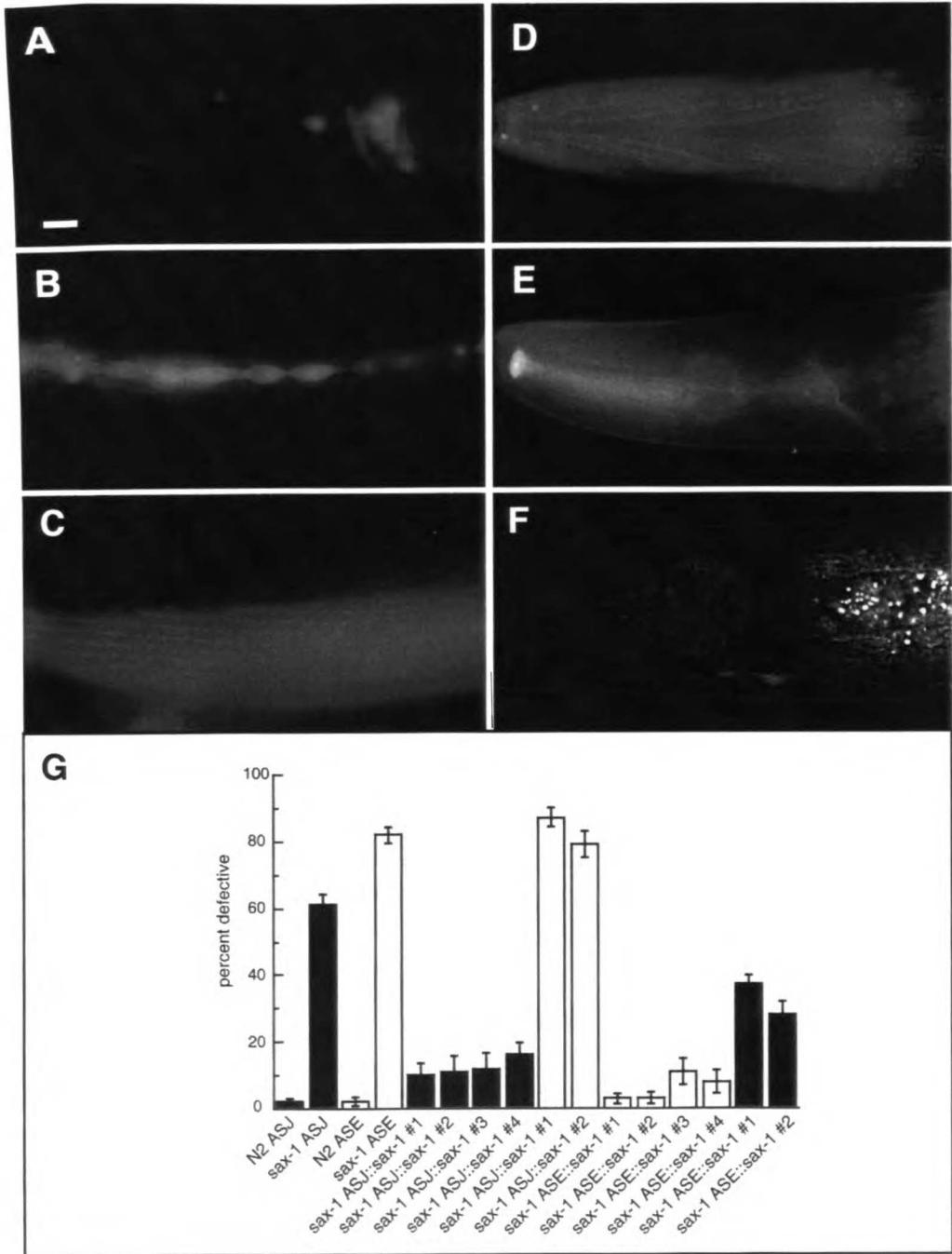


Figure 5. ASJ ectopic neurite defects in *sax-1*, *tax-4*, *unc-43* and *sax-2* single and double mutants. Strains grown at 20°C are shown on the left of each panel, strains grown at 25°C on the right. Error bars indicate the standard error of proportion, n = 110 - 362 animals scored for each data point. Single asterisks indicate double mutants that were significantly more defective than either single mutant at that temperature (p<0.001, Chi-square test). Double asterisks indicate double mutants that were significantly suppressed compared to the more severe single mutant at that temperature (P<0.001, Chi-square test).

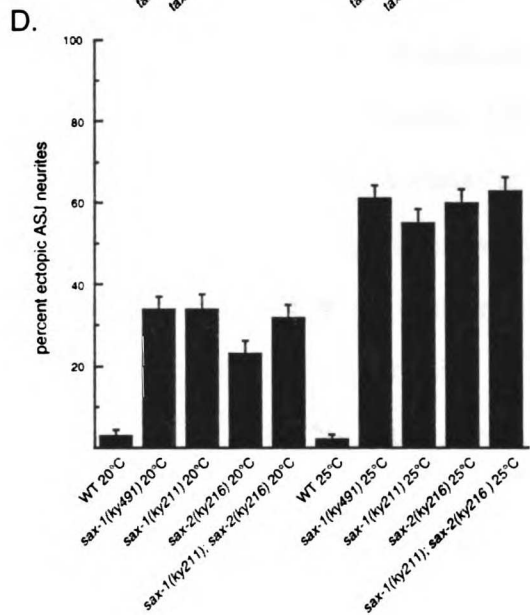
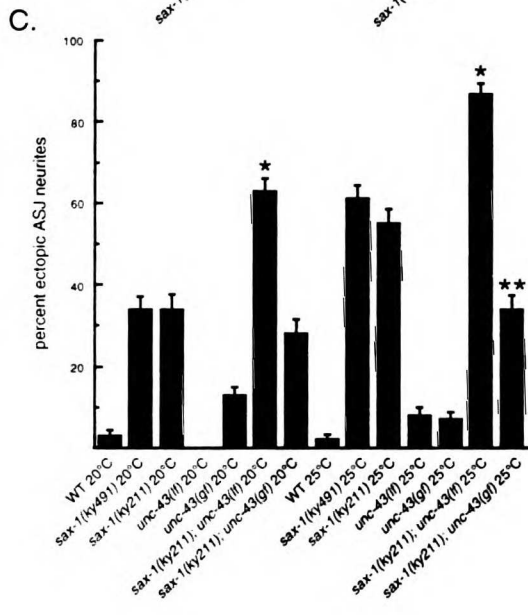
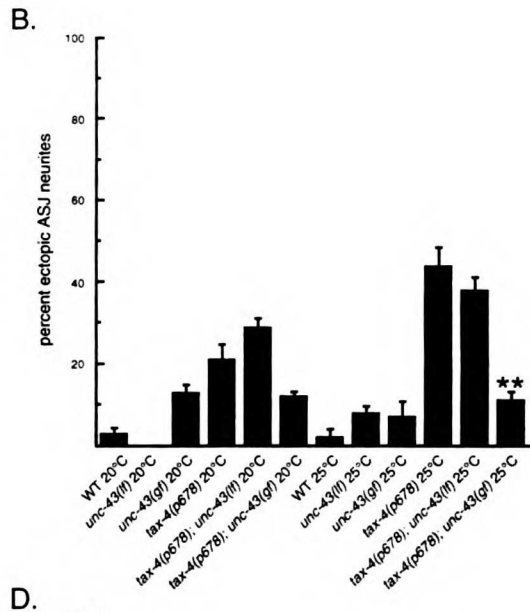
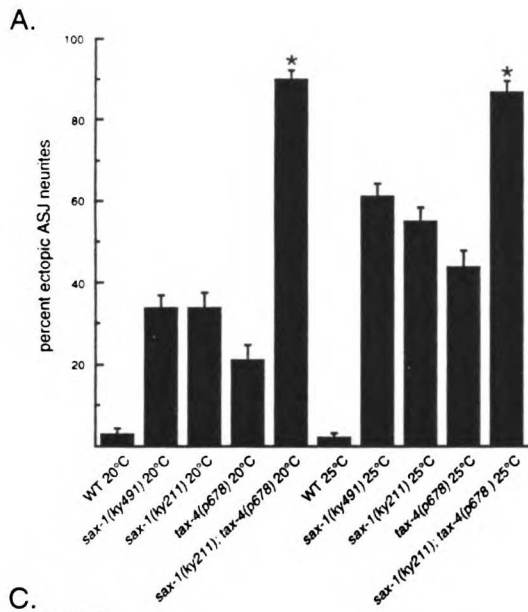


Figure 6. Regulation of ASER amphid neuron morphology by expression of *rhoA* alleles in wild-type and mutant backgrounds. Neuronal morphology was characterized with an integrated transgene that expresses GFP in ASER. All panels show a lateral view of one side of the animal. Anterior is to the left, dorsal at top. Scale bar = 10 μ m. (A) ASER morphology in a wild-type animal. (B) Expanded cell shape defect in an animal expressing *rhoA*^{D13T} in ASER. (C) Expanded cell shape defect in a *sax-1(ky491)* mutant. (D) Wild-type morphology in an animal coexpressing *rhoA*^{D13T} and *sax-1* in ASER. (E) Wild-type morphology in a *sax-1(ky491)* mutant expressing wild-type *rhoA* in ASER. (F-H) Quantitation of effects of *rhoA* (*rhoA*^{wt}), *rhoA*^{Q63L} or *rhoA*^{D13T} expression in ASER in wild-type and mutant backgrounds. Control animals were injected with the coinjection marker alone. Error bars indicate the standard error of proportion, combining animals from four (F,G) or three (H) independent transgenic lines, n>50 animals scored for each line. Single asterisks indicate transgenic animals that were significantly different from control animals (P<0.001, Chi-square test). (F) Expression of *rhoA* alleles in wild-type animals. The double asterisk indicates transgenic animals that were significantly less defective than animals expressing *rhoA*^{D13T} and significantly more defective than wild type. (G) Expression of *rhoA* alleles in *sax-1(ky491)* animals. (H) Expression of *rhoA* alleles in *tax-4(p678)* animals. *gcy-5::rhoA* alleles were injected at 50 ng/ μ l. *gcy-5::sax-1* was injected at 50 ng/ μ l in F and 100 ng/ μ l in H. In all experiments, the dominant *rol-6* pRF4 coinjection marker was injected at 100 ng/ μ l. As an additional control, *rhoA*^{D13T} was coinjected with the *gcy-5* promoter at 50 ng/ μ l, to address the possibility that coexpression of *gcy-5::sax-1* produced nonspecific suppression of the defects caused by *rhoA*^{D13T}.

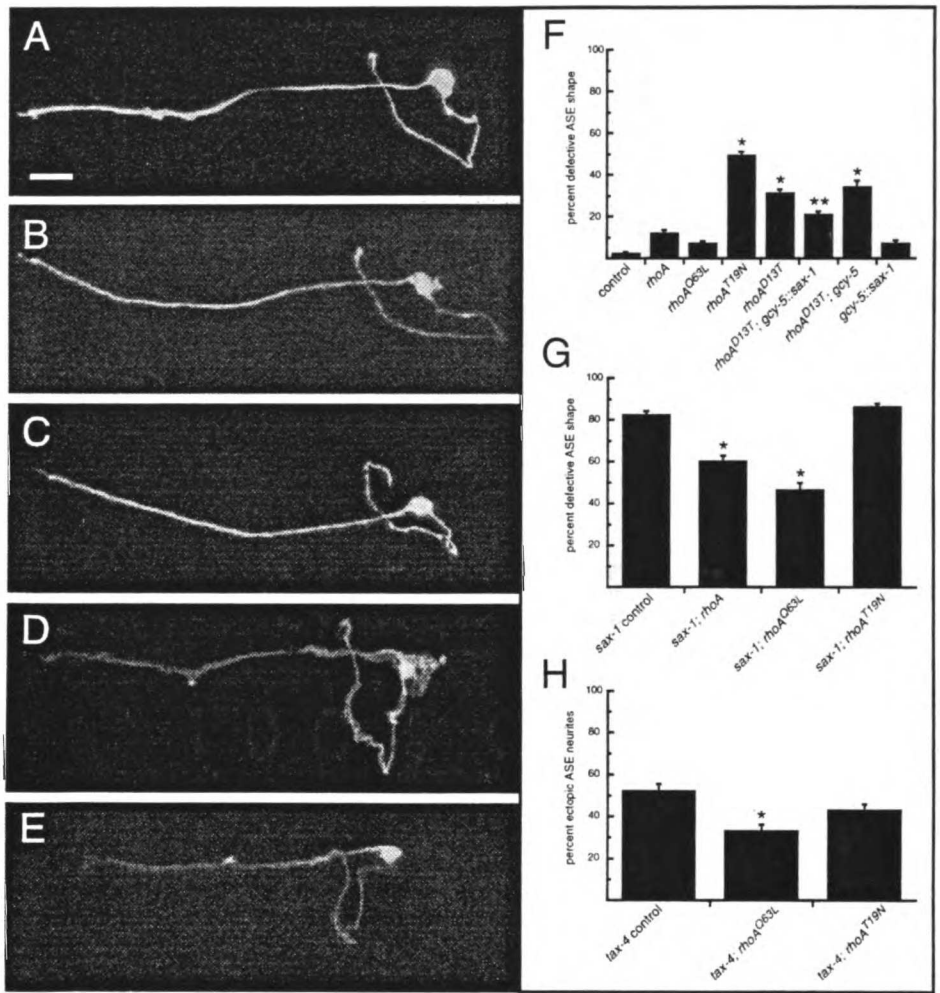


Table 1. Some neuronal morphology defects in *sax-1* and *sax-2* mutants are temperature sensitive

	ASE		ASJ		AWC	
	25°	20°	25°	20°	25°	20°
WT	2 (n=110)	1 (n=114)	4 (n=154)	0 (n=203)	0 (n=136)	2 (n=118)
<i>sax-1(ky211)</i>	84 (n=102)*	43 (n=106)	62 (n=180)*	27 (n=241)	92 (n=129)*	68 (n=287)
<i>sax-1(ky491)</i>	82 (n=265)*	64 (n=110)	59 (n=286)*	13 (n=214)	79 (n=179)	86 (n=332)
<i>sax-2(ky216)</i>	85 (n=150)	89 (n=131)	80 (n=246)*	28 (n=167)	97 (n=150)	94 (n=185)

Axon and cell shape phenotypes were scored in adult animals raised at 25°C or 20°C using GFP fusion genes *gcy-5::gfp* (ASE), *tax-2Δ::gfp* (ASJ) or *str-2::gfp* (AWC). Animals with cell bodies greater than or equal to twice the normal size or ectopic neurites longer than the diameter of the cell body were scored as defective. Asterisks represent values that differ between 25°C and 20°C at $p < 0.001$. n = number of animals scored. ND = not determined.

Chapter Five
Future Directions

This thesis describes the identification and characterization of genes required for axon outgrowth and guidance in *C. elegans*. Screens for mutants with sensory axon defects led to the identification of eight new *sax* genes required for the establishment (*sax-3*, *sax-5* and *sax-9*) or maintenance (*sax-1*, *sax-2*, *sax-6*, *sax-7* and *sax-8*) of sensory neuron morphology. The SAX-3/Robo immunoglobulin superfamily member regulates axon crossing at the ventral midline and functions as a receptor in the ventral guidance of axons to the midline. SAX-3 is also required for multiple guidance events in the nerve ring, where it acts in parallel to the VAB-1/Eph receptor and the UNC-6/netrin, UNC-40/DCC guidance systems for ventral guidance. SAX-1, a serine/threonine kinase related to the *Drosophila* and human Ndr kinases, is involved in a later developmental process that functions in the maintenance of amphid cell shape, a process that is also affected by the RHOA GTPase. In addition, SAX-1 is required for aspects of sensory neuron polarity and acts in parallel to activity-dependent morphological regulation. The identification of proteins required for early and late phases of amphid neuron development provides a basis for future analysis of the molecular and cell biological mechanisms that contribute to the elaboration of cell morphology during development.

Future directions: SAX-3/Robo

The characterization of other components of the SAX-3 signaling pathway will be essential to an understanding of the chain of events leading from engagement of the SAX-3 receptor at the cell surface to the regulation of growth cone orientation at the level of the cytoskeleton. Candidate approaches based on sequence homologies in the SAX-3/Robo coding region and phenotypic similarities *in vivo* have identified several proteins that are likely to be important for SAX-3/Robo signaling. For example, members of the Slit family of secreted molecules interact genetically and biochemically with Robo receptors (Brose *et al.*, 1999; Kidd *et al.*, 1999; Li *et al.*, 1999). These observations, combined with the identification of a *C. elegans* Slit homolog (J. Hao, J. A. Z. and C. Bargmann,

unpublished results), generate the strong prediction that Slit may function as a SAX-3 ligand in *C. elegans*. In support of this model, misexpression of *C. elegans* Slit can repel growing axons in a SAX-3-dependent manner (J. Hao and C. Bargmann, personal communication). Generation of a Slit mutant will help to definitively establish the function of Slit *in vivo* and the role of its interaction with the SAX-3 receptor (J. Hao and C. Bargmann, in progress).

Several domains in the SAX-3 cytoplasmic region are highly conserved among Robo family members, consistent with the observation that SAX-3/Robo proteins display some receptor functions (Kidd *et al.*, 1998a; Zallen *et al.*, 1998/Chapter 3). In particular, three conserved proline-rich motifs (Kidd *et al.*, 1998a), termed motifs A, B and C in SAX-3 (T. Yu and C. Bargmann, personal communication), may participate in signaling interactions that contribute to SAX-3 function. Biochemical analysis demonstrates that SAX-3 motif C can associate directly with the enabled protein (T. Yu, D. Li, K. Prehoda, W. Lim and C. Bargmann, personal communication). Enabled associates with the actin-binding protein profilin (Reinhard *et al.*, 1995; Gertler *et al.*, 1996) and has been implicated in axon guidance in vertebrates and invertebrates (Gertler *et al.*, 1996; Lanier *et al.*, 1999; M. Dell and G. Garriga, personal communication). These interactions suggest a mechanism for communication between the SAX-3 guidance receptor and the actin cytoskeleton. In addition, SAX-3 motif B interacts directly with a *C. elegans* homolog of the DOCK/Nck SH2/SH3 adapter protein (T. Yu and C. Bargmann, personal communication) and DOCK is required for normal axon guidance in *Drosophila* (Garrity *et al.*, 1996). These results raise the possibility that DOCK may function as a cytoplasmic effector of the SAX-3 receptor. The proteins that associate with motif A remain to be identified, although these may include SH2-domain proteins. Deletion of SAX-3 motifs B and C, and further characterization of the *C. elegans* DOCK and enabled homologs, will demonstrate whether these interactions are required for SAX-3 function *in vivo* (T. Yu and C. Bargmann, in progress). It will be interesting to determine if different signaling

interactions are relevant in different cell contexts, since *sax-3* mutants are defective in multiple axon guidance events, as well as the cell migrations of epidermal and mesodermal cell types (Chapter 2; C. Branda and M. Stern, personal communication).

In addition to the three proline-rich motifs that are shared among Robo homologs, SAX-3 contains two alternatively-spliced exons in its cytoplasmic domain — VSYVQ and DIFQ — whose roles in SAX-3 regulation have not been examined. The *mec-7::sax-3* fusion used in Chapter 2 to demonstrate that SAX-3 expression in the AVM neuron is sufficient for normal AVM axon guidance contain several small (<100 bp) introns that allow SAX-3 alternative splicing. Therefore, it is not known if the three identified SAX-3 isoforms differ in function, perhaps through altered spacing of the proline-rich motifs or tyrosine phosphorylation. Interestingly, the VSYVQ alternative exon resembles the conserved VYIVQ sequence in a set of transmembrane Ephrin ligands that are phosphorylated on tyrosine in response to Eph receptor association (Holland *et al.*, 1997). This sequence may therefore be relevant to SAX-3 activation upon association with a ligand or receptor partner. Further characterization of the SAX-3 isoforms responsible for its different roles *in vivo* may provide information about the cytoplasmic sequences required for SAX-3 function.

While much evidence has accumulated in favor of SAX-3/Robo receptor function, it is also possible that SAX-3 may perform as a ligand in certain contexts. It has not been possible to demonstrate a cell autonomous role for SAX-3 in the circumferential and longitudinal guidance of amphid sensory axons, and mosaic experiments are in fact consistent with a non-autonomous function (Appendix). Mosaic analysis indicates that SAX-3 activity is required in a small number of cells to regulate development of the nerve ring, suggesting two models: SAX-3 could act as a receptor in axons that pioneer the nerve ring or as a ligand on the substrate. SAX-3 could even play more than one role, for example as a receptor in ventral guidance and as a ligand in the prevention of anterior axon misrouting. Interestingly, the *C. elegans* Slit homolog, a candidate SAX-3 ligand, is

expressed in epidermal cells in the anterior head region and the RIH neuron whose axon defines the anterior boundary of the nerve ring (J. Hao and C. Bargmann, personal communication). RIH lies immediately adjacent to the large RMEV axon, which forms a wide barrier that is in a position to prevent nerve ring axons from inappropriately invading the anterior head region. Furthermore, RIH and RMEV are among the earliest axons to grow into the nerve ring (C. Norris and E. Hedgecock, personal communication). It would be interesting to examine whether SAX-3 functions cell autonomously in RMEV, perhaps in an epidermis-RMEV or RIH-RMEV interaction mediated by the Slit ligand.

Further mosaic analysis, combined with cell-specific *sax-3* expression and cell ablation experiments in the embryo, will help to define the site of SAX-3 action. It will also be necessary to directly demonstrate whether the SAX-3 cytoplasmic domain is required for SAX-3 functions. For example, SAX-3 may act in a subset of neurons to mediate nerve ring axon guidance; however, it could still function as a receptor or a ligand in these cells. Use of the *sax-3* promoter to drive expression of a truncated SAX-3 fusion with its cytoplasmic domain replaced by GFP produced dominant negative effects in wild-type animals, leading to aberrant midline crossover defects detected by GFP fluorescence (J. A. Z. and C. Bargmann, unpublished data). These results indicate that the SAX-3 fusion without a cytoplasmic domain is expressed. However, it was not possible to generate transgenic lines expressing this fusion in *sax-3(ky123)* mutant animals. However, it should be possible to generate transgenic lines with the truncated SAX-3 fusion in the healthier *sax-3(ky200ts)* strain at the permissive temperature, and then examine specific axon phenotypes at the restrictive temperature. The combination of these experimental approaches will help to define the regions of SAX-3 that function in specific axon guidance events.

Another way to identify components of the SAX-3 pathway is to examine mutants with *sax-3*-like phenotypes *in vivo*. The characterization of numerous axon guidance mutants conducted during the course of this thesis and in the published literature did not

identify any mutants with an identical set of phenotypes. However, the *unc-5*, *unc-6* and *unc-40* genes in the netrin signaling pathway exhibit distinct overall phenotypes, although certain cell types display common defects. It is possible that SAX-3 utilizes different signaling pathways in different cell types, such that examination of mutants with specific phenotypes in common with *sax-3* may provide information about cell-specific guidance pathways. For example, axon crossover at the midline is also caused by mutations in *unc-6*, *unc-40* (Wadsworth *et al.*, 1996), *sax-5*, *sax-9* (Chapter 2), *epi-1*, *vab-13* and *unc-34* (Appendix). It will be interesting to examine whether these genes are involved in SAX-3-mediated midline guidance. *epi-1* encodes a laminin alphaB chain (K. Joh and E. Hedgecock, personal communication). Slit can bind to laminin (Brose *et al.*, 1999), raising the possibility that EPI-1 may function to localize a midline-specific guidance molecule such as Slit (Brose *et al.*, 1999) or s-laminin (Hunter *et al.*, 1992). *vab-13* maps to a small region on LGXR (Jonathan Hodgkin, personal communication) that contains a *C. elegans* homolog of the secreted F-spondin protein which has been implicated in axon guidance in vertebrates (T. Burstyn-Cohen *et al.*, 1999); however, cosmids from this region did not rescue the *vab-13* mutant phenotype (Appendix).

unc-34 encodes a *C. elegans* enabled homolog (M. Dell and G. Garriga, personal communication) that is required to prevent axon crossing of the ventral midline (Appendix). Double mutant analysis should indicate whether SAX-3 and UNC-34 function together in this process, since each mutant has only partially penetrant defects on its own. It is interesting to note that, among all the axon guidance mutants characterized in the course of this thesis and in the published literature, only *unc-34* and *sax-5* exhibit near complete phenotypic overlap. Both *unc-34* and *sax-5* mutants have amphid axon termination defects (Chapter 2; J. A. Z. and C. Bargmann, unpublished data), CAN cell migration defects (Chapter 2; Forrester *et al.*, 1998), AVM ventral guidance defects (Chapter 2; T. Yu and C. Bargmann, personal communication) and interneuron midline crossover defects (Chapter 2; Appendix). Many of these phenotypes are also present in

sax-3 mutants (Chapter 2). Moreover, both *unc-34* and *sax-5* mutations enhance the anterior misrouting of amphid axons in double mutant combinations with *sax-3* (Appendix; T. Yu and C. Bargmann, personal communication). Therefore, UNC-34 and SAX-5 may define a class of mutants that participates in a common signaling pathway with SAX-3.

Genetic screens provide an opportunity to identify additional components of the SAX-3 guidance system in an unbiased manner. The first two immunoglobulin domains constitute the most highly conserved region among Robo family members (Kidd *et al.*, 1998a), and a missense mutation in this region in the *sax-3(ky200ts)* allele causes temperature-sensitive axon guidance defects (Zallen *et al.*, 1998/Chapter 3). Mutations that suppress the *sax-3(ky200ts)* mutation may include extracellular SAX-3-binding proteins such as Slit or novel ligand/receptor partners. Conversely, mutations that suppress defects caused by SAX-3 overexpression (Appendix) may identify downstream signaling proteins. Enhancer screens with a starting strain that is defective in one of the guidance systems that function in parallel to SAX-3 (Chapter 2; Appendix) may also help to identify genes in the SAX-3 guidance pathway.

The identification of components involved in SAX-3-dependent axon guidance will provide a foundation for studying the spatial and temporal regulation of pathways that direct axon guidance. An Appendix describes the construction of a GFP-tagged SAX-3 construct that appears to retain some aspects of SAX-3 function. It will be interesting to examine SAX-3::GFP localization in the growth cone of a growing axon such as HSN or AVM. Is SAX-3 localization dynamic in the growth cone, and is it regulated by endogenous or ectopic sources of Slit? Does the *sax-3(ky200ts)* mutation in the first immunoglobulin domain disrupt this localization? How does SAX-3 influence the localization of other molecules involved in axon guidance such as UNC-34/enabled or actin binding proteins?

Direct observations of growing axons will help to distinguish between different models for SAX-3-mediated axon guidance. For example, does SAX-3 prevent the initiation or stabilization of inappropriate axon contacts? If SAX-3 association with enabled recruits profilin and therefore actin polymerization to the plasma membrane, are these interactions disrupted upon SAX-3 engagement with a repulsive ligand? Further characterization of the SAX-3 signaling pathway will surely raise questions that can be addressed by this type of analysis.

Future directions: SAX-1/Ndr

The SAX-1/Ndr serine/threonine kinase is required for amphid cell shape and polarity in *C. elegans* and is related to the Orb6, Warts and COT-1 kinases that function in the regulation of cell morphology in other organisms. The signaling pathways mediated by these kinases — including proteins that may provide spatial and regulation of kinase activity as well as downstream substrates that communicate to the cytoskeleton — are largely unknown. In *S. pombe*, there is evidence that the Orb6 kinase may function downstream of the Cdc42-regulated Pak1/Shk1 kinase. Consistent with the possibility that SAX-1 may function downstream of GTPase signaling, mutations in the *C. elegans* RHOA GTPase caused aberrant cell shape phenotypes similar to those of *sax-1* mutants and these defects were partially rescued by SAX-1 overexpression. However, GTPase signaling also performs some SAX-1-independent functions, and the relationship between SAX-1 and GTPase pathways requires further characterization.

Genetic approaches will provide a powerful means to identify additional components involved in SAX-1 signaling. *sax-2* is the only other reported mutant with phenotypes in common with *sax-1*, and *sax-2* maps to a small region on LGIII (Chapter 2; Appendix). While SAX-1 overexpression can rescue the defects caused by dominant negative *rhoA* (Chapter 4), SAX-1 overexpression was not able to rescue *sax-2* mutant defects (J. A. Z. and C. Bargmann, unpublished results), suggesting that SAX-2 may

function downstream of SAX-1. The cloning of *sax-2* may provide information about the SAX-1 signaling pathway (M. Gallegos and C. Bargmann, in progress). The strong selection used as an enrichment in the *daf-11* suppression screening strategy greatly facilitated the isolation of the single *sax-1* and *sax-2* alleles; however, this screen is far from saturation and may lead to the identification of new genes if repeated. In addition, results in Chapter 4 demonstrate that modification of GTPase signaling through expression of *rhoA* mutant alleles can suppress the cell shape defects of *sax-1* null mutants. Therefore, a *sax-1* suppressor screen may identify components of GTPase signaling pathways.

Biochemical analysis of SAX-1 kinase activity on candidate target substrates and its regulation by other proteins will provide useful information about whether identified genetic relationships occur through direct interactions. Extensive biochemical characterization of different Ndr domains has been carried out *in vitro* (Millward *et al.*, 1995; Millward *et al.*, 1998). It will be interesting to determine whether these domains are required for SAX-1 function *in vivo*. For example, the spacer region within the Ndr kinase domain (KRKAETWKRNR) is required for its nuclear localization (Millward *et al.*, 1995) and this region is absolutely conserved in SAX-1. An additional SAX-1 nuclear localization motif (KRKIHHSKETDYLRLKRT) was predicted by the NUCDISC sequence analysis program. A functional SAX-1::GFP tag is localized throughout the cell body of the ASJ neurons, consistent with a role in either the nucleus or the cytoplasm. Deletion of each putative nuclear localization signal in this construct should provide information about whether SAX-1 protein is subsequently mislocalized and/or nonfunctional. In addition, Millward and colleagues have identified a conserved domain that is required for Ndr regulation by calcium (residues 62 - 86 of hNdr, corresponding to residues 53 - 77 of SAX-1) and a peptide from this region can disrupt calcium activation of Ndr in cultured cells. Characterization of SAX-1 mutants lacking this domain will provide evidence for the regulation of Ndr kinases by calcium *in vivo*.

The SDG-1 gene 3' of SAX-1 in the genome contains sequences that are present in other serine/threonine kinases, although *sax-1* and *sdg-1* appear to encode separate transcripts. It is possible that SDG-1 could function in trans to regulate the activity of the SAX-1 kinase. One way to test this model is to examine the phenotype of an *sdg-1* mutant. Alternatively, a dominant R → P mutation has been identified in a conserved pseudosubstrate site of protein kinase C (Nonaka *et al.*, 1995) that may normally function to inhibit kinase activity (Hug and Sarre, 1993). The RKGKK motif of SDG-1 is conserved at three of five residues with the pseudosubstrate site of PKC α ; alternatively, other arginine and lysine-rich sequences phosphorylated by hNdr *in vitro* (Millward *et al.*, 1998) could function as SAX-1 pseudosubstrate sites. Expression of an SDG-1 mutant defective in a candidate pseudosubstrate site may dominantly disrupt endogenous SDG-1 function and reveal whether SDG-1 and SAX-1 function in common processes.

SDG-1 also contains regions with homology to the domain of Rho kinases that associates specifically with GTP-bound Rho (Leung *et al.*, 1995; Ishizaki *et al.*, 1996; Matsui *et al.*, 1996). Biochemical analysis using SDG-1 and RHOA will be necessary to test whether this region of SDG-1 can function as a Rho-binding domain. It is interesting to speculate that SDG-1 may localize to sites of active GTPase signaling within the cell, perhaps in a pathway that confers spatial regulation on SAX-1 kinase activity. This could be analogous to observations in *S. cerevisiae*, where the Cdc42 and Rho1 GTPases required for regulation of bud formation and growth are localized to the bud site (Ziman *et al.*, 1993; Yamochi *et al.*, 1994). A first step in testing this model will be to determine whether a tagged SDG-1 protein exhibits specific subcellular localization within a cell such as the ASJ neuron, and whether this localization is altered by coexpression of dominant negative or gain of function RHOA mutants.

Conclusion

The identification of genes required for axon outgrowth, axon guidance and cell shape in *C. elegans* suggests several directions for future analysis. These include the use of focused genetic screens to identify additional components of these pathways *in vivo* along with biochemical assays to define physical and regulatory interactions *in vitro*. An understanding of SAX-1 and SAX-3 signaling pathways may provide information about the mechanisms by which extrinsic and intrinsic signals regulate the polarized distribution of cytoskeletal components to create unique and dynamic properties of cell morphology.

Bibliography

- Ackerman, S. L., Kozak, L. P., Przyborski, S. A., Rund, L. A., Boyer, B. B. and Knowles, B. B.** (1997). The mouse rostral cerebellar malformation gene encodes an UNC-5-like protein. *Nature* **386**, 838-842.
- Adams, A. E., Johnson, D. I., Longnecker, R. M., Sloat, B. F. and Pringle, J. R.** (1990). CDC42 and CDC43, two additional genes involved in budding and the establishment of cell polarity in the yeast *Saccharomyces cerevisiae*. *J Cell Biol* **111**, 131-142.
- Adams, R. H., Lohrum, M., Klostermann, A., Betz, H. and Puschel, A. W.** (1997). The chemorepulsive activity of secreted semaphorins is regulated by furin-dependent proteolytic processing. *Embo J* **16**, 6077-6086.
- Adams, R. H., Wilkinson, G. A., Weiss, C., Diella, F., Gale, N. W., Deutsch, U., Risau, W. and Klein, R.** (1999). Roles of ephrin B ligands and EphB receptors in cardiovascular development: demarcation of arterial/venous domains, vascular morphogenesis, and sprouting angiogenesis. *Genes Dev.* **13**, 295-306.
- Ahmed, S., Kozma, R., Lee, J., Monfries, C., Harden, N. and Lim, L.** (1991). The cysteine-rich domain of human proteins, neuronal chimaerin, protein kinase C and diacylglycerol kinase binds zinc. Evidence for the involvement of a zinc-dependent structure in phorbol ester binding. *Biochem J* **280**, 233-241.
- Amano, M., Chihara, K., Kimura, K., Fukata, Y., Nakamura, N., Matsuura, Y. and Kaibuchi, K.** (1997). Formation of actin stress fibers and focal adhesions enhanced by Rho-kinase. *Science* **275**, 1308-1311.
- Amano, M., Ito, M., Kimura, K., Fukata, Y., Chihara, K., Nakano, T., Matsuura, Y. and Kaibuchi, K.** (1996). Phosphorylation and activation of

myosin by Rho-associated kinase (Rho-kinase). *J Biol Chem* **271**, 20246-20249.

Bagnard, D., Lohrum, M., Uziel, D., Puschel, A. W. and Bolz, J. (1998).

Semaphorins act as attractive and repulsive guidance signals during the development of cortical projections. *Development* **125**, 5043-5053.

Bargmann, C. I., Hartwig, E. and Horvitz, H. R. (1993). Odorant-selective genes and neurons mediate olfaction in *C. elegans*. *Cell* **74**, 515-527.

Barrett, K., Leptin, M. and Settleman, J. (1997). The Rho GTPase and a putative RhoGEF mediate a signaling pathway for the cell shape changes in *Drosophila* gastrulation. *Cell* **91**, 905-915.

Barstead, R. J. and Waterston, R. H. (1989). The basal component of the nematode dense-body is vinculin. *J. Biol. Chem.* **264**, 10177-10185.

Baum, P. D. and Garriga, G. (1997). Neuronal migrations and axon fasciculation are disrupted in *ina-1* integrin mutants. *Neuron* **19**, 51-62.

Behar, O., Golden, J. A., Mashimo, H., Schoen, F. J. and Fishman, M. C. (1996). Semaphorin III is needed for normal patterning and growth of nerves, bones and heart. *Nature* **383**, 525-528.

Bender, A. and Pringle, J. R. (1989). Multicopy suppression of the *cdc24* budding defect in yeast by *CDC42* and three newly identified genes including the ras-related gene *RSR1*. *Proc Natl Acad Sci U S A* **86**, 9976-9980.

Bergemann, A. D., Zhang, L., Chiang, M. K., Brambilla, R., Klein, R. and Flanagan, J. G. (1998). Ephrin-B3, a ligand for the receptor EphB3, expressed at the midline of the developing neural tube. *Oncogene* **16**, 471-480.

Bloom, L. (1993). Genetic and molecular analysis of genes required for axon outgrowth in *Caenorhabditis elegans*. *Ph.D. Thesis Massachusetts Institute of Technology*, Cambridge, Massachusetts.

- Bloom, L. and Horvitz, H. R.** (1997). The *Caenorhabditis elegans* gene *unc-76* and its human homologs define a new gene family involved in axonal outgrowth and fasciculation. *Proc. Natl. Acad. Sci. USA* **94**, 3414-3419.
- Boguski, M. S. and McCormick, F.** (1993). Proteins regulating Ras and its relatives. *Nature* **366**, 643-654.
- Bourne, H. R., Sanders, D. A. and McCormick, F.** (1991). The GTPase superfamily: conserved structure and molecular mechanism. *Nature* **349**, 117-127.
- Brenner, S.** (1974). The genetics of *Caenorhabditis elegans*. *Genetics* **77**, 71-94.
- Bretscher, A.** (1991). Microfilament structure and function in the cortical cytoskeleton. *Annu Rev Cell Biol* **7**, 337-374.
- Brose, K., Bland, K. S., Wang, K. H., Arnott, D., Henzel, W., Goodman, C. S., Tessier-Lavigne, M. and Kidd, T.** (1999). Slit proteins bind Robo receptors and have an evolutionarily conserved role in repulsive axon guidance. *Cell* **96**, 795-806.
- Bruckner, K., Pasquale, E. B. and Klein, R.** (1997). Tyrosine phosphorylation of transmembrane ligands for Eph receptors. *Science* **275**, 1640-3.
- Budnik, V., Zhong, Y. and Wu, C. F.** (1990). Morphological plasticity of motor axons in *Drosophila* mutants with altered excitability. *J. Neurosci.* **10**, 3754-3768.
- Burstyn-Cohen, T., Tzarfaty, V., Frumkin, A., Feinstein, Y., Stoeckli, E. and Klar, A.** (1999). F-spondin is required for accurate pathfinding of commissural axons at the floor plate, *Neuron*, in press.
- Castellani, V., Yue, Y., Gao, P. P., Zhou, R. and Bolz, J.** (1998). Dual action of a ligand for Eph receptor tyrosine kinases on specific populations of axons during the development of cortical circuits. *J Neurosci* **18**, 4663-4672.

- Chalfie, M. and Thomson, J. N.** (1979). Organization of neuronal microtubules in the nematode *Caenorhabditis elegans*. *J. Cell Biol.* **82**, 278-289.
- Chan, S. S., Zheng, H., Su, M. W., Wilk, R., Killeen, M. T., Hedgecock, E. M. and Culotti, J. G.** (1996). UNC-40, a *C. elegans* homolog of DCC (Deleted in Colorectal Cancer), is required in motile cells responding to UNC-6 netrin cues. *Cell* **87**, 187-195.
- Chang, E. C., Barr, M., Wang, Y., Jung, V., Xu, H. P. and Wigler, M. H.** (1994). Cooperative interaction of *S. pombe* proteins required for mating and morphogenesis. *Cell* **79**, 131-141.
- Chant, J., Corrado, K., Pringle, J. R. and Herskowitz, I.** (1991). Yeast BUD5, encoding a putative GDP-GTP exchange factor, is necessary for bud site selection and interacts with bud formation gene BEM1. *Cell* **65**, 1213-1224.
- Chant, J. and Herskowitz, I.** (1991). Genetic control of bud site selection in yeast by a set of gene products that constitute a morphogenetic pathway. *Cell* **65**, 1203-1212.
- Chedotal, A., Del Rio, J. A., Ruiz, M., He, Z., Borrell, V., de Castro, F., Ezan, F., Goodman, C. S., Tessier-Lavigne, M., Sotelo, C. and Soriano, E.** (1998). Semaphorins III and IV repel hippocampal axons via two distinct receptors. *Development* **125**, 4313-4323.
- Chen, H., Chedotal, A., He, Z., Goodman, C. S. and Tessier-Lavigne, M.** (1997). Neuropilin-2, a novel member of the neuropilin family, is a high affinity receptor for the semaphorins Sema E and Sema IV but not Sema III. *Neuron* **19**, 547-559.
- Chen, H., He, Z., Bagri, A. and Tessier-Lavigne, M.** (1998). Semaphorin-neuropilin interactions underlying sympathetic axon responses to class III semaphorins. *Neuron* **21**, 1283-1290.

- Chen, W. and Lim, L.** (1994). The *Caenorhabditis elegans* small GTP-binding protein RhoA is enriched in the nerve ring and sensory neurons during larval development. *J Biol Chem* **269**, 32394-32404.
- Cheng, H. J., Nakamoto, M., Bergemann, A. D. and Flanagan, J. G.** (1995). Complementary gradients in expression and binding of ELF-1 and Mek4 in development of the topographic retinotectal projection map. *Cell* **82**, 371-381.
- Chihara, K., Amano, M., Nakamura, N., Yano, T., Shibata, M., Tokui, T., Ichikawa, H., Ikebe, R., Ikebe, M. and Kaibuchi, K.** (1997). Cytoskeletal rearrangements and transcriptional activation of c-fos serum response element by Rho-kinase. *J Biol Chem* **272**, 25121-25127.
- Chisholm, A. D. and Horvitz, H. R.** (1995). Patterning of the *Caenorhabditis elegans* head region by the Pax-6 family member *vab-3*. *Nature* **377**, 52-65.
- Chrzanowska-Wodnicka, M. and Burridge, K.** (1996). Rho-stimulated contractility drives the formation of stress fibers and focal adhesions. *J Cell Biol* **133**, 1403-1415.
- Coburn, C. M. and Bargmann, C. I.** (1996). A putative cyclic nucleotide-gated channel is required for sensory development and function in *C. elegans*. *Neuron* **17**, 695-706.
- Coburn, C. M., Mori, I., Ohshima, Y. and Bargmann, C. I.** (1998). A cyclic nucleotide-gated channel inhibits sensory axon outgrowth in larval and adult *C. elegans*: a distinct pathway for maintenance of sensory axon structure. *Development* **125**, 249-258.
- Colamarino, S. A. and Tessier-Lavigne, M.** (1995a). The axonal chemoattractant netrin-1 is also a chemorepellent for trochlear motor axons. *Cell* **81**, 621-629.
- Colamarino, S. A. and Tessier-Lavigne, M.** (1995b). The role of the floor plate in axon guidance. *Annu Rev Neurosci* **18**, 497-529.

- Colavita, A. and Culotti, J. G.** (1998). Suppressors of ectopic UNC-5 growth cone steering identify eight genes involved in axon guidance in *Caenorhabditis elegans*. *Dev Biol* **194**, 72-85.
- Comeau, M. R., Johnson, R., DuBose, R. F., Petersen, M., Gearing, P., VandenBos, T., Park, L., Farrah, T., Buller, R. M., Cohen, J. I., Strockbine, L. D., Rauch, C. and Spriggs, M. K.** (1998). A poxvirus-encoded semaphorin induces cytokine production from monocytes and binds to a novel cellular semaphorin receptor, VESPR. *Immunity* **8**, 473-482.
- Constantine-Paton, M., Cline, H. T. and Debski, E.** (1990). Patterned activity, synaptic convergence, and the NMDA receptor in developing visual pathways. *Annu Rev Neurosci* **13**, 129-154.
- Culotti, J. G. and Merz, D. C.** (1998). DCC and netrins. *Curr. Opin. Cell Biol.* **10**, 609-613.
- Davletov, B. A. and Sudhof, T. C.** (1993). A single C2 domain from synaptotagmin I is sufficient for high affinity Ca²⁺/phospholipid binding. *J Biol Chem* **268**, 26386-26390.
- de la Torre, J. R., Hopker, V. H., Ming, G. L., Poo, M. M., Tessier-Lavigne, M., Hemmati-Brivanlou, A. and Holt, C. E.** (1997). Turning of retinal growth cones in a netrin-1 gradient mediated by the netrin receptor DCC. *Neuron* **19**, 1211-1224.
- Deiner, M. S., Kennedy, T. E., Fazeli, A., Serafini, T., Tessier-Lavigne, M. and Sretavan, D. W.** (1997). Netrin-1 and DCC mediate axon guidance locally at the optic disc: loss of function leads to optic nerve hypoplasia. *Neuron* **19**, 575-589.
- Der, C. J., Finkel, T. and Cooper, G. M.** (1986a). Biological and biochemical properties of human rasH genes mutated at codon 61. *Cell* **44**, 167-176.

- Der, C. J., Pan, B. T. and Cooper, G. M.** (1986b). rasH mutants deficient in GTP binding. *Mol Cell Biol* **6**, 3291-3294.
- Dernburg, A. F., McDonald, K., Moulder, G., Barstead, R., Dresser, M. and Villeneuve, A. M.** (1998). Meiotic recombination in *C. elegans* initiates by a conserved mechanism and is dispensable for homologous chromosome synapsis. *Cell* **94**, 387-398.
- Desai, C., Garriga, G., McIntire, S. L. and Horvitz, H. R.** (1988). A genetic pathway for the development of the *Caenorhabditis elegans* HSN motor neurons. *Nature* **336**, 638-646.
- Devreotes, P. N. and Zigmond, S. H.** (1988). Chemotaxis in eukaryotic cells: a focus on leukocytes and Dictyostelium. *Annu Rev Cell Biol* **4**, 649-686.
- Di Cunto, F., Calautti, E., Hsiao, J., Ong, L., Topley, G., Turco, E. and Dotto, G. P.** (1998). Citron rho-interacting kinase, a novel tissue-specific ser/thr kinase encompassing the Rho-Rac-binding protein Citron. *J Biol Chem* **273**, 29706-29711.
- Drechsel, D. N., Hyman, A. A., Hall, A. and Glotzer, M.** (1997). A requirement for Rho and Cdc42 during cytokinesis in *Xenopus* embryos. *Curr Biol* **7**, 12-23.
- Drescher, U., Kremoser, C., Handwerker, C., Loschinger, J., Noda, M. and Bonhoeffer, F.** (1995). In vitro guidance of retinal ganglion cell axons by RAGS, a 25 kDa tectal protein related to ligands for Eph receptor tyrosine kinases. *Cell* **82**, 359-370.
- Durbin, R. M.** (1987). Studies on the development and organisation of the nervous system of *Caenorhabditis elegans*. *Ph.D. Thesis University of Cambridge*, Cambridge, England.

- Dwyer, N. D., Troemel, E. R., Sengupta, P. and Bargmann, C. I.** (1998). Odorant receptor localization to olfactory cilia is mediated by ODR-4, a novel membrane-associated protein. *Cell* **93**, 455-466.
- Eaton, S., Auvinen, P., Luo, L., Jan, Y. N. and Simons, K.** (1995). CDC42 and Rac1 control different actin-dependent processes in the *Drosophila* wing disc epithelium. *J Cell Biol* **131**, 151-164.
- Edelman, G. M. and Cunningham, B. A.** (1990). Place-dependent cell adhesion, process retraction, and spatial signaling in neural morphogenesis. *Cold Spring Harbor Symp. Quant. Biol.* **LV**, 303-318.
- Fan, J. and Raper, J. A.** (1995). Localized collapsing cues can steer growth cones without inducing their full collapse. *Neuron* **14**, 263-274.
- Fawell, E., Bowden, S. and Armstrong, J.** (1992). A homologue of the ras-related CDC42 gene from *Schizosaccharomyces pombe*. *Gene* **114**, 153-154.
- Fazeli, A., Dickinson, S. L., Hermiston, M. L., Tighe, R. V., Steen, R. G., Small, C. G., Stoeckli, E. T., Keino-Masu, K., Masu, M., Rayburn, H., Simons, J., Bronson, R. T., Gordon, J. I., Tessier-Lavigne, M. and Weinberg, R. A.** (1997). Phenotype of mice lacking functional Deleted in colorectal cancer (Dcc) gene. *Nature* **386**, 796-804.
- Feig, L. A. and Cooper, G. M.** (1988). Relationship among guanine nucleotide exchange, GTP hydrolysis, and transforming potential of mutated ras proteins. *Mol Cell Biol* **8**, 2472-2478.
- Flanagan, J. G. and Vanderhaeghen, P.** (1998). The ephrins and Eph receptors in neural development. *Annu Rev Neurosci* **21**, 309-345.
- Forrester, W. C., Perens, E., Zallen, J. A. and Garriga, G.** (1998). Identification of *Caenorhabditis elegans* genes required for neuronal differentiation and migration. *Genetics* **148**, 151-165.

- Fujisawa, H., Takagi, S. and Hirata, T. (1995).** Growth-associated expression of a membrane protein, neuropilin, in *Xenopus* optic nerve fibers. *Dev Neurosci* **17**, 343-349.
- Fujisawa, K., Fujita, A., Ishizaki, T., Saito, Y. and Narumiya, S. (1996).** Identification of the Rho-binding domain of p160ROCK, a Rho-associated coiled-coil containing protein kinase. *J Biol Chem* **271**, 23022-23028.
- Fukui, Y., Kozasa, T., Kaziro, Y., Takeda, T. and Yamamoto, M. (1986).** Role of a ras homolog in the life cycle of *Schizosaccharomyces pombe*. *Cell* **44**, 329-336.
- Garrett, M. D., Self, A. J., van Oers, C. and Hall, A. (1989).** Identification of distinct cytoplasmic targets for ras/R-ras and rho regulatory proteins. *J Biol Chem* **264**, 10-13.
- Garrity, P. A., Rao, Y., Salecker, I., McGlade, J., Pawson, T. and Zipursky, S. L. (1996).** *Drosophila* photoreceptor axon guidance and targeting requires the dreadlocks SH2/SH3 adapter protein. *Cell* **85**, 639-650.
- Gebbink, M. F., Kranenburg, O., Poland, M., van Horck, F. P., Houssa, B. and Moolenaar, W. H. (1997).** Identification of a novel, putative Rho-specific GDP/GTP exchange factor and a RhoA-binding protein: control of neuronal morphology. *J Cell Biol* **137**, 1603-1613.
- George, S. E., Simokat, K., Hardin, J. and Chisholm, A. D. (1998).** The VAB-1 Eph receptor tyrosine kinase functions in neural and epithelial morphogenesis in *C. elegans*. *Cell* **92**, 633-643.
- Gertler, F. B., Niebuhr, K., Reinhard, M., Wehland, J. and Soriano, P. (1996).** Mena, a relative of VASP and *Drosophila* Enabled, is implicated in the control of microfilament dynamics. *Cell* **87**, 227-239.
- Goodman, C. S. and Shatz, C. J. (1993).** Developmental mechanisms that generate precise patterns of neuronal connectivity. *Cell* **72 Suppl.**, 77-98.

- Goshima, Y., Nakamura, F., Strittmatter, P. and Strittmatter, S. M.** (1995). Collapsin-induced growth cone collapse mediated by an intracellular protein related to UNC-33. *Nature* **376**, 509-514.
- Hall, A.** (1994). Small GTP-binding proteins and the regulation of the actin cytoskeleton. *Annu Rev Cell Biol* **10**, 31-54.
- Hamelin, M., Zhou, Y., Su, M., Scott, I. and Culotti, J.** (1993). Expression of the UNC-5 guidance receptor in the touch neurons of *C. elegans* steers their axons dorsally. *Nature* **364**, 327-330.
- Hanson, P. I. and Schulman, H.** (1992). Neuronal Ca²⁺/calmodulin-dependent protein kinases. *Annu Rev Biochem* **61**, 559-601.
- Harden, N., Loh, H. Y., Chia, W. and Lim, L.** (1995). A dominant inhibitory version of the small GTP-binding protein Rac disrupts cytoskeletal structures and inhibits developmental cell shape changes in *Drosophila*. *Development* **121**, 903-914.
- Harris, R., Sabatelli, L. M. and Seeger, M. A.** (1996). Guidance cues at the *Drosophila* CNS midline: identification and characterization of two *Drosophila* Netrin/UNC-6 homologs. *Neuron* **17**, 217-228.
- Hartwell, L. H.** (1973). Three additional genes required for deoxyribonucleic acid synthesis in *Saccharomyces cerevisiae*. *J Bacteriol* **115**, 966-974.
- He, Z. and Tessier-Lavigne, M.** (1997). Neuropilin is a receptor for the axonal chemorepellent Semaphorin III. *Cell* **90**, 739-751.
- Hedgecock, E. M., Culotti, J. G., Thomson, J. N. and Perkins, L. A.** (1985). Axonal guidance mutants of *Caenorhabditis elegans* identified by filling sensory neurons with fluorescein dyes. *Dev. Biol.* **111**, 158-70.
- Hedgecock, E. M., Culotti, J. G. and Hall, D. H.** (1990). The *unc-5*, *unc-6*, and *unc-40* genes guide circumferential migrations of pioneer axons and mesodermal cells on the epidermis in *C. elegans*. *Neuron* **4**, 61-85.

- Henkemeyer, M., Orioli, D., Henderson, J. T., Saxton, T. M., Roder, J., Pawson, T. and Klein, R.** (1996). Nuk controls pathfinding of commissural axons in the mammalian central nervous system. *Cell* **86**, 35-46.
- Herman, R. K. and Hedgecock, E. M.** (1990). Limitation of the size of the vulval primordium of *Caenorhabditis elegans* by *lin-15* expression in surrounding hypodermis. *Nature* **348**, 169-171.
- Holland, S. J., Gale, N. W., Gish, G. D., Roth, R. A., Songyang, Z., Cantley, L. C., Henkemeyer, M., Yancopoulos, G. D. and Pawson, T.** (1997). Juxtamembrane tyrosine residues couple the Eph family receptor EphB2/Nuk to specific SH2 domain proteins in neuronal cells. *Embo J* **16**, 3877-3888.
- Huang, L. S., Tzou, P. and Sternberg, P. W.** (1994). The *lin-15* locus encodes two negative regulators of *Caenorhabditis elegans* vulval development. *Mol. Biol. Cell* **5**, 395-412.
- Hug, H. and Sarre, T. F.** (1993). Protein kinase C isoenzymes: divergence in signal transduction? *Biochem J* **291**, 329-343.
- Hunter, D. D., Llinas, R., Ard, M., Merlie, J. P. and Sanes, J. R.** (1992). Expression of s-laminin and laminin in the developing rat central nervous system. *J Comp Neurol* **323**, 238-251.
- Ishii, N., Wadsworth, W. G., Stern, B. D., Culotti, J. G. and Hedgecock, E. M.** (1992). UNC-6, a laminin-related protein, guides cell and pioneer axon migrations in *C. elegans*. *Neuron* **9**, 873-881.
- Ishizaki, T., Maekawa, M., Fujisawa, K., Okawa, K., Iwamatsu, A., Fujita, A., Watanabe, N., Saito, Y., Kakizuka, A., Morii, N. and Narumiya, S.** (1996). The small GTP-binding protein Rho binds to and activates a 160 kDa Ser/Thr protein kinase homologous to myotonic dystrophy kinase. *Embo J* **15**, 1885-1893.

- Ishizaki, T., Naito, M., Fujisawa, K., Maekawa, M., Watanabe, N., Saito, Y. and Narumiya, S.** (1997). p160ROCK, a Rho-associated coiled-coil forming protein kinase, works downstream of Rho and induces focal adhesions. *Febs Lett* **404**, 118-124.
- Itoh, A., Miyabayashi, T., Ohno, M. and Sakano, S.** (1998). Cloning and expressions of three mammalian homologues of *Drosophila* slit suggest possible roles for Slit in the formation and maintenance of the nervous system. *Brain Res Mol Brain Res* **62**, 175-186.
- Johnson, D. I. and Pringle, J. R.** (1990). Molecular characterization of CDC42, a *Saccharomyces cerevisiae* gene involved in the development of cell polarity. *J Cell Biol* **111**, 143-152.
- Justice, R. W., Zilian, O., Woods, D. F., Noll, M. and Bryant, P. J.** (1995). The *Drosophila* tumor suppressor gene warts encodes a homolog of human myotonic dystrophy kinase and is required for the control of cell shape and proliferation. *Genes Dev* **9**, 534-546.
- Kaech, S. M., Whitfield, C. W. and Kim, S. K.** (1998). The LIN-2/LIN-7/LIN-10 complex mediates basolateral membrane localization of the *C. elegans* EGF receptor LET-23 in vulval epithelial cells. *Cell* **94**, 761-772.
- Kawakami, A., Kitsukawa, T., Takagi, S. and Fujisawa, H.** (1996). Developmentally regulated expression of a cell surface protein, neuropilin, in the mouse nervous system. *J Neurobiol* **29**, 1-17.
- Keino-Masu, K., Masu, M., Hinck, L., Leonardo, E. D., Chan, S. S., Culotti, J. G. and Tessier-Lavigne, M.** (1996). Deleted in Colorectal Cancer (DCC) encodes a netrin receptor. *Cell* **87**, 175-185.
- Kennedy, T. E., Serafini, T., de la Torre, J. R. and Tessier-Lavigne, M.** (1994). Netrins are diffusible chemotropic factors for commissural axons in the embryonic spinal cord. *Cell* **78**, 425-435.

- Kidd, T., Bland, K. S. and Goodman, C. S. (1999).** Slit is the midline repellent for the Robo receptor in *Drosophila*. *Cell* **96**, 785-794.
- Kidd, T., Brose, K., Mitchell, K. J., Fetter, R. D., Tessier-Lavigne, M., Goodman, C. S. and Tear, G. (1998a).** Roundabout controls axon crossing of the CNS midline and defines a novel subfamily of evolutionarily conserved guidance receptors. *Cell* **92**, 205-215.
- Kidd, T., Russell, C., Goodman, C. S. and Tear, G. (1998b).** Dosage-sensitive and complementary functions of roundabout and commissureless control axon crossing of the CNS midline. *Neuron* **20**, 25-33.
- Kimura, K., Ito, M., Amano, M., Chihara, K., Fukata, Y., Nakafuku, M., Yamamori, B., Feng, J., Nakano, T., Okawa, K., Iwamatsu, A. and Kaibuchi, K. (1996).** Regulation of myosin phosphatase by Rho and Rho-associated kinase (Rho-kinase). *Science* **273**, 245-248.
- Kitsukawa, T., Shimizu, M., Sanbo, M., Hirata, T., Taniguchi, M., Bekku, Y., Yagi, T. and Fujisawa, H. (1997).** Neuropilin-semaphorin III/D-mediated chemorepulsive signals play a crucial role in peripheral nerve projection in mice. *Neuron* **19**, 995-1005.
- Kolodkin, A. L. (1996).** Growth cones and the cues that repel them. *Trends Neurosci* **19**, 507-513.
- Kolodkin, A. L. and Ginty, D. D. (1997).** Steering clear of semaphorins: neuropilins sound the retreat. *Neuron* **19**, 1159-1162.
- Kolodkin, A. L., Levensgood, D. V., Rowe, E. G., Tai, Y. T., Giger, R. J. and Ginty, D. D. (1997).** Neuropilin is a semaphorin III receptor. *Cell* **90**, 753-762.
- Kolodkin, A. L., Matthes, D. J. and Goodman, C. S. (1993).** The semaphorin genes encode a family of transmembrane and secreted growth cone guidance molecules. *Cell* **75**, 1389-1399.

- Kolodney, M. S. and Elson, E. L.** (1993). Correlation of myosin light chain phosphorylation with isometric contraction of fibroblasts. *J Biol Chem* **268**, 23850-23855.
- Kolodziej, P. A., Timpe, L. C., Mitchell, K. J., Fried, S. R., Goodman, C. S., Jan, L. Y. and Jan, Y. N.** (1996). frazzled encodes a *Drosophila* member of the DCC immunoglobulin subfamily and is required for CNS and motor axon guidance. *Cell* **87**, 197-204.
- Komatsu, H., Jin, Y. H., L'Etoile, N., Mori, I., Bargmann, C. I., Akaike, N. and Ohshima, Y.** (1999). Functional reconstitution of a heteromeric cyclic nucleotide-gated channel of *Caenorhabditis elegans* in cultured cells. *Brain Res* **821**, 160-168.
- Komatsu, H., Mori, I., Rhee, J.-S., Akaike, N. and Ohshima, Y.** (1996). Mutations in a cyclic nucleotide-gated channel lead to abnormal thermosensation and chemosensation in *C. elegans*. *Neuron* **17**, 707-718.
- Kozma, R., Ahmed, S., Best, A. and Lim, L.** (1995). The Ras-related protein Cdc42Hs and bradykinin promote formation of peripheral actin microspikes and filopodia in Swiss 3T3 fibroblasts. *Mol Cell Biol* **15**, 1942-1952.
- Krull, C. E., Lansford, R., Gale, N. W., Collazo, A., Marcelle, C., Yancopoulos, G. D., Fraser, S. E. and Bronner-Fraser, M.** (1997). Interactions of Eph-related receptors and ligands confer rostrocaudal pattern to trunk neural crest migration. *Curr. Biol.* **7**, 571-580.
- Lamarche, N. and Hall, A.** (1994). GAPs for rho-related GTPases. *Trends Genet* **10**, 436-440.
- Lamb, N. J., Fernandez, A., Conti, M. A., Adelstein, R., Glass, D. B., Welch, W. J. and Feramisco, J. R.** (1988). Regulation of actin microfilament integrity in living nonmuscle cells by the cAMP-dependent protein kinase and the myosin light chain kinase. *J Cell Biol* **106**, 1955-1971.

- Lang, P., Gesbert, F., Delespine-Carmagnat, M., Stancou, R., Pouchelet, M. and Bertoglio, J.** (1996). Protein kinase A phosphorylation of RhoA mediates the morphological and functional effects of cyclic AMP in cytotoxic lymphocytes. *Embo J* **15**, 510-519.
- Lanier, L. M., Gates, M. A., Witke, W., Menzies, A. S., Wehman, A. M., Macklis, J. D., Kwiatkowski, D., Soriano, P. and Gertler, F. B.** (1999). Mena is required for neurulation and commissure formation. *Neuron* **22**, 313-325.
- Leonardo, E. D., Hinck, L., Masu, M., Keino-Masu, K., Ackerman, S. L. and Tessier-Lavigne, M.** (1997). Vertebrate homologues of *C. elegans* UNC-5 are candidate netrin receptors. *Nature* **386**, 833-838.
- Leung, T., Chen, X. Q., Manser, E. and Lim, L.** (1996). The p160 RhoA-binding kinase ROK alpha is a member of a kinase family and is involved in the reorganization of the cytoskeleton. *Mol Cell Biol* **16**, 5313-5327.
- Leung, T., Chen, X. Q., Tan, I., Manser, E. and Lim, L.** (1998). Myotonic dystrophy kinase-related Cdc42-binding kinase acts as a Cdc42 effector in promoting cytoskeletal reorganization. *Mol Cell Biol* **18**, 130-140.
- Leung, T., Manser, E., Tan, L. and Lim, L.** (1995). A novel serine/threonine kinase binding the Ras-related RhoA GTPase which translocates the kinase to peripheral membranes. *J Biol Chem* **270**, 29051-29054.
- Leung-Hagesteijn, C., Spence, A. M., Stern, B. D., Zhou, Y., Su, M. W., Hedgecock, E. M. and Culotti, J. G.** (1992). UNC-5, a transmembrane protein with immunoglobulin and thrombospondin type I domains, guides cell and pioneer axon migrations in *C. elegans*. *Cell* **71**, 289-299.
- Levin, D. E., Fields, F. O., Kunisawa, R., Bishop, J. M. and Thorner, J.** (1990). A candidate protein kinase C gene, PKC1, is required for the *S. cerevisiae* cell cycle. *Cell* **62**, 213-224.

- Li, H. S., Chen, J. H., Wu, W., Fagaly, T., Zhou, L., Yuan, W., Dupuis, S., Jiang, Z. H., Nash, W., Gick, C., Ornitz, D. M., Wu, J. Y. and Rao, Y.** (1999). Vertebrate slit, a secreted ligand for the transmembrane protein roundabout, is a repellent for olfactory bulb axons. *Cell* **96**, 807-818.
- Luo, L., Lee, T., Tsai, L., Tang, G., Jan, L. Y. and Jan, Y. N.** (1997). Genghis Khan (Gek) as a putative effector for *Drosophila* Cdc42 and regulator of actin polymerization. *Proc Natl Acad Sci U S A* **94**, 12963-12968.
- Luo, L., Liao, Y. J., Jan, L. Y. and Jan, Y. N.** (1994). Distinct morphogenetic functions of similar small GTPases: *Drosophila* Drac1 is involved in axonal outgrowth and myoblast fusion. *Genes Dev* **8**, 1787-1802.
- Luo, Y., Raible, D. and Raper, J. A.** (1993). Collapsin: a protein in brain that induces the collapse and paralysis of neuronal growth cones. *Cell* **75**, 217-227.
- Madaule, P., Eda, M., Watanabe, N., Fujisawa, K., Matsuoka, T., Bito, H., Ishizaki, T. and Narumiya, S.** (1998). Role of citron kinase as a target of the small GTPase Rho in cytokinesis. *Nature* **394**, 491-494.
- Madaule, P., Furuyashiki, T., Reid, T., Ishizaki, T., Watanabe, G., Morii, N. and Narumiya, S.** (1995). A novel partner for the GTP-bound forms of rho and rac. *Febs Lett* **377**, 243-248.
- Maestrini, E., Tamagnone, L., Longati, P., Cremona, O., Gulisano, M., Bione, S., Tamanini, F., Neel, B. G., Toniolo, D. and Comoglio, P. M.** (1996). A family of transmembrane proteins with homology to the MET-hepatocyte growth factor receptor. *Proc Natl Acad Sci U S A* **93**, 674-678.
- Marcus, S., Polverino, A., Chang, E., Robbins, D., Cobb, M. H. and Wigler, M. H.** (1995). Shk1, a homolog of the *Saccharomyces cerevisiae* Ste20 and mammalian p65PAK protein kinases, is a component of a Ras/Cdc42

- signaling module in the fission yeast *Schizosaccharomyces pombe*. *Proc Natl Acad Sci U S A* **92**, 6180-6184.
- Maricq, A. V., Peckol, E., Driscoll, M. and Bargmann, C. I.** (1995). Mechanosensory signalling in *C. elegans* mediated by the GLR-1 glutamate receptor. *Nature* **378**, 78-81.
- Matsui, T., Amano, M., Yamamoto, T., Chihara, K., Nakafuku, M., Ito, M., Nakano, T., Okawa, K., Iwamatsu, A. and Kaibuchi, K.** (1996). Rho-associated kinase, a novel serine/threonine kinase, as a putative target for small GTP binding protein Rho. *Embo J* **15**, 2208-2216.
- Matsui, Y. and Toh-E, A.** (1992). Yeast RHO3 and RHO4 ras superfamily genes are necessary for bud growth, and their defect is suppressed by a high dose of bud formation genes CDC42 and BEM1. *Mol Cell Biol* **12**, 5690-5699.
- McIntire, S. L., Garriga, G., White, J. G., Jacobson, D. and Horvitz, H. R.** (1992). Genes necessary for directed axonal elongation or fasciculation in *Caenorhabditis elegans*. *Neuron* **8**, 307-322.
- Mello, C. C., Kramer, J. M., Stinchcomb, D. and Ambros, V.** (1991). Efficient gene transfer in *C. elegans*: Extrachromosomal maintenance and integration of transforming sequences. *EMBO J.* **10**, 3959-3970.
- Mello, C. and Fire, A.** (1995). DNA transformation. *Methods Cell Biol.* **48**, 451-482.
- Messersmith, E. K., Leonardo, E. D., Shatz, C. J., Tessier-Lavigne, M., Goodman, C. S. and Kolodkin, A. L.** (1995). Semaphorin III can function as a selective chemorepellent to pattern sensory projections in the spinal cord. *Neuron* **14**, 949-959.
- Miller, P. J. and Johnson, D. I.** (1994). Cdc42p GTPase is involved in controlling polarized cell growth in *Schizosaccharomyces pombe*. *Mol Cell Biol* **14**, 1075-1083.

- Millward, T., Cron, P. and Hemmings, B. A.** (1995). Molecular cloning and characterization of a conserved nuclear serine(threonine) protein kinase. *Proc Natl Acad Sci U S A* **92**, 5022-5026.
- Millward, T. A., Heizmann, C. W., Schafer, B. W. and Hemmings, B. A.** (1998). Calcium regulation of Ndr protein kinase mediated by S100 calcium-binding proteins. *Embo J* **17**, 5913-5922.
- Ming, G. L., Song, H. J., Berninger, B., Holt, C. E., Tessier-Lavigne, M. and Poo, M. M.** (1997). cAMP-dependent growth cone guidance by netrin-1. *Neuron* **19**, 1225-1235.
- Mitani, S., Du, H., Hall, D. H., Driscoll, M. and Chalfie, M.** (1993). Combinatorial control of touch receptor neuron expression in *Caenorhabditis elegans*. *Development* **119**, 773-783.
- Mitchell, K. J., Doyle, J. L., Serafini, T., Kennedy, T. E., Tessier-Lavigne, M., Goodman, C. S. and Dickson, B. J.** (1996). Genetic analysis of Netrin genes in *Drosophila*: Netrins guide CNS commissural axons and peripheral motor axons. *Neuron* **17**, 203-215.
- Monschau, B., Kremoser, C., Ohta, K., Tanaka, H., Kaneko, T., Yamada, T., Handwerker, C., Hornberger, M. R., Loschinger, J., Pasquale, E. B., Siever, D. A., Verderame, M. F., Muller, B. K., Bonhoeffer, F. and Drescher, U.** (1997). Shared and distinct functions of RAGS and ELF-1 in guiding retinal axons. *Embo J* **16**, 1258-1267.
- Mueller, B. K.** (1999). Growth cone guidance: first steps towards a deeper understanding. *Annu Rev Neurosci* **22**, 351-388.
- Nakagawa, O., Fujisawa, K., Ishizaki, T., Saito, Y., Nakao, K. and Narumiya, S.** (1996). ROCK-I and ROCK-II, two isoforms of Rho-associated coiled-coil forming protein serine/threonine kinase in mice. *Febs Lett* **392**, 189-193.

- Nakamoto, M., Cheng, H. J., Friedman, G. C., McLaughlin, T., Hansen, M. J., Yoon, C. H., O'Leary, D. D. and Flanagan, J. G. (1996).** Topographically specific effects of ELF-1 on retinal axon guidance in vitro and retinal axon mapping in vivo. *Cell* **86**, 755-766.
- Nakayama, M., Nakajima, D., Nagase, T., Nomura, N., Seki, N. and Ohara, O. (1998).** Identification of high-molecular-weight proteins with multiple EGF-like motifs by motif-trap screening. *Genomics* **51**, 27-34.
- Nguyen Ba-Charvet, K. T., Brose, K., Marillat, V., Kidd, T., Goodman, C. S., Tessier-Lavigne, M., Sotelo, C. and Chedotal, A. (1999).** Slit2-Mediated chemorepulsion and collapse of developing forebrain axons. *Neuron* **22**, 463-473.
- Nishizuka, Y. (1984).** The role of protein kinase C in cell surface signal transduction and tumour promotion. *Nature* **308**, 693-698.
- Nobes, C. D. and Hall, A. (1995).** Rho, rac, and cdc42 GTPases regulate the assembly of multimolecular focal complexes associated with actin stress fibers, lamellipodia, and filopodia. *Cell* **81**, 53-62.
- Nonaka, H., Tanaka, K., Hirano, H., Fujiwara, T., Kohno, H., Umikawa, M., Mino, A. and Takai, Y. (1995).** A downstream target of RHO1 small GTP-binding protein is PKC1, a homolog of protein kinase C, which leads to activation of the MAP kinase cascade in *Saccharomyces cerevisiae*. *Embo J* **14**, 5931-5938.
- Ohta, K., Mizutani, A., Kawakami, A., Murakami, Y., Kasuya, Y., Takagi, S., Tanaka, H. and Fujisawa, H. (1995).** Plexin: a novel neuronal cell surface molecule that mediates cell adhesion via a homophilic binding mechanism in the presence of calcium ions. *Neuron* **14**, 1189-1199.
- Ono, Y., Fujii, T., Igarashi, K., Kuno, T., Tanaka, C., Kikkawa, U. and Nishizuka, Y. (1989).** Phorbol ester binding to protein kinase C requires a

cysteine-rich zinc- finger-like sequence. *Proc Natl Acad Sci U S A* **86**, 4868-4871.

Orioli, D., Henkemeyer, M., Lemke, G., Klein, R. and Pawson, T. (1996). Sek4 and Nuk receptors cooperate in guidance of commissural axons and in palate formation. *Embo J* **15**, 6035-6049.

Otsuka, A. J., Franco, R., Yang, B., Shim, K. H., Tang, L. Z., Zhang, Y. Y., Boontrakulpoontawee, P., Jeyaprakash, A., Hedgecock, E., Wheaton, V. I. and Sobery, A. (1995). An ankyrin-related gene (*unc-44*) is necessary for proper axonal guidance in *Caenorhabditis elegans*. *J. Cell Biol.* **129**, 1081-1092.

Ottillie, S., Miller, P. J., Johnson, D. I., Creasy, C. L., Sells, M. A., Bagrodia, S., Forsburg, S. L. and Chernoff, J. (1995). Fission yeast *pak1+* encodes a protein kinase that interacts with Cdc42p and is involved in the control of cell polarity and mating. *Embo J* **14**, 5908-5919.

Ozaki, K., Tanaka, K., Imamura, H., Hihara, T., Kameyama, T., Nonaka, H., Hirano, H., Matsuura, Y. and Takai, Y. (1996). Rom1p and Rom2p are GDP/GTP exchange proteins (GEPs) for the Rho1p small GTP binding protein in *Saccharomyces cerevisiae*. *Embo J* **15**, 2196-2207.

Park, H. O., Chant, J. and Herskowitz, I. (1993). BUD2 encodes a GTPase-activating protein for Bud1/Rsr1 necessary for proper bud-site selection in yeast. *Nature* **365**, 269-274.

Park, S., Frisen, J. and Barbacid, M. (1997). Aberrant axonal projections in mice lacking EphA8 (Eek) tyrosine protein kinase receptors. *Embo J* **16**, 3106-3114.

Paterson, H. F., Self, A. J., Garrett, M. D., Just, I., Aktories, K. and Hall, A. (1990). Microinjection of recombinant p21rho induces rapid changes in cell morphology. *J Cell Biol* **111**, 1001-1007.

- Peckol, E. L., Zallen, J. A., Yarrow, J. C. and Bargmann, C. I.** (1999). Sensory activity affects sensory axon development in *C. elegans*. *Development* **126**, 1891-1902.
- Perkins, L. A., Hedgecock, E. M., Thomson, J. N. and Culotti, J. G.** (1986). Mutant sensory cilia in the nematode *Caenorhabditis elegans*. *Dev. Biol.* **117**, 456-487.
- Puschel, A. W.** (1996). The semaphorins: a family of axonal guidance molecules? *Eur J Neurosci* **8**, 1317-1321.
- Puschel, A. W., Adams, R. H. and Betz, H.** (1995). Murine semaphorin D/collapsin is a member of a diverse gene family and creates domains inhibitory for axonal extension. *Neuron* **14**, 941-948.
- Quilliam, L. A., Khosravi-Far, R., Huff, S. Y. and Der, C. J.** (1995). Guanine nucleotide exchange factors: activators of the Ras superfamily of proteins. *Bioessays* **17**, 395-404.
- Reinhard, M., Giehl, K., Abel, K., Haffner, C., Jarchau, T., Hoppe, V., Jockusch, B. M. and Walter, U.** (1995). The proline-rich focal adhesion and microfilament protein VASP is a ligand for profilins. *Embo J* **14**, 1583-1589.
- Riddle, D. L., Swanson, M. M. and Albert, P. S.** (1981). Interacting genes in nematode dauer larva formation. *Nature* **290**, 668-671.
- Ridley, A. J. and Hall, A.** (1992). The small GTP-binding protein rho regulates the assembly of focal adhesions and actin stress fibers in response to growth factors. *Cell* **70**, 389-399.
- Ridley, A. J., Paterson, H. F., Johnston, C. L., Diekmann, D. and Hall, A.** (1992). The small GTP-binding protein rac regulates growth factor-induced membrane ruffling. *Cell* **70**, 401-410.

- Rongo, C., Whitfield, C. W., Rodal, A., Kim, S. K. and Kaplan, J. M.** (1998). LIN-10 is a shared component of the polarized protein localization pathways in neurons and epithelia. *Cell* **94**, 751-760.
- Roskies, A. L. and O'Leary, D. D.** (1994). Control of topographic retinal axon branching by inhibitory membrane-bound molecules. *Science* **265**, 799-803.
- Rothberg, J. M., Hartley, D. A., Walther, Z. and Artavanis-Tsakonas, S.** (1988). slit: an EGF-homologous locus of *D. melanogaster* involved in the development of the embryonic central nervous system. *Cell* **55**, 1047-1059.
- Rothberg, J. M., Jacobs, J. R., Goodman, C. S. and Artavanis-Tsakonas, S.** (1990). slit: an extracellular protein necessary for development of midline glia and commissural axon pathways contains both EGF and LRR domains. *Genes Dev* **4**, 2169-2187.
- Seabra, M. C.** (1998). Membrane association and targeting of prenylated Ras-like GTPases. *Cell Signal* **10**, 167-172.
- Seeger, M., Tear, G., Ferres-Marco, D. and Goodman, C. S.** (1993). Mutations affecting growth cone guidance in *Drosophila*: genes necessary for guidance toward or away from the midline. *Neuron* **10**, 409-426.
- Schackwitz, W. S., Inoue, T. and Thomas, J. H.** (1996). Chemosensory neurons function in parallel to mediate a pheromone response in *C. elegans*. *Neuron* **17**, 719-728.
- Sengupta, P., Chou, J. C. and Bargmann, C. I.** (1996). *odr-10* encodes a seven transmembrane domain olfactory receptor required for responses to the odorant diacetyl. *Cell* **84**, 899-909.
- Serafini, T., Kennedy, T. E., Galko, M. J., Mirzayan, C., Jessell, T. M. and Tessier-Lavigne, M.** (1994). The netrins define a family of axon outgrowth-promoting proteins homologous to *C. elegans* UNC-6. *Cell* **78**, 409-424.

- Serafini, T., Colamarino, S. A., Leonardo, E. D., Wang, H., Beddington, R., Skarnes, W. C. and Tessier-Lavigne, M.** (1996). Netrin-1 is required for commissural axon guidance in the developing vertebrate nervous system. *Cell* **87**, 1001-1014.
- Shirasaki, R., Katsumata, R. and Murakami, F.** (1998). Change in chemoattractant responsiveness of developing axons at an intermediate target. *Science* **279**, 105-107.
- Shirasaki, R., Mirzayan, C., Tessier-Lavigne, M. and Murakami, F.** (1996). Guidance of circumferentially growing axons by netrin-dependent and -independent floor plate chemotropism in the vertebrate brain. *Neuron* **17**, 1079-1088.
- Shirasaki, R., Tamada, A., Katsumata, R. and Murakami, F.** (1995). Guidance of cerebellofugal axons in the rat embryo: directed growth toward the floor plate and subsequent elongation along the longitudinal axis. *Neuron* **14**, 961-972.
- Siddiqui, S. S.** (1990). Mutations affecting axonal outgrowth and guidance of motor neurons and mechanosensory neurons in the nematode *Caenorhabditis elegans*. *Neurosci. Res.(Suppl.)* **13**, 171-190.
- Siddiqui, S. S. and Culotti, J. G.** (1991). Examination of neurons in wild type and mutants of *Caenorhabditis elegans* using antibodies to horseradish peroxidase. *J. Neurogenet.* **7**, 193-211.
- Smith, A., Robinson, V., Patel, K. and Wilkinson, D. G.** (1997). The EphA4 and EphB1 receptor tyrosine kinases and ephrin-B2 ligand regulate targeted migration of branchial neural crest cells. *Curr Biol* **7**, 561-570.
- Sonnenfeld, M. J. and Jacobs, J. R.** (1994). Mesectodermal cell fate analysis in *Drosophila* midline mutants. *Mech Dev* **46**, 3-13.

- St. John, M. A., Tao, W., Fei, X., Fukumoto, R., Carcangiu, M. L., Brownstein, D. G., Parlow, A. F., McGrath, J. and Xu, T. (1999).** Mice deficient of Lats1 develop soft-tissue sarcomas, ovarian tumours and pituitary dysfunction. *Nat Genet* **21**, 182-186.
- Steven, R., Kubiseski, T. J., Zheng, H., Kulkarni, S., Mancillas, J., Ruiz Morales, A., Hogue, C. W., Pawson, T. and Culotti, J. (1998).** UNC-73 activates the Rac GTPase and is required for cell and growth cone migrations in *C. elegans*. *Cell* **92**, 785-795.
- Strutt, D. I., Weber, U. and Mlodzik, M. (1997).** The role of RhoA in tissue polarity and Frizzled signalling. *Nature* **387**, 292-295.
- Sulston, J. E., Schierenberg, E., White, J. G. and Thomson, J. N. (1983).** The embryonic cell lineage of the nematode *Caenorhabditis elegans*. *Dev. Biol.* **100**, 64-119.
- Symons, M. (1996).** Rho family GTPases: the cytoskeleton and beyond. *Trends Biochem Sci* **21**, 178-181.
- Takagi, S., Hirata, T., Agata, K., Mochii, M., Eguchi, G. and Fujisawa, H. (1991).** The A5 antigen, a candidate for the neuronal recognition molecule, has homologies to complement components and coagulation factors. *Neuron* **7**, 295-307.
- Takagi, S., Kasuya, Y., Shimizu, M., Matsuura, T., Tsuboi, M., Kawakami, A. and Fujisawa, H. (1995).** Expression of a cell adhesion molecule, neuropilin, in the developing chick nervous system. *Dev Biol* **170**, 207-222.
- Takahashi, T., Nakamura, F., Jin, Z., Kalb, R. G. and Strittmatter, S. M. (1998).** Semaphorins A and E act as antagonists of neuropilin-1 and agonists of neuropilin-2 receptors. *Nat Neurosci* **1**, 487-493.

- Tan, J. L., Ravid, S. and Spudich, J. A.** (1992). Control of nonmuscle myosins by phosphorylation. *Annu Rev Biochem* **61**, 721-759.
- Taniguchi, M., Yuasa, S., Fujisawa, H., Naruse, I., Saga, S., Mishina, M. and Yagi, T.** (1997). Disruption of semaphorin III/D gene causes severe abnormality in peripheral nerve projection. *Neuron* **19**, 519-530.
- Tapon, N. and Hall, A.** (1997). Rho, Rac and Cdc42 GTPases regulate the organization of the actin cytoskeleton. *Curr Opin Cell Biol* **9**, 86-92.
- Tear, G., Harris, R., Sutaria, S., Kilomanski, K., Goodman, C. S. and Seeger, M. A.** (1996). *commissureless* controls growth cone guidance across the CNS midline in *Drosophila* and encodes a novel membrane protein. *Neuron* **16**, 501-514.
- Tessier-Lavigne, M. and Goodman, C. S.** (1996). The molecular biology of axon guidance. *Science* **274**, 1123-1133.
- Troemel, E. R., Kimmel, B. E. and Bargmann, C. I.** (1997). Reprogramming chemotaxis responses: sensory neurons define olfactory preferences in *C. elegans*. *Cell* **91**, 161-169.
- Turner, C. E. and Burridge, K.** (1991). Transmembrane molecular assemblies in cell-extracellular matrix interactions. *Curr Opin Cell Biol* **3**, 849-853.
- Varela-Echavarría, A., Tucker, A., Puschel, A. W. and Guthrie, S.** (1997). Motor axon subpopulations respond differentially to the chemorepellents netrin-1 and semaphorin D. *Neuron* **18**, 193-207.
- Verde, F., Mata, J. and Nurse, P.** (1995). Fission yeast cell morphogenesis: identification of new genes and analysis of their role during the cell cycle. *J Cell Biol* **131**, 1529-1538.
- Verde, F., Wiley, D. J. and Nurse, P.** (1998). Fission yeast orb6, a ser/thr protein kinase related to mammalian rho kinase and myotonic dystrophy kinase, is

- required for maintenance of cell polarity and coordinates cell morphogenesis with the cell cycle. *Proc Natl Acad Sci U S A* **95**, 7526-7531.
- Vowels, J. J. and Thomas, J. H.** (1992). Genetic analysis of chemosensory control of dauer formation in *Caenorhabditis elegans*. *Genetics* **130**, 105-123.
- Wadsworth, W. G., Bhatt, H. and Hedgecock, E. M.** (1996). Neuroglia and pioneer neurons express UNC-6 to provide global and local netrin cues for guiding migrations in *C. elegans*. *Neuron* **16**, 35-46.
- Wang, B. B., Muller-Immergluck, M. M., Austin, J., Robinson, N. T., Chisholm, A. and Kenyon, C.** (1993). A homeotic gene cluster patterns the anteroposterior body axis of *C. elegans*. *Cell* **74**, 29-42.
- Wang, F. S., Wolenski, J. S., Cheney, R. E., Mooseker, M. S. and Jay, D. G.** (1996). Function of myosin-V in filopodial extension of neuronal growth cones. *Science* **273**, 660-663.
- Wang, H. U. and Anderson, D. J.** (1997). Eph family transmembrane ligands can mediate repulsive guidance of trunk neural crest migration and motor axon outgrowth. *Neuron* **18**, 383-396.
- Wang, J., Renger, J. J., Griffith, L. C., Greenspan, R. J. and Wu, C. F.** (1994). Concomitant alterations of physiological and developmental plasticity in *Drosophila* CaM kinase II-inhibited synapses. *Neuron* **13**, 1373-1384.
- Wang, K. H., Brose, K., Arnott, D., Kidd, T., Goodman, C. S., Henzel, W. and Tessier-Lavigne, M.** (1999). Biochemical purification of a mammalian slit protein as a positive regulator of sensory axon elongation and branching. *Cell* **96**, 771-784.
- Ward, S., Thomson, N., White, J. G. and Brenner, S.** (1975). Electron microscopical reconstruction of the anterior sensory anatomy of the nematode *Caenorhabditis elegans*. *J. Comp. Neurol.* **160**, 313-337.

- Ware, R. W., Clark, D., Crossland, K. and Russell, R. L.** (1975). The nerve ring of the nematode *Caenorhabditis elegans*: sensory input and motor output. *J. Comp. Neur.* **162**, 71-110.
- White, J. G., Southgate, E., Thomson, J. N. and Brenner, S.** (1976). The structure of the ventral nerve cord of *Caenorhabditis elegans*. *Phil. Transact. R. Soc. Lond. B* **275**, 327-348.
- White, J. G., Southgate, E., Thomson, J. N. and Brenner, S.** (1986). The structure of the nervous system of the nematode *Caenorhabditis elegans*. *Phil. Transact. R. Soc. Lond. B* **314**, 1-340.
- Winberg, M. L., Noordermeer, J. N., Tamagnone, L., Comoglio, P. M., Spriggs, M. K., Tessier-Lavigne, M. and Goodman, C. S.** (1998). Plexin A is a neuronal semaphorin receptor that controls axon guidance. *Cell* **95**, 903-916.
- Winslow, J. W., Moran, P., Valverde, J., Shih, A., Yuan, J. Q., Wong, S. C., Tsai, S. P., Goddard, A., Henzel, W. J., Hefti, F. and et, a.** (1995). Cloning of AL-1, a ligand for an Eph-related tyrosine kinase receptor involved in axon bundle formation. *Neuron* **14**, 973-981.
- Wissmann, A., Ingles, J., McGhee, J. D. and Mains, P. E.** (1997). *Caenorhabditis elegans* LET-502 is related to Rho-binding kinases and human myotonic dystrophy kinase and interacts genetically with a homolog of the regulatory subunit of smooth muscle myosin phosphatase to affect cell shape. *Genes Dev* **11**, 409-422.
- Wu, G. Y. and Cline, H. T.** (1998). Stabilization of dendritic arbor structure in vivo by CaMKII. *Science* **279**, 222-226.
- Xu, T., Wang, W., Zhang, S., Stewart, R. A. and Yu, W.** (1995). Identifying tumor suppressors in genetic mosaics: the *Drosophila lats* gene encodes a putative protein kinase. *Development* **121**, 1053-1063.

- Yamada, K. M. and Geiger, B.** (1997). Molecular interactions in cell adhesion complexes. *Curr Opin Cell Biol* **9**, 76-85.
- Yamochi, W., Tanaka, K., Nonaka, H., Maeda, A., Musha, T. and Takai, Y.** (1994). Growth site localization of Rho1 small GTP-binding protein and its involvement in bud formation in *Saccharomyces cerevisiae*. *J Cell Biol* **125**, 1077-1093.
- Yarden, O., Plamann, M., Ebbole, D. J. and Yanofsky, C.** (1992). cot-1, a gene required for hyphal elongation in *Neurospora crassa*, encodes a protein kinase. *Embo J* **11**, 2159-2166.
- Yu, H. H., Araj, H. H., Ralls, S. A. and Kolodkin, A. L.** (1998). The transmembrane Semaphorin Sema I is required in *Drosophila* for embryonic motor and CNS axon guidance. *Neuron* **20**, 207-220.
- Yu, S., Avery, L., Baude, E. and Garbers, D. L.** (1997). Guanylyl cyclase expression in specific sensory neurons: a new family of chemosensory receptors. *Proc. Natl. Acad. Sci. USA* **94**, 3384-3387.
- Zallen, J. A., Yi, B. A. and Bargmann, C. I.** (1998). The conserved immunoglobulin superfamily member SAX-3/Robo directs multiple aspects of axon guidance in *C. elegans*. *Cell* **92**, 217-227.
- Ziman, M., Preuss, D., Mulholland, J., O'Brien, J. M., Botstein, D. and Johnson, D. I.** (1993). Subcellular localization of Cdc42p, a *Saccharomyces cerevisiae* GTP-binding protein involved in the control of cell polarity. *Mol Biol Cell* **4**, 1307-1316.
- Zinn, K. and Sun, Q.** (1999). Slit branches out: a secreted protein mediates both attractive and repulsive axon guidance. *Cell* **97**, 1-4.
- Zipkin, I. D., Kindt, R. M. and Kenyon, C. J.** (1997). Role of a new Rho family member in cell migration and axon guidance in *C. elegans*. *Cell* **90**, 883-894.

Zorio, D. A., Cheng, N. N., Blumenthal, T. and Spieth, J. (1994). Operons as a common form of chromosomal organization in *C. elegans*. *Nature* **372**, 270-272.

Appendices

Appendix A. Double mutant analysis between genes involved in axon guidance. Percent defective animals (A), axon segments (B, see Chapter 3) or amphids (C-F) are indicated on the x axis. Error bars represent the standard error of proportion.

A. *sax-3; sax-5* double mutants scored for anterior misrouting in amphid axons visualized by DiI filling.

B. *sax-3; vab-1* double mutants scored for HSN axon crossover defects visualized with antibodies to serotonin.

C. *sax-3; vab-3* double mutants scored for ventral guidance defects in amphid axons visualized by DiI filling.

D. *sax-3; vab-2* double mutants scored for ventral guidance defects in amphid axons visualized by DiI filling.

E. *sax-3; unc-5* double mutants scored for ventral guidance defects in amphid axons visualized by DiI filling.

F. *vab-2; unc-40* double mutants scored for ventral guidance defects in amphid axons visualized by DiI filling.

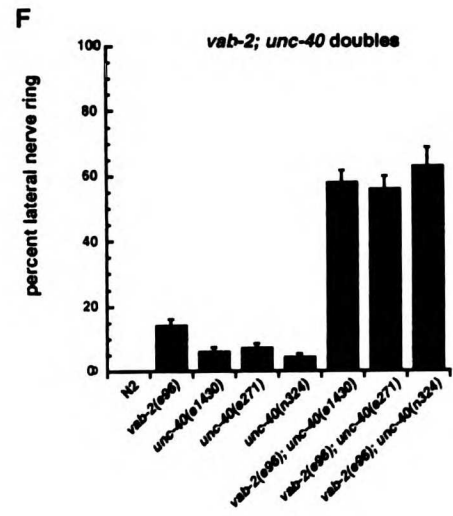
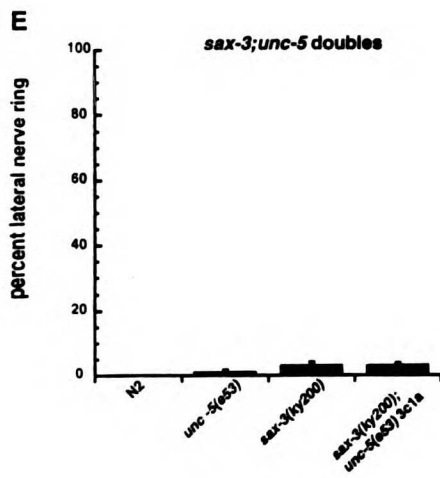
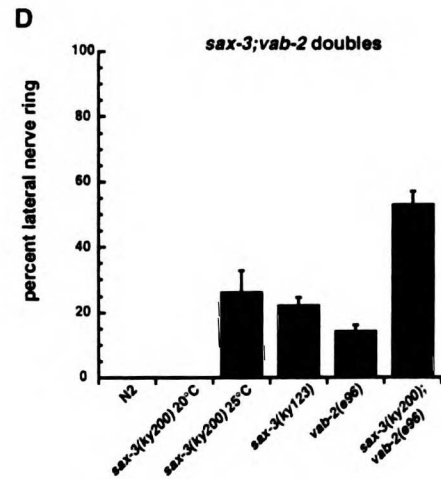
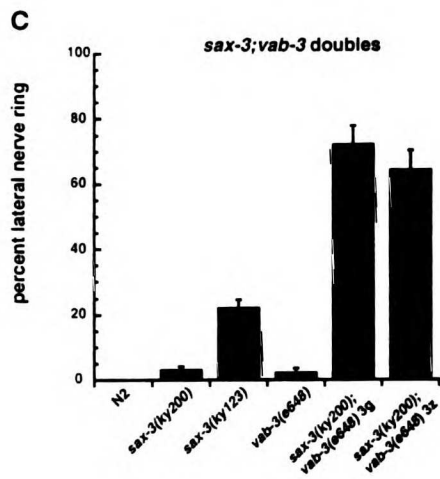
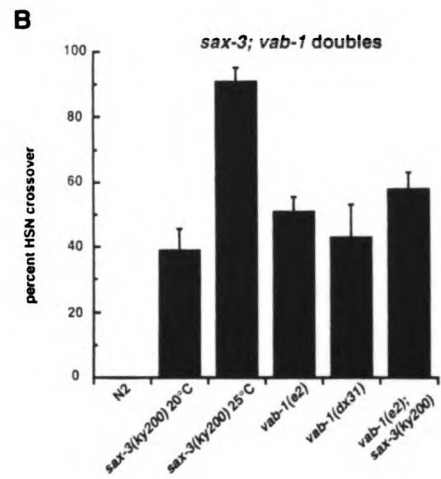
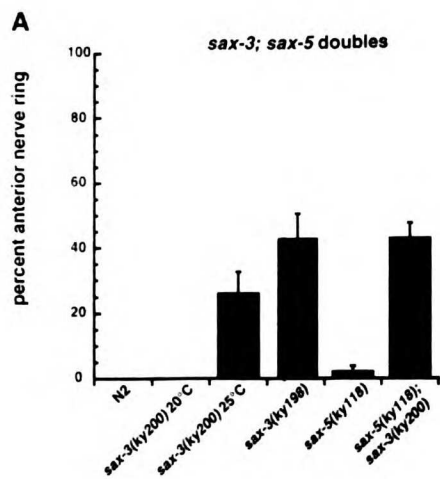








Table. Amphid axon pathfinding and cell migration defects in *sax-3* mutants.

							n	Viability ³
	Wild type	Defasciculated	Anterior axon	Anterior nerve ring ¹	Anterior cells ²	Notched head		
wild type	100%						>100	100%
<i>ky200</i> 20°C	68%	7%	17%		7%	5%	41	85%
<i>ky200</i> 25°C	14%	26%	23%	26%	12%	42%	43	34%
<i>ky203</i> 20°C	2%	40%	33%	16%	9%	28%	43	31%
<i>ky123</i> 20°C		20%	33%	25%	20%	43%	40	18%
<i>ky198</i> 20°C		20%	14%	43%	23%	57%	44	7%

Amphid axon phenotypes were characterized in adults with the *ceh-23::GFP* marker. Schematic drawings show the head of the animal. Anterior is to the left, dorsal at top. n = number of animals scored for amphid axon and notched head phenotypes. Animals with more than one phenotype were scored in the more severe category, with phenotypes listed from left to right in order of increasing severity.






¹In these mutants, all amphid axons were found in an abnormal location with respect to their cell bodies. In *sax-3(ky123)*, similar displacement of axons from nerve ring interneurons was also observed (see Methods).

²Axons were not scored in mutants with anterior cell bodies.

³Viability was scored as the percentage of eggs laid during a three hour period that survived to adulthood (n>150/strain). Most of the lethality occurred in embryos.

Appendix C. High copy transgenes containing the rescuing *sax-3* Apa1-Pst1 subclone of the R06A1 cosmid cause axon termination defects in the ASI amphid sensory neuron pair labeled with the *str-3::gfp* marker. These transgenes may overexpress SAX-3 protein in the cells in which it is normally expressed.

Table. Axon outgrowth and cell migration defects in the ASI neuron produced by a high copy *sax-3(+)* transgene

											n
	Wild type	Anterior axon	Axon termination	Wild type	Anterior cell	Posterior cell	Wild type	Anterior cell	Posterior cell		
wild type coincjection marker alone	100%						97 - 100%			8 lines, 48-122/line	
<i>sax-3</i> recessive mutation <i>sax-3(ly123)</i>		71%	29%				88%	6%		35	
high copy <i>sax-3(+)</i> high penetrance lines	51 - 75%	0 - 2%	25 - 49%				89 - 94%		6 - 11%	3 lines, 53 - 63/line	
medium penetrance lines	83 - 87%	0 - 1%	13 - 17%				93 - 96%		4 - 7%	3 lines, 30-276/line	
low penetrance lines	94 - 97%	0 - 1%	3 - 6%				94 - 97%		3 - 6%	3 lines, 69-89/line	
wild-type lines	100%						97 - 100%		0 - 3%	3 lines, 87-155/line	

Amphid axon phenotypes were characterized in adults using the *stx-3::GFP* marker. Schematic drawings show the head of the animal. Anterior is to the left, dorsal at top.
n = number of animals scored.

High copy *sax-3(+)* lines contained the *sax-3(+)* rescuing subclone and a *rol-6(dominant)* coincjection marker, while wild type animals contained the *rol-6* coincjection marker alone.

Appendix D. Map positions of *sax* mutants: data not included in Chapters Two, Three and Four

sax-2(ky216) III

dpy-17 non *unc-32* (0/4 mutant)
unc-32 non *dpy-17* (15/15 mutant)
unc-36 non *sma-4* (6/6 mutant)
sma-4 non *unc-36* (0/3 mutant)

sax-4(ky112) X

lon-2 non *egl-15* (3/6 mutant)
egl-15 non *lon-2* (2/19 mutant)
dpy-6 non *unc-18* (0/14 mutant)
unc-18 non *dpy-6* (4/4 mutant)
dpy-6 non *unc-115* (9/9 mutant)

sax-5(ky118) IV

dpy-4 non *unc-17* (0/3 mutant)
unc-17 non *dpy-4* (4/5 mutant)
dpy-4 non *tra-3* (2/4 mutant)
dpy-4 non *unc-26* (13/19 mutant)
unc-22 ky118 dpy-4 2i isolate/ep75 (RW7000)
dpy-4 non-ep75 non-*unc-22* (0/2) mutant
unc-22 ep75 non-dpy-4 (0/8 mutant)
unc-22 non-ep75 non-dpy-4 (3/3 mutant)

sax-6(ky214) I

homoz *sax-6* from non-*bli3 unc-54* (5 mutant, 2 het)
uncovered by sDf5
not uncovered by sDf6
dpy-5 non *unc-13* (1/4 mutant)
unc-13 non *dpy-5* (1/5 mutant)
lin-11 non *unc-13* (4/7 mutant)
unc-13 non *dpy-14* (3/3 mutant)

Appendix E. Mosaic analysis of *sax-3*.

An injection mix containing 10 ng/ul of pJAZ1 (an *ApaI*-*PstI* subclone of the R06A1 *sax-3* cosmid) and 160 ng/ul of PTG96 *sur-5::gfp* was injected into *sax-3(ky123)* mutant animals to generate mosaics. Mosaic animals were identified by the pattern of *sur-5::gfp* expression and scored for amphid axon defects by single-animal DiI filling.

- | | |
|-------------------|---|
| mosaic F1: | ABar- ABpl+ ABprap- |
| amphid phenotype: | left side — mostly wild-type, one axon slightly posteriorly displaced within the amphid commissure
right side — wild-type |
|
 | |
| mosaic F2: | ABa- ABpr- ABpl+ |
| amphid phenotype: | left side — major defasciculation, anterior axon
right side — mild defasciculation, maybe premature termination? |
|
 | |
| mosaic F3: | mostly ABp- (all right and two on left gfp-) ABar+ |
| amphid phenotype: | left side — wild-type
right side — wild-type |
|
 | |
| mosaic F4: | ABalpp+ (four on left +) ABprp+ (ASI ++) ABpra- |
| amphid phenotype: | left side — wild-type
right side — wild-type |
|
 | |
| mosaic C1: | ABa+? ABp- E+ MS+ C+ D+ P4+ |
| amphid phenotype: | left side — all axons anterior, slightly anterior cell bodies
right side — some termination (not all) |
|
 | |
| mosaic C2: | ABar- ABplap- ABa- (ABal- ar+?) ABp+ ABplap- E+ MS+ C+ D+ P4+ |
| amphid phenotype: | left side — slightly defasciculated
right side — anterior nerve ring, anterior cell bodies, defasciculation |
|
 | |
| mosaic C3: | AB- ABa- (?) ABp- E+ MS+ C+ D+ (P4+) |
| amphid phenotype: | left side — anterior nerve ring
right side — slight anterior nerve ring, ~wild-type |
|
 | |
| mosaic C4: | AB- complex ABa- (but a few +) ABp- (but a few +) (a few motor neurons on the right are +, SIA/SMB) E+ MS+ C+ D+ (P4+) |
| amphid phenotype: | left side — wild-type
right side — few dyefill (dendrite termination?), see one wild-type axon and one short anterior axon |

- mosaic C5: ABpl+ EMS+ ABa- ABpr- E+ MS+ C- D-
 amphid phenotype: left side — wild-type
 right side — poor dyefill, can't score
- mosaic E1: AB+ P1-
 amphid phenotype: left side — wild-type
 right side — wild-type
- mosaic G1: EMS- ABa+ ABp+ C+ D+
 strange lateral notched head (bulbous), egl, sick
 poor dyefill
- mosaic G2: AB- P1-
 unc, egl
 amphid phenotype: left side — mild defasciculation, termination
 right side — no dyefill
- mosaic G3: MS- ABpr- ABpl+ ABa+ E+ C+
 mild notch, not unc or egl
 amphid phenotype: left side — ~wild-type, poor fill
 right side — ~wild-type, poor fill
- mosaic G4: ABp loss perfect
 not unc or egl
 amphid phenotype: left side — anterior and posterior axons, termination
 right side — ~wild-type
- mosaic H1: AB++ (overexpression?) E- C- D- MS+
 dpy, roller
 poor dyefill
- mosaic H2: AB++ (overexpression?) E- MS- C- D-
 twisted pharynx, mild egl, mild unc, mild notch
 poor dyefill
- mosaic H3: AB+ P1-
 not unc or egl
 poor dyefill
- mosaic H4: AB+ P1-
 not unc or egl
 amphid phenotype: left side — wild-type
 right side — wild-type

Appendix F. Axon defects in amphid sensory neurons and HSN motor neurons in known mutants.

vab-13(e2627)

HSN ventral guidance defects (anti-serotonin staining): 0% mutant, n=82 neurons
HSN crossover defects (anti-serotonin staining): 28% mutant, n=36 axon segments
HSN cell migration defects (anti-serotonin staining): 7% mutant, n=60 neurons

one of the two amphids fails to dye fill (DiI filling, 25°C): 31%, n=61 animals
neither amphid fills (DiI filling, 25°C): 7%, n=61 animals

ina-1(gm144)

amphid axon termination (DiI filling, 20°C): 74% mutant (n=62 animals)

ina-1(gm39)

lateral axon misrouting (DiI filling, 20°C): 5% mutant (n=76 amphids)

mig-2(rh17)

amphid axon termination (DiI filling, 20°C): 73% mutant (n=137 animals)
posterior axons (DiI filling, 20°C): 12% mutant (n=137 animals)

mig-2(mu28)

wild-type amphid axons (DiI filling, 20°C): 0% mutant (n=339)

Appendix G. Candidate cosmids injected into *sax-2* and *vab-13* mutants did not rescue their amphid axon defects.

SAX-2 candidates

pool 1 (at 10 ng/ul each)

F56G1 (CaM kinase)
F20H6 (CaM kinase)
T06C9 (CaM kinase)
F55A10 (transducin)
rol-6 (100 ng/ul)

injected into CX3147 *sax-2(ky216) III; kyls4 X*
no rescue (4 lines)

pool 2 (at 10 ng/ul each)

ZC401 (a-actinin)
F52C9 (a-actinin)
F25F2 (myosin light chain kinase)
F22A4 (myosin light chain kinase)
rol-6 (100 ng/ul)

injected into CX3147 *sax-2(ky216) III; kyls4 X*
no rescue (14 lines)

CaMKII overexpression mix (at 30 ng/ul each)

F56G1
F20H6
T06C9
rol-6 (100 ng/ul)

injected into CX2627 *kyls4 X*
no defects observed at 20°C or 25°C (14 lines)

mix 1 (at 9 ng/ul)

C34E10 (*skb-1*)
rol-6 (100 ng/ul)

injected into CX3147 *sax-2(ky216) III; kyls4 X*
no rescue (x lines)

mix 2 (at varying concentrations)

C17F7 (10 ng/ul)

C12H31 (4 ng/ul)

C35H91 (or H9?) (3 ng/ul)

C55F6 (3 ng/ul)

rol-6 (100 ng/ul)

injected into CX3147 *sax-2(ky216) III; kyls4 X*

no rescue (x lines)

VAB-13 candidates (at 10 ng/ul each)

F10E7

F11F5

PTG96 (check name) (100 ng/ul)

injected into *vab-13(e2623) X* (from Jonathan Hodgkin)

no rescue of amphid dyefilling defect (5 lines)

Cosmids between the left breakpoint of nDf16 and lin-39 on III

injected into *sax-2(ky216) III; kyls4 X* in 7 pools of 4-5 cosmids each (each cosmid at ~10 ng/ul) with *rol-6(d)* pRF4 at 100 ng/ul as a coinjection marker

listed from left to right on the physical map

- the Q# on the tube indicates the number of the Qiagen prep
- concentrations are in units of nanograms / microliter; they may be slightly inaccurate due to spec variation and low yields
- some cosmids were misplaced so there are gaps in this region

F37A4 Q3 (from ND) 240 ng/ul

C28A6 (from ND) 50 ng/ul

C02B12 Q1 63 ng/ul

K07E12 Q3 (from ND) 230 ng/ul

R02D2 Q4 138 ng/ul

F39C7 (canonical for R121) QP27 from ND

R06H12 Q4 1100 ng/ul

C07C3 Q1 20 ng/ul

R01H2 Q1 315 ng/ul

C45A11 Q1 98 ng/ul

C17A11 Q1a 40 ng/ul

C24D3 Q1 775 ng/ul

C03F2 Q4 3900 ng/ul

C17A3 Q1 85 ng/ul

B0361! Q1 100 ng/ul

C47B12 Q1 270 ng/ul

R13H12 1130 ng/ul

T20B12 Q1 243 ng/ul

R13A5 Q1 775 ng/ul

K07D8 Q4 500 ng/ul

Cosmids between *tra-3* and *dpy-4* on LGIV

injected into *sax-5(ky118) III; kyls4 X* in 7 pools of 2-6 phage/cosmids each (each at ~7 ng/ul) with *rol-6(d)* pRF4 at 100 ng/ul as a coinjection marker

listed from left to right on the physical map

- the Q# on the tube indicates the number of the Qiagen prep
- concentrations are in units of nanograms / microliter; they may be slightly inaccurate due to spec variation and low yields!
- concentrations shown are those of the cosmid stock, not the concentration of cosmid in the injected pool
- phage preps gave exceptionally low yields, each tube represents a Qiagen prep from three combined 15 cm phage plates
- notes from Tom Barnes, who identified the phage in this region:
anything with A is the same as without the A
1384=1400, 1405=1412

pool 1:

1382 50 ng/ul (2/19)
1398 30 ng/ul
CCCA7 Q1 140 ng/ul
F55B11 Q1 50 ng/ul (and Q2 50 ng/ul)
Pla29 Q2 65 ng/ul

pool 2:

1494 53 ng/ul
1405 41 ng/ul
1384 113 ng/ul (and other isolate 25 ng/ul)
C28B4 Q1 128 ng/ul (and Q2 163 ng/ul)
LLC1 Q1 1690 ng/ul

pool 3:

1253 18 ng/ul
1248 183 ng/ul (and other isolate 5 ng/ul)
T27E7 Q1 85 ng/ul
T27E10 Q1 238 ng/ul

pool 4:

1222 20 ng/ul
1219 30 ng/ul

pool 5:

1231 35 ng/ul
I 272 80 ng/ul (and other isolate 35 ng/ul)
I 216S 75 ng/ul
1-406 20 ng/ul
E03E10 Q1a 175 ng/ul (and other isolate Q1b 855 ng/ul)
F13G11

pool 6:

1268B 65 ng/ul (and 1268A 53 ng/ul)
1232B 30 ng/ul (and 1232A 18 ng/ul)
1240 193 ng/ul
1269 175 ng/ul

pool 7:

1297 38 ng/ul
1290 100 ng/ul
1292 30 ng/ul
1294 20 ng/ul
1298 68 ng/ul

Cosmids between *fax-1* and stP40 on LGX

injected into *sax-3(ky123) kyls4 X* in 5 pools of 4-6 cosmids each (each at ~10 ng/ul) with *rol-6(d)* pRF4 at 100 ng/ul as a coinjection marker

listed from left to right on the physical map

- the Q# on the tube indicates the number of the Qiagen prep
- concentrations are in units of nanograms / microliter; they may be slightly inaccurate due to low yields and spec variation
- concentrations shown are those of the cosmid stock, not the concentration of cosmid in the injected pool

C38F12

C35G3 Q4 363 ng/ul

W05A4 Q3 1030 ng/ul

R16 Q3 105 ng/ul

M01F12 Q1 140 ng/ul

C42G10 Q4 600 ng/ul

C43E10

T09D6 Q1 910 ng/ul

T07B8 Q3 1210 ng/ul

ZK832 Q1 1450 ng/ul

C48D3 Q2 95 ng/ul

F11D5 Q 200 ng/ul

C50H7 Q3 128 ng/ul

C04F6 Q1 50 ng/ul

R06A1 (*sax-3* cosmid, in other boxes)

C05C4 Q4 270 ng/ul

C24E12 Q1 2240 ng/ul

ZK818 Q1 1780 ng/ul

B0015 Q1 200 ng/ul

BB7 Q1 55 ng/ul

F39A7

Cosmids between stP40 and *lin-18* on LGX

injected into *sax-1(ky211) kyls4 X* in 8 pools of 3-5 cosmids each (each at ~10 ng/ul) with *rol-6(d)* pRF4 at 100 ng/ul as a coinjection marker

listed from left to right on the physical map

-the Q# on the tube indicates the number of the Qiagen prep

-concentrations are in units of nanograms / microliter; they may be slightly inaccurate due to spec variation and low yields

C11H11 Q1 40 ng/ul

C08A6 Q3 280 ng/ul

D2071 Q3 73 ng/ul

C03H7 Q9

F34G9 5Q (canonical for C03H7)

C05F6 Q1

R11G1 Q1 133 ng/ul (*sax-1* cosmid, in other boxes)

K10C12 Q3 230 ng/ul

C02F12 Q1 133 ng/ul

C33B7 5Q

C01C4 4Q

F25E11 Q2 133 ng/ul (canonical for C49H7)

T14G12 Q1 1730 ng/ul

F47B7 Q1 63 ng/ul (and one other isolate 6Q)

T09H11 Q3 668 ng/ul (canonical for C28E1)

F35A5 9Q

K03C7 Q2 2100 ng/ul

C50A9 Q2

T08C3 Q3 1440 ng/ul

ZC64 Q3 180 ng/ul

R05F10 Q5 130 ng/ul

F47F2 Q2 1670 ng/ul

T22B2 Q1 353 ng/ul

C38D3

F47B7 6Q

B0451 Q2 2000 ng/ul (canonical for C13E11)

C16B8 Q3A 318 ng/ul (and one other isolate 3Q 145 ng/ul)

C26A2 Q3 (canonical for C16B8)

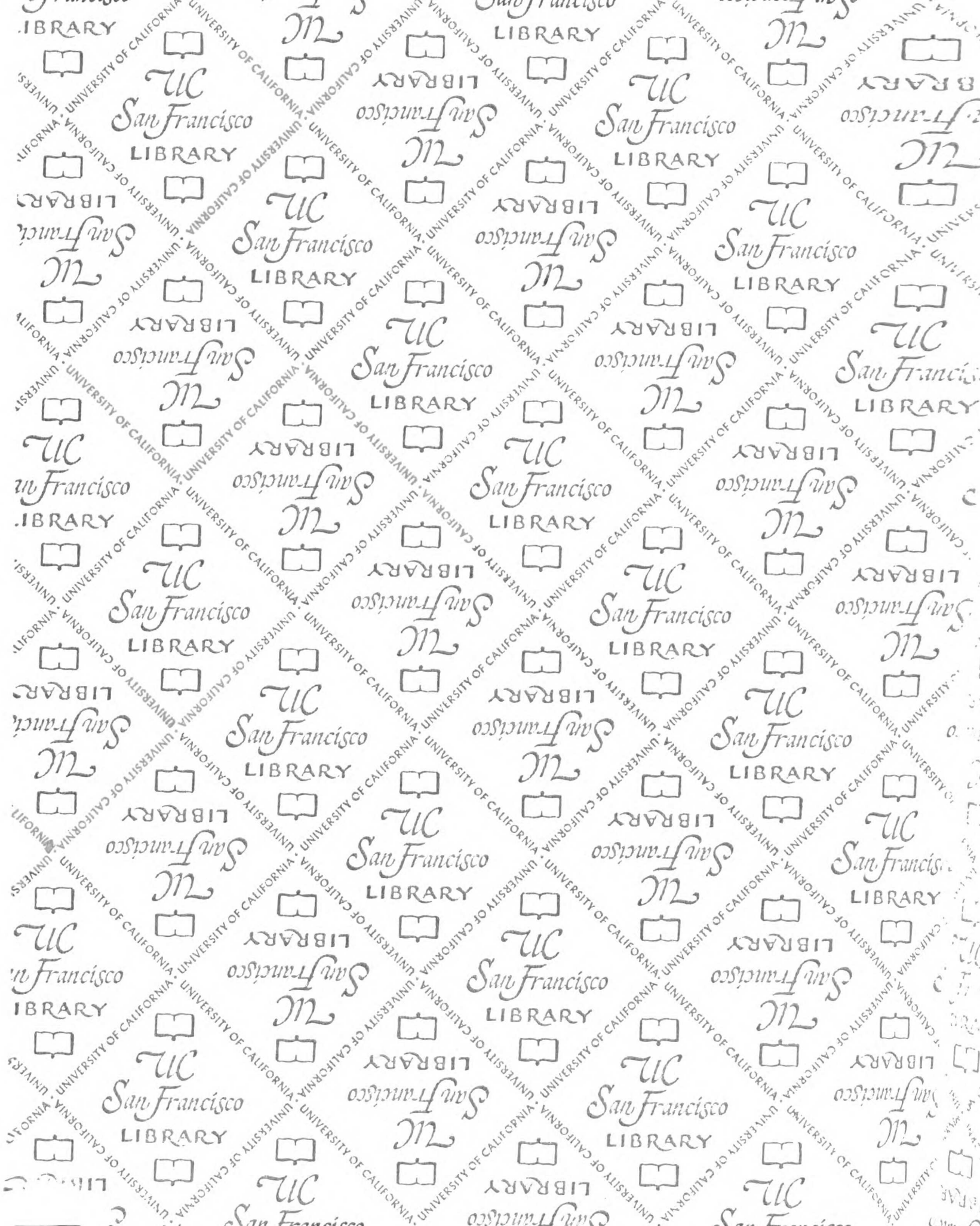
C27B6 58 ng/ul (canonical for C16B8)

F28E4 Q2 1700 ng/ul

T06F4 Q5 783 ng/ul

F09F9 Q2 110 ng/ul

C07F2 Q2 78 ng/ul



UCSF LIBRARY

For Not to be taken
from the room.
reference

7065090



3 1378 00706 5090

